iScience

CellPress
OPEN ACCESS

Review

Unlocking CO_2 conversion potential with single atom catalysts and machine learning in energy application

Esraa Kotob,[1] Mohammed Mosaad Awad,[1] Mustapha Umar,[2] Omer Ahmed Taialla,[1] Ijaz Hussain,[2] Shaima' Ibrahim Alsabbahen,[1] Khalid Alhooshani,[1,3] and Saheed A. Ganiyu[1,3,*]

[1]Department of Chemistry, King Fahd University of Petroleum and Minerals, Dhahran 31261, Saudi Arabia

[2]Department of Chemical Sciences, Faculty of Science and Computing, North-Eastern University, P. M. B. 0198, Gombe, Gombe State, Nigeria

[3]Interdisciplinary Center for Refining & Advanced Chemicals, King Fahd University of Petroleum & Minerals, Dhahran 31261, Saudi Arabia

*Correspondence: gsadewale@kfupm.edu.sa

https://doi.org/10.1016/j.isci.2025.112306

SUMMARY

SACs are transforming CO_2 conversion and energy applications due to their high catalytic efficiency, unique electronic structures, and maximal atom utilization. They have shown great promise in CO_2 electroreduction, hydrogenation, and dry reforming, yet challenges remain in their synthesis, stability, and scalable production. This review explores advances in SAC design, support interactions, and electronic tuning to enhance catalytic performance. It also analyzed state-of-the-art characterization techniques used to probe SAC structures and reaction mechanisms. Machine learning is emerging as a powerful tool for predicting SAC stability and optimizing reaction pathways. By examining recent breakthroughs and existing limitations, this work provides insights into the future of SACs in energy applications and CO_2 utilization, highlighting their role in sustainable chemical transformations and carbon-neutral technologies.

INTRODUCTION

Over the past century, the Earth's temperatures have been increasing because of the growing emissions of carbon dioxide (CO_2).[1,2] By 2040, global energy consumption is projected to rise by over 48%. Fossil fuels, which remain the primary source of energy, are major contributors to the emission of CO_2 into the atmosphere.[3,4] Renewable energies like wind and solar energy offer viable alternatives to fossil fuels, helping to mitigate this issue.[5,6] However, these sources are subject to seasonal, nocturnal, and geographical variations. Furthermore, various industries such as textiles, paper and pulp, aluminum refineries, iron, cement, steel, and landfills generate additional CO_2 emissions during their processes.[7,8] In fact, CO_2 alone accounts for approximately 77% of total greenhouse gas (GHG) emissions.[9,10] While natural processes like ocean absorption and forest growth do remove some CO_2 from the atmosphere, they are insufficient to counterbalance the excess CO_2 present in the air.[11]

The Paris Agreement commits countries to cutting CO_2 emissions, aiming to limit global warming below 2°C. The agreement prioritizes reducing human activities that generate CO_2 and developing technologies that can reduce and transform CO_2 emissions into value-added products within a circular economy framework.[12] To meet these goals, a sustainable method for removing 800 Gt (gigaton) of CO_2 from the atmosphere between 2010 and 2150 must be established.[13–15] Currently, the world can utilize just 10% of global CO_2 emissions, or 3.7 Gt/year. Nonetheless, the possibility of CO_2 sequestration may be greatly expanded by combining companies with suitable carbon capture and storage (CCS) mechanism.[16] This integration might also allow for continuous generation of fuels and other valuable products. This worldwide effort has the potential to generate a $0.8–1.1 trillion yearly market for carbon-based products, even if it just uses 10% of the CO_2 supply.[9] As a result, carbon capture, utilization, and storage (CCUS), and another energy application like the CO_2 and methane reforming provides a medium-term strategy for lowering global CO_2 emissions.[17,18] Advancements in technology that focus on decreasing energy consumption and adapting current facilities for CO_2 utilization are expected to be promising in the coming years.[3] Implementing CCS technology in fossil fuel–dependent power production systems is the only way to meet the 40% reduction in GHG emissions objective set by Europe's energy road plan toward a low-carbon energy system by 2030.[19]

Recent research has focused on catalytic processes that transform CO_2 into valuable chemicals and fuels for energy applications.[20] Essentially, there are multiple strategies for reducing CO_2 emissions: physical, biochemical, electrochemical, photochemical, radiochemical, thermochemical, carbon sequestration and storage, and chemical. Physical methods, such as deep-sea sequestration and geological storage, are limited by high costs and complexity.[21,22] Chemical approaches for CO_2 conversion include the use of homogeneous[23] and

heterogeneous catalysts,[24] as well as biochemical,[25] electrochemical,[26] photochemical,[27] radiochemical,[28] and thermochemical processes.[29,30] While these methods show promise for producing valuable chemicals, several challenges hinder their advancement. These include the exceptional stability of CO_2, high energy and temperature requirements,[23] scalability issues in industrial applications, the need for multifunctional active phases, the complex nature of tandem cascade reactions, and the difficulties in understanding and controlling reaction mechanisms. These obstacles lead to inefficiencies and economic disadvantages. Nonetheless, the exploration and extensive development of innovative alternatives provide promising opportunities for improvement.[31]

SACs and metal-single atom catalysts (M-SACs) have recently developed as potential catalysts for CO_2 utilization processes (CO_2UPs) due to their outstanding performance.[32,33] SACs, which contain separated metal atoms dispersed on a conductive support, introduce an innovative approach to catalysis by merging the benefits of both heterogeneous and homogeneous catalysts.[34,35] SACs are catalysts in which individual metal atoms are dispersed and stabilized on a supporting material, often exhibiting unique catalytic properties due to their atomic level dispersion. Unlike zeolites and metal-organic frameworks (MOFs), which are porous materials that primarily function as hosts for catalytic sites or reactants, SACs rely on isolated metal atoms as the active sites. These isolated atoms often achieve higher atomic utilization and exhibit distinct electronic structures compared to the clusters or nanoparticles found in zeolites and MOFs, leading to unique catalytic behavior.[36]

The downsizing of metal sites to the atomic scale offers several benefits, including unique low coordination of metal atoms, strong metal support interactions, electronic structures, and maximum utilization of metal atoms.[37–39] Solid-state heterogeneous SACs with analogous M-Nx moieties have recently attracted significant attention for various CO_2 utilization methods. This is due to their ease of preparation, unique electronic and geometric structures, excellent conductivity (particularly when supported on carbon materials), structural stability, and outstanding CO_2UPs performance and durability.[40–42] In a short period, the field of SACs for CO_2UPs has grown fast, resulting in the research of diverse single metal sites and reduction products.[43] Nonetheless, as the specific surface area of SACs rises, their surface free energy experiences a pronounced increase, which in turn facilitates the tendency for agglomeration coupling and the creation of sizable clusters during both their preparation and reaction processes.[44] Maiden research on catalysts with isolated metal atomic sites can be traced back to 1979, when Ji et al. confirmed the presence of isolated rhodium (Rh) single atoms on the surface of Al_2O_3 using nuclear magnetic resonance and ^{13}C relaxation time distribution.[38] In addition to oxide systems, Meshitsuka et al.[39] designed a Ti single site catalyst in 1995 by directly attaching a metal-organic combination onto the inner surface of mesoporous silica. This catalyst demonstrated exceptional selectivity and efficiency in the process of epoxidizing cyclohexene and pinene with *tert*-butyl hydroperoxide. In 1999, Meshitsuka et al.,[39] demonstrated that atomically dispersed Pt ions stabilized on magnesium oxide exhibited comparable activity to Pt nanoparticles in the combustion of propane at low temperatures. They used X-ray absorption fine structure (XAFS) data to verify the absence of platinum particles. Subsequently, Abbet et al.,[45] prepared Pdn (1–30) clusters and single Pd sites on magnesium oxide films using a selective soft-landing method. The single Pd atoms catalyzed the formation of benzene at a low temperature of 300 K. During this period, numerous studies were conducted on supported catalysts, particularly single metal species on oxide substrates. The soft-landing method for precise nanoclusters was widely developed, and significant progress was made in catalytic research for various important conversions. Atomically dispersed metal sites are the principal active centers in these catalysts, whereas coordinated atoms (mostly carbon and nitrogen) surrounding the metal sites contribute to CO_2 activation or intermediate dissociation via electronic polarization.[46–48] The synergetic effects of heterogeneous SACs considerably improve the catalytic performance of CO_2UPs.

This article gives a comprehensive and critical review of recent advancements and prospects of SACs for CO_2UPs, with a focus on the production of valuable products. It offers an extensive overview of how SACs influence product formation and enhance the production of multicarbon compounds. Moreover, it explores the synergistic effects of single atoms and cascade systems, emphasizing the cutting-edge approach of integrating SACs into cascade systems for CO_2 conversion research (CO_2CR). The combination of the unique properties of single atoms and the efficiency of cascade systems holds great potential to achieve unparalleled selectivity and conversion rates in transforming CO_2 into valuable products. SACs can serve as fundamental building blocks within individual catalytic stages of cascade systems. Each SAC can be strategically placed at specific stages to perform targeted chemical transformations, creating a highly tailored and efficient reaction pathway. Furthermore, the review delves into the characterization methods of SACs supported by computational studies, drawing on recent published works of SACs for CO_2UPs. It also addresses the challenges associated with utilizing SACs for CO_2UPs and offers valuable recommendations for realizing the full potential of SACs in CO_2 reduction.

SINGLE ATOM CATALYSTS (SAC)

From bulk to atomic, a history of single-atom catalyst development

The concept of isolated atoms acting as catalysts is not new. Even before its application in modern heterogeneous catalysts with supported metals, nature utilized single atoms in various forms to drive crucial chemical reactions. Examples include metalloenzymes, organometallic complexes, and open framework structures.[49] Pioneering work by Flytzani-Stephanopoulos et al.,[50] and Bashyam and Zelenay[51] challenged the traditional view of metal nanoparticles in catalysis. These researchers demonstrated that isolated ionic gold/platinum and oxidized cobalt/iron species were responsible for activity in the water-gas shift and oxygen reduction reactions, respectively. Advancements in experimental techniques later confirmed the presence of these isolated centers, solidifying the concept of SACs as in Figure 1 showing the timeline for SACs concept.

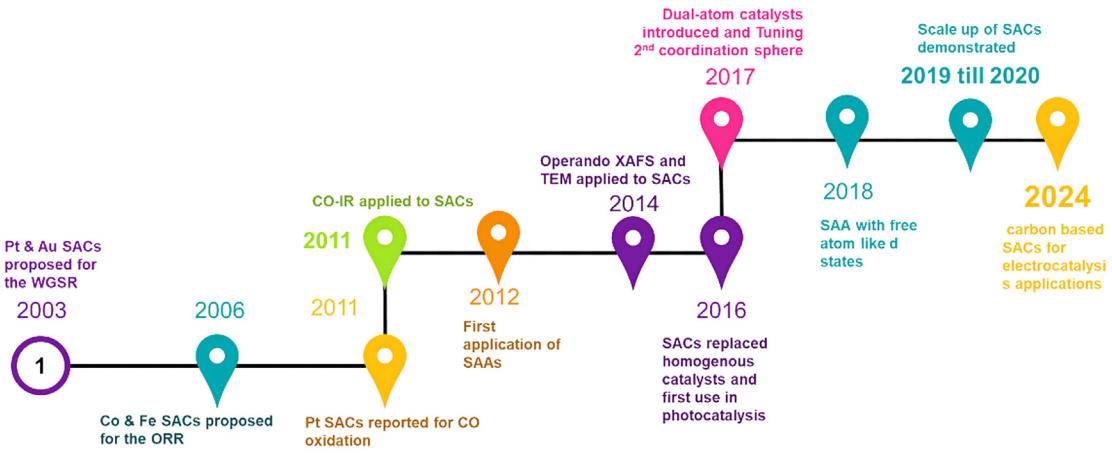

Figure 1. SACs: a decade of stunning advancement and the ability for a bright future (Data obtained from Web of Science)

Notably, Zhang et al.'s landmark work showcased the high productivity of platinum single atoms on iron oxide for CO oxidation, ushering in a new era in heterogeneous catalysis.[52,53] Single-atom catalysis has exploded in popularity over the past decade, becoming a major focus in modern chemical research. Early researchers soon realized the potential cost advantages of using atomically dispersed species for precious metals, and enhancing their utilization became a key focus in the field.[54] Over the 10-year journey since the topic's consolidation, single-atom catalysis has explored the entire periodic table. The variety of host materials has also grown. Although metal oxides were initially the most extensively studied, customized carbons have become the most dominant in recent years. The range of applications has broadened, with an increasing emphasis on heterogeneous catalysis.[55] Iron (Fe), cobalt (Co), and nickel (Ni) atoms dispersed individually on nitrogen-doped carbon materials have exhibited remarkable catalytic activity in key energy-related processes, such as oxygen reduction,[51] hydrogen evolution reaction,[56] and CO_2 conversion.[57] While research on single atom photocatalysts is still in its infancy compared to electrocatalysts, this field also holds great promise for addressing the energy crisis.[58] The starting point for single atoms was the concept of subnanometer clusters, which paved the way for moving beyond the nanoparticle scale.[59]

Advantages of subnanometer clusters and single atoms over nanoparticles

The significance of particle sizes in determining catalytic properties is well-established, leading to the development of various catalyst forms, including nanoparticles, nanosized clusters, and monatomic catalysts, to enhance their effectiveness.[40,60] Transitioning metal active sites from nanoparticles to sub-nanometer clusters and then to single atoms introduces differences in metal atom aggregation and coordination structures in supported catalysts.[61–63] Homogeneous catalysts, heterogeneous nanoparticles, and SACs of the same metal often exhibit distinct catalytic behaviors due to differences in atomic utilization and coordination environments.[37] For instance, homogeneous nickel complexes demonstrate high activity for CO_2 activation in hydrogenation reactions but suffer from poor stability and recyclability, limiting their practical applications.[64] In contrast, nickel nanoparticles supported on oxides offer improved durability; however, their catalytic activity and selectivity are largely influenced by particle size, leading to variations in performance.[65] Single-atom Ni catalysts anchored on nitrogen-doped carbon overcome these limitations by achieving nearly 100% atomic utilization, significantly enhancing CO_2 conversion efficiency and selectivity.[66] Similarly, copper-based homogeneous catalysts efficiently catalyze CO_2 reduction but require ligand stabilization to maintain their activity.[67,68] While Cu nanoparticles supported on zirconia provide better stability, their performance is hindered by low selectivity due to the presence of multiple active sites.[69] In contrast, Cu-SACs anchored on carbon-based supports demonstrate superior catalytic efficiency, attributed to their well-defined single-atom active sites that optimize electronic interactions with the support material.[66,70,71] For instance, Yang et al. reported that Cu-SACs exhibit significantly enhanced CO_2 hydrogenation selectivity compared to Cu nanoparticles, achieving higher conversion efficiency and product specificity.[72] These examples underscore the critical role of SACs in bridging the gap between homogeneous and heterogeneous catalysis, offering a promising avenue for advancing CO_2 utilization technologies by improving activity, stability, and selectivity. However, stabilizing high-surface-energy metal particles on supporting materials is challenging, as it requires significantly reducing the loading and consequently the availability of active sites for the catalytic route.[73]

Supported sub-nanometer cluster catalysts (SNCCs, <2 nm) offer nearly fully exposed active atoms, maximizing atom utilization and enhancing specific activity.[74] Notably, studies by Hu et al. and Wang et al. have shown that reducing metal particles to ~1 nm shifts the d-band center closer to the Fermi level, enhancing electron delocalization, reducing activation energy, and improving catalytic activity.[75,76] Positioned between nanoparticles and SACs, sub-nano clusters balance active site availability with oxidation state modulation, making them advantageous for catalytic reactions.[76,77] Their unique geometric structures and metal–support interactions can be flexibly

regulated to optimize intermediate adsorption and reaction pathways, offering unique catalytic performances and high selectivity[78–82]

In contrast, SACs represent the ultimate downscaling of catalysts, with isolated metal atoms stabilized on supports.[83] SACs achieve 100% atom utilization efficiency and precise active site control, addressing challenges in adsorption and activation of intermediates.[84,85] Since the groundbreaking work of Qiao et al. in 2011, where SACs with separated Pt atoms were synthesized, SACs have demonstrated high activity and stability.[58] For instance, Pt-based SACs are active for specific reactions but may lack efficiency in others due to the absence of metal–metal bonds.[86,87] The development of robust support materials and advanced techniques, such as aberration-corrected microscopy, has enabled better stabilization and characterization of SACs.[88] Despite their reduced number of active sites compared to SNCCs, SACs exhibit unique electronic properties due to the isolation of metal atoms, making them effective for specific reactions such as CO_2 conversion and oxygen reduction.[63,89–92] Two-dimensional (2D) materials, such as $Ti_3C_2T_x$ MXene, are promising supports for SACs due to their high specific surface area, excellent conductivity, and active basal planes.[93–99] These supports enhance the exposure and stability of active sites, improving catalytic performance.[100,101] Furthermore, SACs anchored on oxide supports benefit from surface imperfections that act as anchoring sites for metal clusters and individual atoms.[102–104] The practical fabrication of SACs remains challenging due to their inherent mobility and sintering tendencies under realistic reaction conditions.[105] Nevertheless, advancements in synthesis methods and support materials continue to push the boundaries of SAC applications.

The concept of SACs has advanced significantly since its inception, with applications in thermocatalysis, electrocatalysis, and photocatalysis.[106] For example, SACs have shown promise in fuel cell reactions and CO_2 conversion due to their precise engineering of active sites.[107–110] However, challenges such as synthesis scalability, stability under reaction conditions, and limitations in adsorption and activation for complex reactions persist. Comparatively, while nanoparticles provide abundant active sites, their interior atoms remain inaccessible, limiting overall efficiency.[86,87] Sub-nanometer clusters, with their high surface atom fraction and tunable electronic properties, offer a middle ground between nanoparticles and SACs.[46,62,84,111] By leveraging their distinct advantages, SACs and SNCCs complement each other in advancing catalytic technologies, paving the way for sustainable and efficient processes.

Synergetic effect of single atom and cascade system

In the pursuit of sustainable and effective solutions to address the global challenge of CO_2 emissions, researchers have delved into innovative approaches within CO_2 conversion technologies. One groundbreaking concept involves the implementation of cascade systems for CO_2 conversion. This approach integrates multiple catalytic stages, each conducting distinct chemical transformations, to convert CO_2 into valuable products. By harnessing synergistic effects through sequential catalytic reactions, cascade systems promise improved selectivity and overall conversion efficiency. This novel approach opens possibilities to transform CO_2 into a diverse range of valuable multicarbon products, including hydrogen, hydrocarbons, alcohols, and other high-value chemicals.[112] Previously explored cascade systems have included permutations of electrochemical, thermochemical, and biochemical reactions in CO_2 upgrades to multicarbon products.[94,113–121] However, these often rely on harsh reaction conditions (high temperature and pressure) and generate byproducts, necessitating costly separation.[122–126] Cascade electrochemical and biochemical processes utilize ambient conditions but have, thus far, led to limited productivity of C_4 chemicals. Cascade systems for CO_2 conversion encompass various innovative designs, each optimized to achieve specific product selectivity and overall efficiency. A common type involves the integration of multiple catalysts in a tandem arrangement, where the product of one catalytic[116] stage becomes the feedstock for the subsequent stage. For instance, the first catalyst may convert CO_2 to an intermediate, such as CO, which is then fed to a second catalyst for further transformation into hydrocarbons with yields exceeding 60% or alcohols. An alternative variant employs a multifunctional catalyst with separate active sites, which enables consecutive reactions to efficiently convert CO_2 into desired products in a single reactor. Researchers have also explored photocascade systems, where light-driven catalysis initiates specific reactions followed by subsequent thermal catalytic steps. These multistage configurations offer the potential to unlock higher selectivity and synergistic effects, facilitating the conversion of CO_2 into a different of valuable fuels and chemicals.[118] The incorporation of SACs into cascade systems represents a cutting-edge approach in CO_2 conversion research. By combining the exceptional properties of single atoms with the efficiency of cascade systems, researchers aim to accomplish unprecedented selectivity and conversion rates in transforming CO_2 into value-added products. In such a setup, SACs can serve as the building blocks of individual catalytic stages within the cascade system. Placing each single-atom catalyst strategically at specific stages enables targeted chemical transformations, creating a highly tailored and efficient reaction pathway. The utilization of SACs ensures atomic precision, allowing for precise control over reaction intermediates and products.[127] Moreover, the high surface area and tunable properties of SACs can be leveraged to enhance the interaction among different catalytic stages, advancing efficient mass and energy transfer within the cascade system. Despite the challenges, the integration of SACs into cascade systems holds immense promise in advancing CO_2 conversion technologies, providing a sustainable and versatile solution to mitigate CO_2 emissions while producing valuable chemicals and fuels.[61] Nevertheless, the process of obtaining controlled production of SACs continues to be difficult because of the rapid migration as well as aggregation of active atoms throughout manufacturing or later application procedures. The most practical and efficient method to achieve SACs is to sustain monodispersed atoms on suitable substrates. Various techniques, including confinement impacts, coordination effects, and chemical bonding, have been documented to provide isolated metal sites on supports. These methods involve restricting the loading quantity of the active component, enhancing interactions among metal atoms and supports, and utilizing defects or voids on the

support.[84,128–130] A recent study explored the tandem conversion of CO_2 to 1-butene (1-C_4H_8) through a system combining a CO_2-to-C_2H_4 electrolyzer with a C_2H_4 dimerization step. Using a bimetallic metal-organic framework (MOF) with tunable pore structures and periodic channels, the study optimized selectivity and activity for the dimerization process. The most effective MOF, containing Ru and Ni catalytic sites, achieved a 1-C_4H_8 production rate of 1.3 mol g_{cat}^{-1} h^{-1} with 97% C_2H_4 conversion. The cradle-to-gate carbon intensity was estimated at −2.1 kg CO_2e/kg 1-C_4H_8, assuming CO_2 from direct air capture and wind-powered electricity, demonstrating the potential of cascade systems for sustainable CO_2 utilization.[131]

Characterizations

The development of SACs has necessitated advanced characterization methods to elucidate their structural and electronic properties.[132,133] These techniques provide critical insights into the atomic dispersion, coordination environment, and catalytic mechanisms of SACs, facilitating their optimization for CO_2 conversion.[134] However, SAC characterization presents several challenges, including the difficulty of detecting isolated atoms, distinguishing them from nanoparticles, and understanding their dynamic behavior under reaction conditions.[135,136] A combination of microscopic, spectroscopic, and operando techniques is often required to achieve a comprehensive characterization of SACs.[132,137–139]

Microscopic techniques provide direct visualization of SAC structures, offering insights into atomic dispersion and morphology. High-angle annular dark-field scanning transmission electron microscopy (HAADF-STEM) and transmission electron microscopy (TEM) are commonly used to confirm single-atom dispersion.[140] For example, HAADF-STEM imaging (Figure 2D) of Cu-SA/$Ti_3C_2T_x$ identifies individual Cu atoms as bright dots uniformly distributed across the $Ti_3C_2T_x$ lattice, indicating the absence of Cu clusters and confirming atomic dispersion. TEM imaging (Figure 2C) further reveals the nanosheet morphology of the catalyst, which enhances surface area and facilitates electron transfer, improving catalytic performance. Although X-ray diffraction (XRD) is useful for determining structural properties,[128,141–144] it lacks the sensitivity to detect isolated atoms.[145] Bao et al. employed XRD to confirm that the Cu-SA/$Ti_3C_2T_x$ catalyst retains its $Ti_3C_2T_x$-like crystal structure, with the absence of diffraction peaks for copper species (Figure 2B) suggesting that Cu atoms remain atomically dispersed rather than forming nanoparticles or clusters. Additional microscopic techniques, such as high-resolution transmission electron microscopy (HR-TEM), may be required to further resolve atomic structures.[36]

Spectroscopic methods provide elemental, electronic, and coordination information, which is crucial for understanding the behavior of SACs. X-ray photoelectron spectroscopy (XPS) is commonly used to analyze oxidation states and electronic interactions.[22,146,147] In the case of Cu-SA/$Ti_3C_2T_x$, XPS reveals Cu 2p binding energies at 932.5 and 952.4 eV, indicating a mixed Cu^0 and Cu^{1+} oxidation state. This suggests partial electron transfer between Cu and $Ti_3C_2T_x$, influencing catalytic selectivity.[36] X-ray absorption spectroscopy (XAS), including X-ray absorption near-edge structure (XANES) and extended X-ray absorption fine structure (EXAFS), offers additional structural insights.[148] XANES analysis at the Cu K-edge (Figure 2E) confirms that the Cu valence state lies between metallic Cu^0 and Cu^{1+}, while EXAFS (Figure 2F) reveals a dominant Cu–O coordination peak at ∼1.6 Å, with no Cu–Cu scattering at 2.2 Å, reinforcing atomic dispersion. Further EXAFS fitting (Figure 2G) suggests a Cu–O_3 coordination environment, aligning with Bader charge analysis (+0.42), which indicates electronic interactions between Cu and surface oxygen groups. Inductively coupled plasma-optical emission spectrometry (ICP-OES) quantifies Cu loading at 0.2 wt. %, validating the effectiveness of the synthesis approach in achieving a well-defined SAC structure.[36]

Operando and *in situ* characterization techniques are essential for studying the dynamic behavior of SACs under reaction conditions. Yang et al. investigated the structural evolution of Cu nanocatalysts during CO_2 reduction using operando analysis, including 4D electrochemical liquid-cell scanning TEM. Their findings revealed that metallic Cu nanograins oxidize into single-crystal Cu_2O nanocubes upon exposure to air after electrolysis, highlighting the dynamic nature of SACs.[147] Additionally, Amirbeigiarab et al. demonstrated the spontaneous formation of low-coordinated Cu surface species at the onset of CO_2 electroreduction using *in situ* scanning tunneling microscopy (STM), surface XRD (SXRD), and Raman spectroscopy. STM imaging showed a disordered adlayer on Cu terraces, suggesting the presence of immobile molecular species, while SXRD provided atomic-level insights into surface restructuring. Raman spectroscopy further confirmed the formation of bidentate carbonates and carbonate anions, which are crucial for catalytic performance.[149]

Despite advancements in characterization techniques, significant challenges remain in fully understanding SACs. The primary difficulties include detecting single atoms, as conventional techniques like XRD lack the sensitivity to identify isolated atomic sites, necessitating advanced imaging methods like HAADF-STEM. Distinguishing single atoms from nanoparticles requires complementary techniques such as XAS and EXAFS to confirm atomic dispersion and avoid misinterpretation of agglomeration. Understanding dynamic changes under reaction conditions remains complex, even with operando techniques, as real-time tracking of atomic-scale transformations is challenging. Additionally, correlating structure with catalytic performance demands a multi-technique approach integrating spectroscopy, electrochemical analysis, and theoretical modeling to establish structure-activity relationships in SACs. Future research should focus on improving *in situ* and operando techniques, developing higher-resolution imaging methods, and integrating computational simulations with experimental data to gain deeper insights into SAC behavior. Addressing these challenges will enhance the design and optimization of SACs for CO_2 conversion and other catalytic applications.

SACs BASED CATALYSTS

SACs have lately gained prominence in catalysis due to their ability to use the advantages of both homogeneous and heterogeneous catalysts, while also incorporating distinctive characteristics that bridge the gap between them.[34] In contrast to

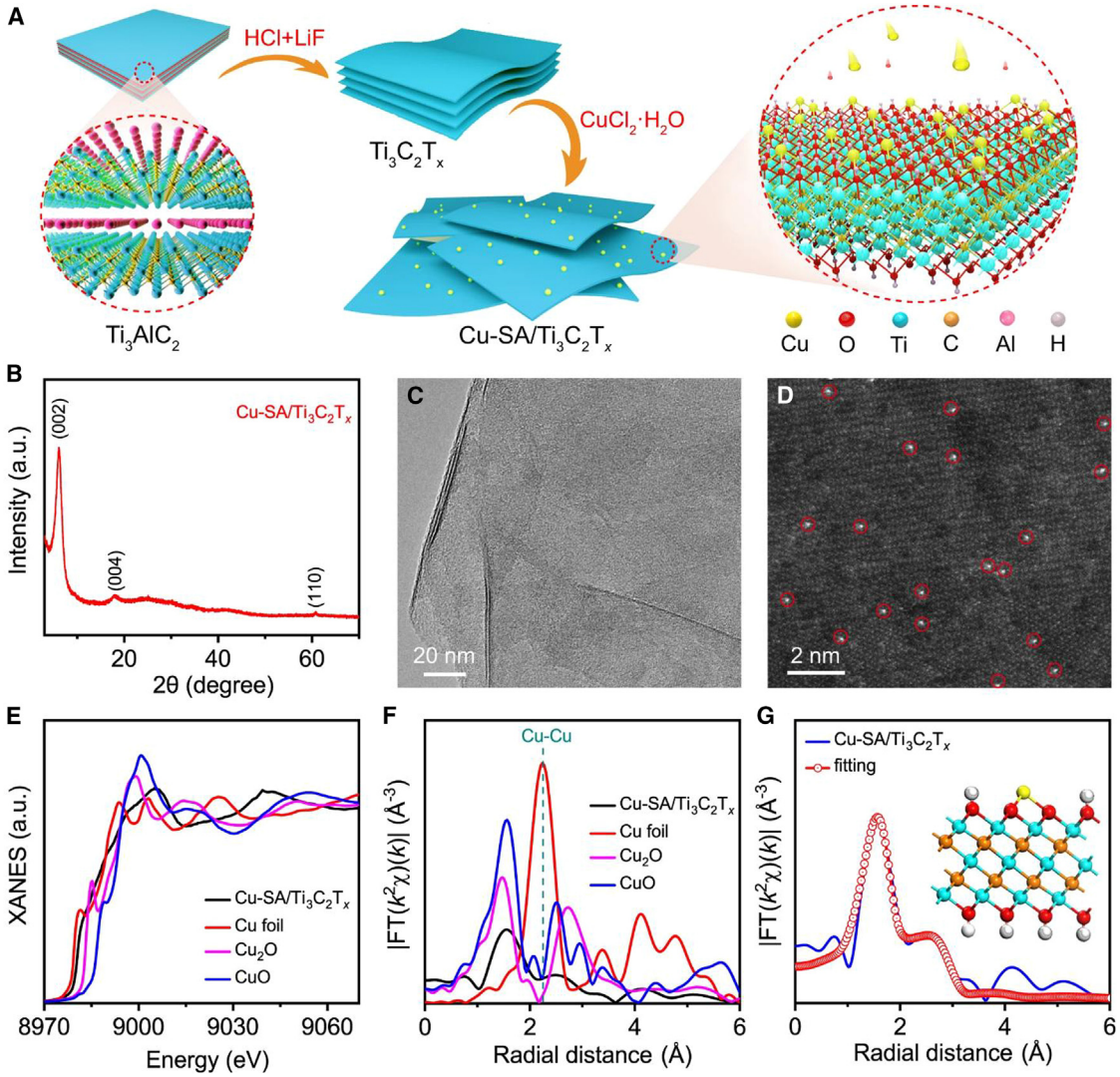

Figure 2. Physical characterization

(A) Preparation and structural characterization of Cu-SA/$Ti_3C_2T_x$.

(B) XRD pattern.

(C) TEM image.

(D) HAADF-STEM image in which some of the Cu SAs are highlighted by red circles.

(E) XANES spectra at the Cu K-edge with CuO, Cu_2O and Cu foil as reference.

(F) The k^2-weighted Fourier transform (FT) EXAFS curves in which $\chi(k)$ denotes the EXAFS oscillation function.

(G) EXAFS fitting curve of Cu-SA/$Ti_3C_2T_x$, insert is an illustration of Cu-SA/$Ti_3C_2T_x$ structure. The yellow, blue, dark yellow, red, and white balls represent Cu, Ti, C, O, and H, respectively. Reprinted with permission from[36].

heterogeneous catalysts, SACs optimize atom utilization and possess homogeneous active sites with adjustable electronic environments, resulting in exceptionally high catalytic activity and selectivity. Additionally, SAC exhibits enhanced stability and exceptional recyclability.[33,61,150,151] The utilization of single atoms in CO_2 conversion represents a groundbreaking approach that holds immense potential for addressing environmental challenges and advancing sustainable chemistry.[141,152] Single atoms, precisely isolated on suitable catalyst materials, offer unique electronic and structural properties that can significantly impact CO_2 conversion reactions.[153] This innovation has far-reaching applications and effects across various aspects of CO_2 conversion.[153] The advantages of SACs for CO_2 conversion include highly active catalytic centers that enhance CO_2 activation and facilitate specific chemical transformations. These catalysts can significantly accelerate reaction rates and improve overall conversion efficiency.[154–156]

Cu-based SAC catalysts

Single site decorated copper catalysts represent a cutting-edge approach in the realm of CO_2 conversion.[157] These catalysts involve the precise placement of individual catalytic centers,

often Cu atoms, onto a supporting material.[158,159] The primary aim of this technology is to efficiently accelerate the conversion of CO_2 molecules into valuable chemical products through catalytic reactions.[159,160] The uniqueness of single site decorated copper catalysts lies in the isolated copper atoms, strategically dispersed on the supporting material.[161] These single atoms possess distinct electronic and geometric properties that enable precise CO_2 activation and subsequent conversion reactions. The isolated nature of the copper atoms minimizes undesired side reactions, leading to enhanced selectivity and catalytic efficiency in CO_2 conversion processes. The supporting material is crucial in maintaining and improving the catalytic efficiency of copper catalysts that are modified with single-site decoration. This material often possesses a high porosity and surface area, ensuring maximum exposure of the active phase to CO_2 molecules. The interaction between the Cu atoms and the supporting material makes an optimal environment for catalytic reactions, resulting in improved overall efficiency.[162] For instance, Chen et al., Both theoretical and experimental evidence have emphasized the crucial function of Lewis acid in a Cu/Al_2O_3 SAC for the electrochemical conversion of CO_2. Through theoretical calculations, it was shown that Lewis's acid sites in metal oxides, such as aluminum oxide and Cr_2O_3, have the ability to adjust the electronic structure of copper atoms by maximizing intermediate absorption. This, in turn, leads to an improvement in CO_2 methanation[163]

Recently, 2D materials have garnered significant attention as a robust platform for supporting SA catalysts due to their large specific surface areas, numerous exposed active sites, and exceptional catalytic activities.[94–96] In particular, 2D $Ti_3C_2T_x$ MXene (where T_x represents surface functional groups) has been extensively studied for various catalytic reactions because of its excellent electronic conductivity, catalytically active basal planes, and unique graphene-like layered structures.[101,164,165] Moreover, its abundant ability to reduce, suitable surface imperfections, and hydrophilic surface properties render it a perfect contender for providing support and stability to individual atoms.[166,167] Bao et al. demonstrated through experimental and theoretical studies that atomically dispersed $Cu–O_3$ sites on 2D $Ti_3C_2T_x$ MXene facilitate C–C coupling of CO molecules, leading to the formation of the key *CO-CHO intermediate. Theoretical simulations further reveal that these $Cu–O_3$ sites lower the free energy barrier of the potential-determining step, thereby enhancing the catalytic activity and selectivity of copper single atoms for CO reduction. This synergistic effect accounts for the remarkable performance of Cu-based SACs in CO_2 conversion.[36]

Fe-based SAC catalysts

Fe-based SACs hold significant promise in addressing the global challenge of CO_2 emissions and advancing sustainable CO_2 utilization technologies.[44,168] These catalyst systems involve the integration of Fe atoms in unique configurations on supporting materials to assist the efficient transformation of CO_2 molecules into valuable chemical products through catalytic reactions. The support material used in Fe-based single-atom catalysts play a crucial role in stabilizing and enhancing their catalytic performance.[169,170] This material typically possesses a large porosity and surface area, ensuring maximum exposure of the active sites to CO_2 molecules.[171] The coordination between the iron atoms and the supporting material establishes a suitable environment for catalytic processes, leading to improved overall efficiency. In CO_2 conversion, the Fe-based SACs interact with CO_2 molecules to initiate various chemical reactions. These reactions often involve reduction pathways that lead to the formation of valuable compounds like CO, formic acid, or methane. The specific reaction mechanisms depend on the unique properties of the Fe atoms, the supporting material, and the reaction conditions.[169] Furthermore, beyond just maximizing the utilization efficiency of their single sites and ensuring well-defined active sites with high selectivity, the precise configurations and synergistic effects significantly boost both catalytic efficiency and selectivity.[169,172,173] This renders them indispensable to advancing effective carbon capture and conversion strategies. Ongoing research seeks to optimize the design of these catalysts, uncover novel reaction pathways, and explore their potential in various CO_2 conversion applications. Fe single atoms exhibit distinctive electronic and geometric properties that enable precise CO_2 activation and subsequent conversion reactions. The isolation of the iron atoms reduces undesired side reactions, leading to improved selectivity and catalytic efficiency in CO_2 conversion processes.[172,174] For instance, Takele et al., and Li et al., described a catalyst composed of atomically dispersed Fe coordinated with nitrogen-doped carbon, which exhibited heightened activity in CO_2 reduction to produce CO.[174,175]

Lately, scientists have been investigating the synergistic interplay between the active sites and the intricate networks of hierarchical carbon nanotubes (CNTs) and graphene nanoribbons (GNRs). This catalytic setup combines two distinct elements: iron-nitrogen (Fe-N) active sites and a complex network of CNTs and GNRs. By optimizing the design and composition of the catalyst, researchers seek to enhance its performance in CO_2 conversion processes. Ultimately, the development of Fe–N sites on hierarchically mesoporous CNTs and GNRs represents a significant advancement in the field of sustainable energy and chemical production. These catalysts offer a tailored approach to addressing CO_2 emissions by harnessing the unique properties of the active sites and the nanostructured support network.[176] The straightforward conversion of commercial CNTs into isolated $Fe–N_4$ sites anchored on carbon CNT and GNR networks Fe-N/CNT@GNR was described by Pan et al. Oxidation-induced partial removal of CNTs leads to the formation of GNR nanolayers connected to the remaining fibrous CNT frameworks. This process reticulates a hierarchically mesoporous complex, allowing for a large active surface area and efficient mass translocation. The Fe residues derived from CNT development seeds operate as sources of iron to create separate $Fe-N_4$ groups situated at the basal plane and margins of CNTs and GNRs. These moieties possess a strong inherent ability to activate CO_2 and inhibit hydrogen evolution, as depicted in Figure 3.[176]

Fe3+-based SAC catalysts

Another class of Fe-based SAC catalysts are atomically dispersed Fe^{3+} sites which play a crucial role in the catalytic conversion of CO_2 into valuable products.[177] These catalytic sites

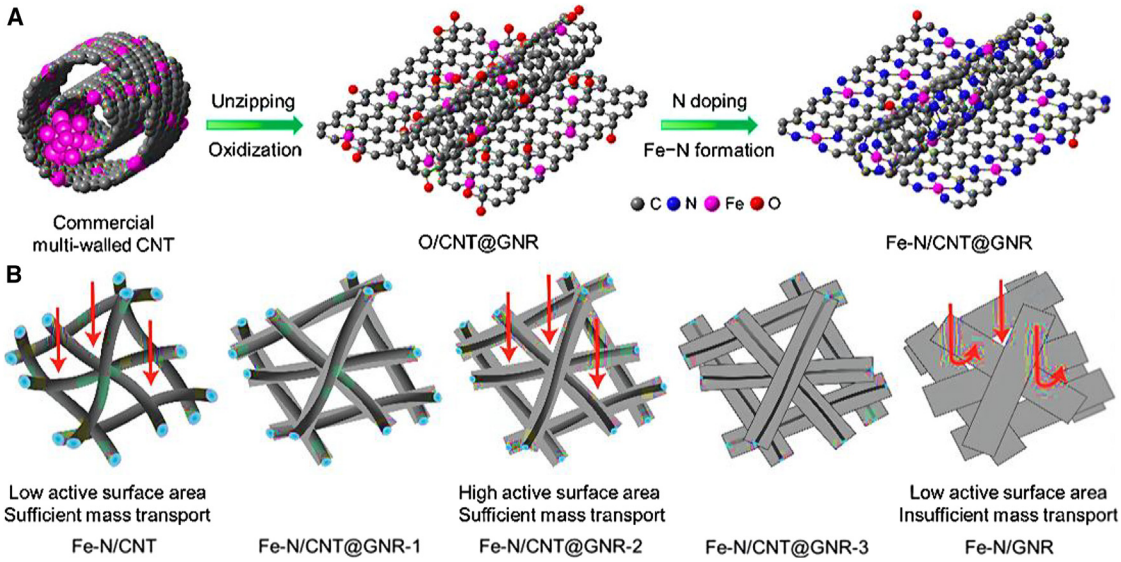

Figure 3. Synthesis method

(A) Schematic representation shows the conversion of multiwalled CNTs into Fe-N/CNT@GNR.

(B) Modifying the mass ratios of $KMnO_4$ and CNTs to induce structural changes from CNTs to CNT@GNR to GNR. Reprinted with permission from.[176]

involve the presence of individual Fe ions, in their trivalent Fe^{3+} state, dispersed on a suitable support material. These sites are designed to facilitate the activation and transformation of CO_2 molecules, contributing to efforts aimed at reducing CO_2 emissions and harnessing this GHG for sustainable chemical processes. The significance of atomically dispersed Fe^{3+} sites lie in their ability to mimic the active sites found in natural enzymes. These sites frequently feature metal ions with unique electronic properties that influence the activation of CO_2 molecules by adsorbing and stabilizing them, facilitating favorable chemical transformations to targeted valuable products, such as CO, formic acid, or other organic compounds, depending on the specific catalytic conditions.[177] Moreover, by preventing the clustering of metals, atomically dispersed Fe^{3+} sites maintain their catalytic effectiveness and ability to selectively promote desired reactions over extended periods of time. For instance, Jun et al. developed a catalyst featuring dispersed single-atom Fe sites, capable of producing carbon monoxide.[117,177] Through operando X-ray absorption spectroscopy, they identified the active sites as isolated Fe^{3+} ions coordinated with pyrrolic nitrogen (N) atoms on an N-doped carbon support. The Fe^{3+} ion remains in its +3-oxidation state during catalysis, likely due to electronic interactions with the conductive carbon matrix as illustrated in Figure 4. The improved catalytic performance of these Fe^{3+} sites is attributed to their enhanced CO_2 adsorption and reduced CO adsorption compared to traditional Fe^{2+} sites. Structural characterization confirmed the atomic dispersion of Fe sites within the carbon matrix. HAADF-STEM imaging (Figure 4A) revealed a well-defined porous structure, while energy dispersive X-ray spectroscopy (EDS) mappings (Figures 4B and 4C) demonstrated a uniform distribution of Fe and N within the carbon framework. Further insights from atomic-resolution aberration-corrected HAADF-STEM imaging (Figure 4D) revealed bright spots (~0.2 nm) corresponding to atomically dispersed Fe and Zn sites. The Fe K-edge XANES spectrum (Figure 4F) and Fe 2p3/2 XPS spectrum exhibited binding and edge energies consistent with Fe_2O_3 and Fe^{3+}-tetraphenylporphyrin-Cl, verifying the +3-oxidation state of Fe. This indicates that Fe ions underwent oxidation from +2 to +3 during pyrolysis, in agreement with previous reports on Fe-containing organic precursors. The Fe K-edge EXAFS spectrum (Figure 4H) further confirmed the atomic dispersion of Fe sites, with spectral fitting suggesting a planar $Fe–X_4$ (X = N or C) coordination structure. The average coordination numbers for Fe–N and Fe–C were 3.4 and 0.5, respectively, with no detectable Fe–Fe bonding.[177–179]

MOF-based SAC catalysts

MOF-SACs, or metal-organic framework-based single-atom catalysts, are novel types of catalysts that show great promise in converting CO_2 into useful chemicals. This catalytic system integrates the accuracy of SAC sites with the special qualities of MOFs. MOFs are porous materials with well-defined nanoporous architectures made of metal nodes joined by organic linkers.[180] The integration of single metal atoms into MOFs results in MOF-SACs, which offer several advantages for CO_2 conversion: The porous nature of MOFs offers a large surface area, enabling efficient CO_2 adsorption and access to the single-atom catalytic sites.[9,181]

Single metal atoms within the MOF structure act as isolated catalytic centers. Their precise arrangement allows for fine-tuning of reactivity and selectivity, mimicking the reactivity of natural enzymes.[182] The electronic properties of both the MOF framework and the single metal atom enhance CO_2 activation and conversion, even under mild reaction conditions. The MOF structure stabilizes and isolates the single metal atoms, preventing agglomeration and maintaining catalytic activity over time.[183] Depending on the specific reaction conditions and the properties of the catalyst, products like CO, formic acid, or more complex

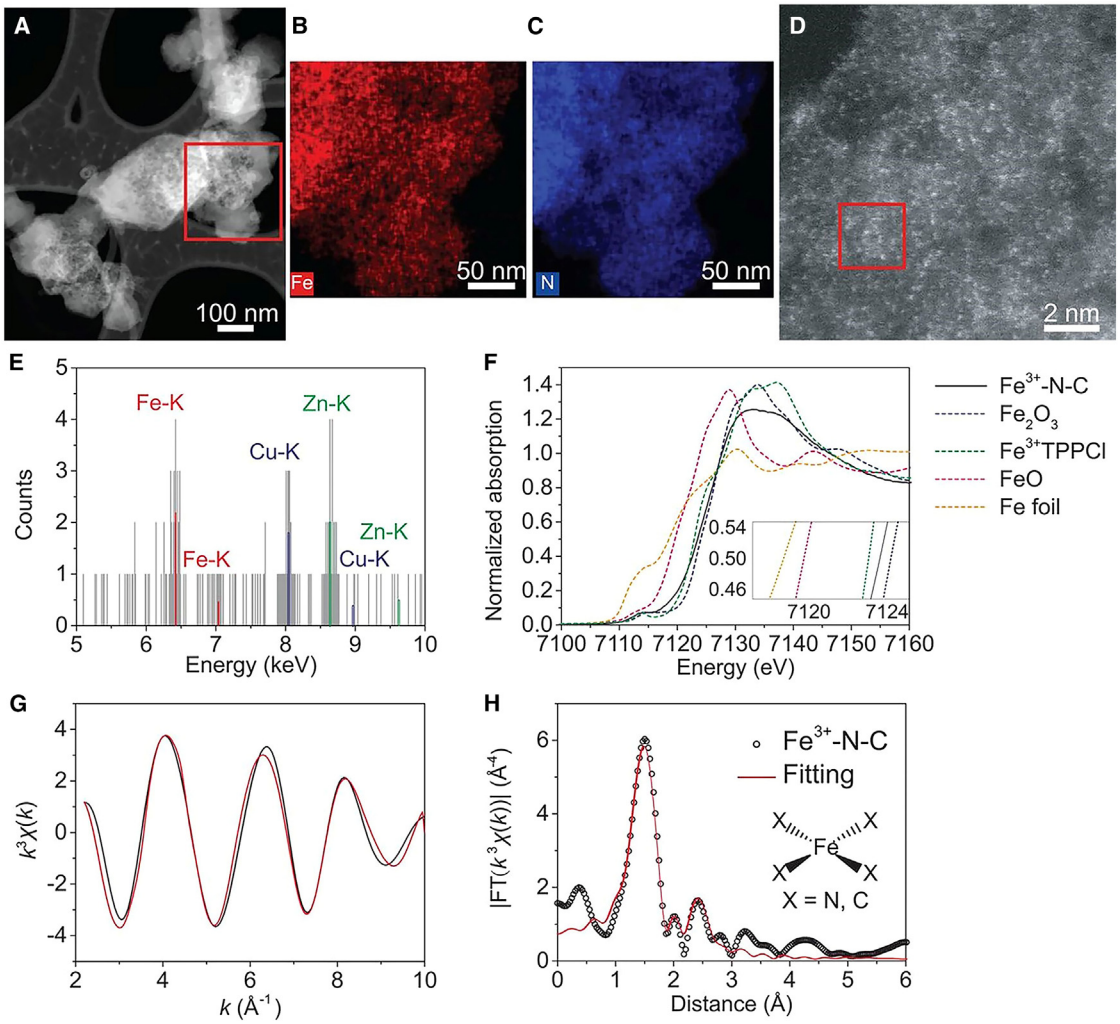

Figure 4. Physical characterization

(A) HAADF-STEM image and EDS mappings of (B) Iron and (C) Nitrogen of the region represented by the red square.

(D) Aberration-corrected HAADF-STEM image and (E) EDS spectrum of the red square region.

(F) Fe K-edge XANES spectra of Fe^{3+}–N–C (black), Fe_2O_3 (blue dashed), Fe^{3+}TPPCl (green dashed), FeO (pink dashed), and Fe foil (orange dashed). (Inset) The enlargement of the main edges.

(G) k-space and (H) R-space Fe K-edge EXAFS spectra. Shown are data (black) and fitting curves (red). Reprinted with permission from.[177]

hydrocarbons can be generated.[184] Ongoing research aims to optimize the synthesis and design of MOF-SACs as depicted in Figures 5A and 5B,[181] uncover their catalytic mechanisms, and develop scalable processes for industrial applications.[185] The development of MOF-based SACs presents an exciting avenue for advancing sustainable CO_2 utilization technologies, bridging the gap between porous materials and precise catalysis[181,186–188]

Ni-based SAC catalysts

Single-atom nickel (Ni) sites are advanced catalysts for efficient CO_2 conversion.[49] These catalysts feature isolated nickel atoms on a high-surface-area support material, working as active sites. The exceptional properties of these single atoms allow precise CO_2 adsorption and activation, minimizing side reactions and enhancing selectivity and efficiency. The support material stabilizes the nickel atoms and enhances catalytic activity by providing an optimal environment for CO_2 interaction. Single-atom Ni sites can convert CO_2 into valuable products like syngas, CO, formic acid, or methane, liable on the catalytic material and reaction parameters as in illustrated Figure 6.[31,132,189,190]

Another category of Ni-based SACs includes nickel dual-atom sites, which represent a state-of-the-art catalyst system designed for the efficient conversion of CO_2 into valuable chemical products. This advanced catalyst involves the strategic arrangement of two nickel atoms within a specific configuration on a supporting material. The primary goal of this technology is to improve the activation and transformation of CO_2 molecules through catalytic reactions.[191] The distinctive feature of nickel dual-atom sites lies in the precise arrangement of two nickel

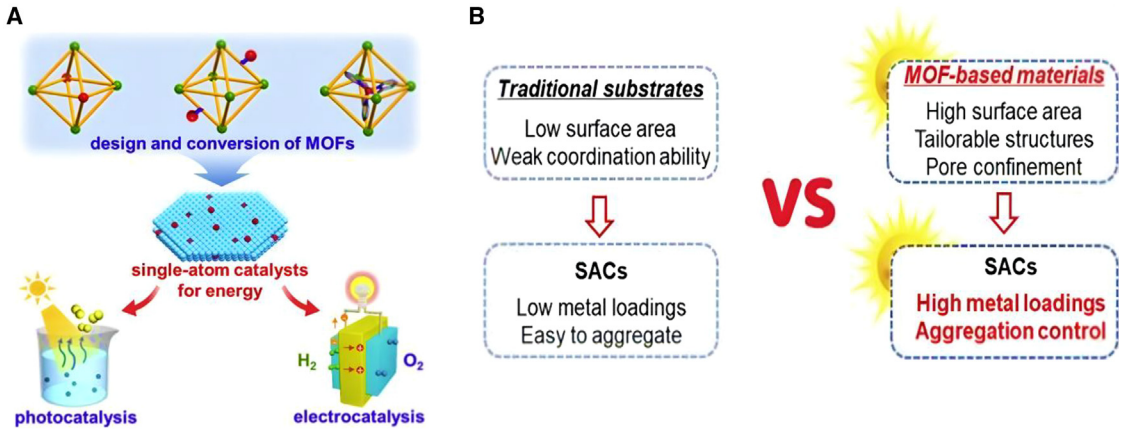

Figure 5. Synthesis method

(A) MOFs based single atom catalysis, (B) Potential advantages of MOFs over traditional substrates for the fabrication of SACs. Copyright with permission from.[188]

atoms in close proximity. This arrangement creates synergistic effects that significantly boost the catalytic selectivity and activity of the catalyst. The close interaction between the dual nickel atoms facilitates efficient CO_2 adsorption, activation, and subsequent transformation into desired products.[192] The supporting material used in this catalyst system provides a stable platform for anchoring and stabilizing the dual nickel atoms.[193] Typically, this material possesses high surface area and porosity, allowing for maximum exposure of the active sites to CO_2 molecules. The combination of the dual nickel atoms and the supporting material creates an optimal environment for catalytic reactions, minimizing unwanted side reactions and enhancing overall efficiency.[171,194] In CO_2 conversion, the nickel dual-atom sites engage with CO_2 molecules to initiate chemical transformations. These reactions often involve reduction pathways that lead to the formation of valuable compounds such as CO, formic acid, or methane.[195] The specific reaction mechanisms depend on the unique properties of the dual nickel atoms, the supporting material, and the reaction conditions. The development of nickel dual-atom sites holds great promise for advancing the field of

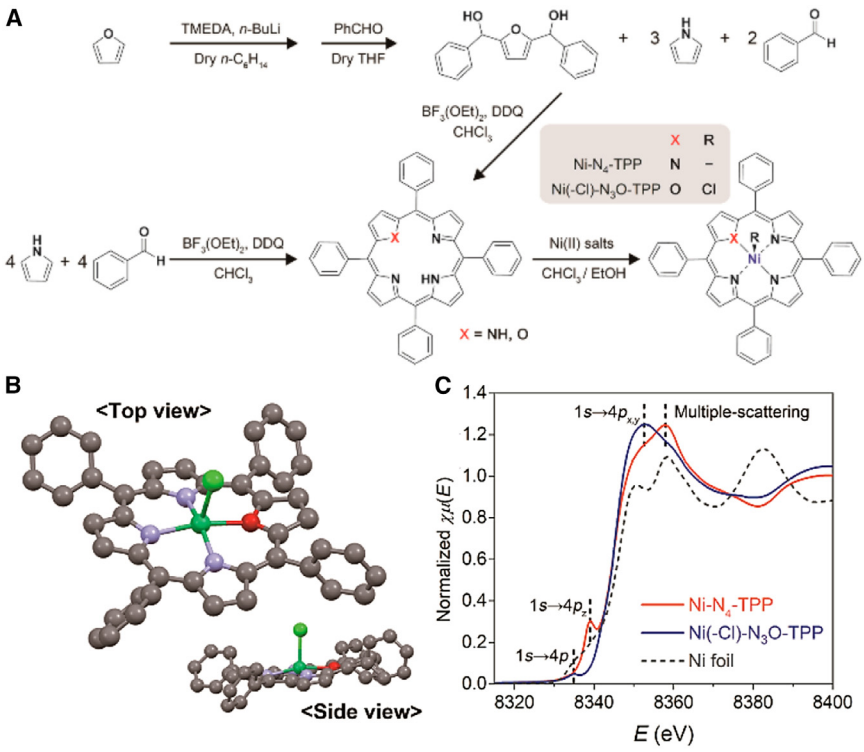

Figure 6. Synthesis and physical properties of prepared porphyrins

(A) Synthetic illustration for Ni–N_4–TPP & Ni(−Cl)–N_3O–TPP by modified Lindsey's methods.

(B) 3D molecular structure of Ni(−Cl)–N_3O–TPP established by SC-XRD.

(C) Ni K-edge XANES spectra of Ni–N_4–TPP, Ni(−Cl)–N_3O–TPP, and Ni foil. Reprinted with permission from.[132]

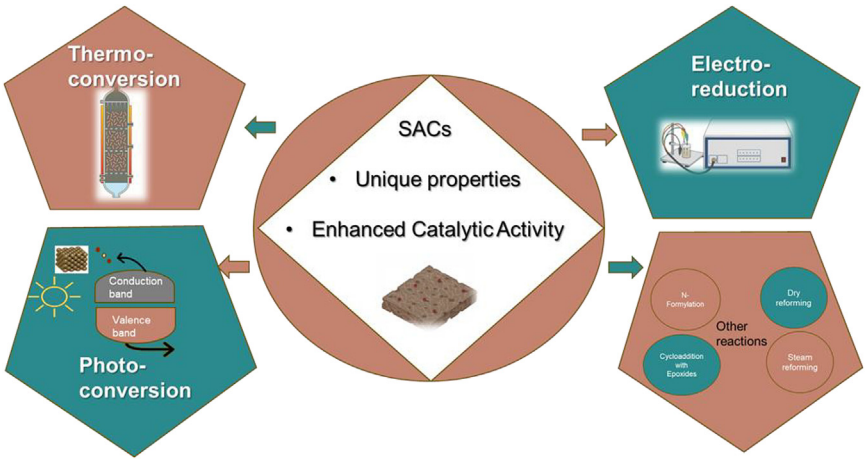

Figure 7. An overview of SACs application in chemical CO_2 conversion displayed in this review

CO utilization and mitigating CO_2 emissions.[196] The synergistic effects resulting from the close arrangement of two nickel atoms enhance the catalyst's efficiency, making it an essential component of sustainable CO_2 conversion technologies. Ongoing research focuses on optimizing the catalyst's design, uncovering new reaction pathways, and exploring its potential in various CO_2 conversion applications.[197] For example, Hao et al., established a catalyst with nickel dual-atom sites through *in situ* conversion of nanoparticles into dual atoms. Both experimental and theoretical investigations showed that during the catalytic process, the Ni dual-atom sites facilitate the adsorption of hydroxyl, creating electron-rich active centers. These centers present a modest reaction kinetic barriers for *COOH production and *CO desorption. This catalytic microenvironment results in faster kinetics compared to either bare dual-atom sites or adsorption of hydroxyl-regulated single-atom sites.[198]

A single Ni atom supported on a hybridized boron, carbon, and nitrogen (BCN) nanosheet represents a promising catalyst system in the realm of CO_2 conversion. This innovation involves the integration of a single nickel atom, a 2D nanosheet composed of BCN, and a specific hybridized structure.[199] The primary objective of this catalyst system is to facilitate the transformation of CO_2 into valuable chemical products through catalytic reactions. The single nickel atom serves as a highly active and selective catalytic site due to its unique catalytic properties and reactivity.[200] The atom is intentionally isolated and distributed on the surface of the BCN nanosheet, allowing for precise control over its interactions with reactant molecules.[201] This isolation enhances the atom's catalytic efficiency, enabling specific CO_2 activation and conversion processes. The hybridized BCN nanosheet offers several advantages in this context. Its composition combines boron, carbon, and nitrogen, which collectively create a versatile platform with tailored chemical properties.[199,202] This composition enhances the nanosheet's affinity for CO_2 adsorption and activation, providing an ideal environment for catalytic reactions.[202,203] The 2D structure also provides a large surface area, ensuring ample exposure of active sites and promoting the accessibility of reactants.[204,205] In CO_2 conversion, the catalyst's single nickel atom interacts with CO_2 molecules adsorbed onto the hybridized BCN nanosheet. These interactions lead to the activation of CO_2 and subsequent chemical transformations, such as reduction reactions that yield valuable products like CO, formic acid, or methane.[206,207] The specific reaction pathways and mechanisms can vary based on factors such as reaction conditions and the unique properties of the catalyst system. The incorporation of a single Ni atom supported on a hybridized BCN nanosheet holds significant potential for addressing the global challenge of CO_2 emissions.[208] By harnessing the atom's reactivity and the nanosheet's tailored properties, this catalyst system offers a pathway to convert CO_2 into useful chemicals, thereby contributing to sustainable and environmentally friendly CO_2 utilization strategies.[209]

Cd-based SAC catalysts

Cd-based SACs represent an emerging and innovative approach in the field of catalytic CO_2 conversion. These catalysts involve the incorporation of individual Cd atoms onto a suitable support material, aiming to efficiently facilitate the transformation of CO_2 molecules into valuable chemical products through catalytic reactions. The uniqueness of Cd-based SACs lies in the isolated Cd atoms that serve as highly active and selective catalytic centers.[210] These single atoms possess distinct electronic and geometric properties that enable precise CO_2 activation and conversion reactions. The isolation of the cadmium atoms minimizes unwanted side reactions, leading to improved selectivity and catalytic efficiency in CO_2 conversion processes.[211] The choice of support material is crucial in stabilizing and enhancing the catalytic activity of Cd-based SACs. This material typically possesses a high surface area and porosity, ensuring optimal exposure of the active sites to CO_2 molecules. The interaction between the Cd atoms and the support material creates an ideal environment for catalytic reactions, resulting in enhanced overall efficiency.[211] Although SACs show significant promise in heterogeneous catalysis, achieving high loading levels of these catalysts continues to be a major challenge. Ongoing research aims to optimize the design of these catalysts, explore novel reaction pathways, and assess their potential in various CO_2 conversion applications. For example, an extremely high loading of Cd-based SACs was achieved through a trapping, emitting strategy and gas migration. This approach resulted in a loading of 30.3 wt. %, with the emitting process enabling the adjustment of the loading amount from 30.3 to 1.4 wt. %. In the context of CO_2RR applications, the Cd-NC SACs with an 18.4 wt. % loading demonstrated optimal Faradaic efficiency (FE) performance.[212]

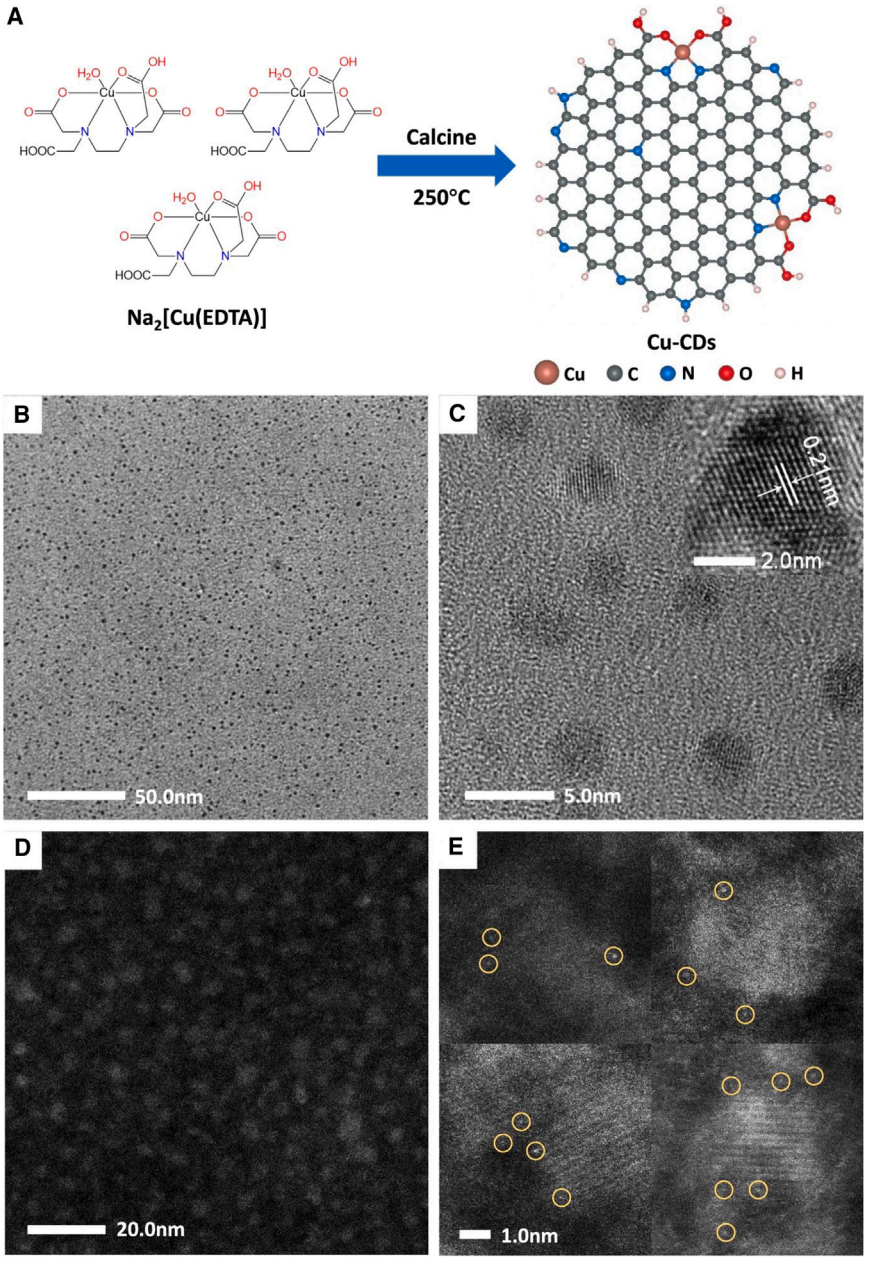

Figure 8. Physical characterization of the catalyst

(A) Diagram of the Cu-CD catalyst prepared using low-temperature calcining process.

(B) large field of view and (C) magnified view of TEM images (the inset is the crystal lattice).

(D) Relatively large-field of view and e typical view of HAADF-STEM images of distributed single Cu atoms in carbon dots. Yellow circles in (E) indicates typical single Cu atoms. Reprinted with permission from.[243]

SACs APPLICATIONS FOR CO_2 CONVERSION

The catalytic transformation of CO_2 into valuable fuels and chemicals presents a promising and economically viable alternative to fossil feedstocks, while also enabling large-scale CO_2 recycling.[22,180] Cost-effective and highly efficient catalysts are crucial for reducing the costs associated with CO_2 utilization as in Figure 7.[213,214] Conventional catalysts based on metal nanoparticles frequently lack efficiency in utilizing active metals, effective catalytic activity, and proper selectivity.[215,216] Consequently, there has been an increasing fascination with SACs, which provide optimal atom usage, a distinctive electrical configuration, and robust metal-support interactions. These characteristics make SACs a promising approach to enhance catalytic efficiency and long-term durability. Additionally, the well-defined structures of SACs facilitate in-depth studies of the mechanisms and active sites involved in CO_2 conversion.[217–219]

CO_2 electrochemical reduction

Advancements in science and technology have led to increased global energy consumption, posing significant environmental challenges in the 21st century.[220] The electrocatalytic conversion of CO_2 into carbon-based fuels has attracted attention due to its ability to operate in ambient conditions, adjust the reduction products via external parameters, store renewable electrons from solar, tidal, and wind energy, and have the potential to reduce global demand for fossil fuels.[221] This method offers a means to close the carbon cycle and utilize off-peak, intermittent renewable electricity.[222–225] However, CO_2 activation presents challenges due to its high thermodynamic stability, requiring substantial overpotentials and reducing energy efficiency. Electrocatalytic CO_2 reduction faces difficulties such as sluggish reaction kinetics, complex reaction pathways, and competing water reduction reactions in aqueous environments.[212,226–228] Despite these obstacles, CO_2RR can yield a variety of products, including carbon monoxide, formic acid, methane, methanol, ethanol, and ethylene.[229] A major obstacle to making CO_2RR viable for renewable energy storage is the similar thermodynamic potential of its products.

Catalysts play a crucial role in CO_2RR, with different metals exhibiting varying adsorption strengths for intermediate products, which influence product distribution.[24] Categorically, metal catalysts can be classified into four types based on their properties and behavior toward products of CO_2RR: formate-selective metals (e.g., Sn, Pb, and In), CO-selective metals (e.g., Ag, Zn, and Au), hydrocarbon-selective Cu, and hydrogen-selective metals (e.g., Pt, Ni, Fe, Co, Pd, and Ga).[230–234] Other extensively investigated catalysts encompass

2D transition metal carbide/nitride,[235,236] transition-metal complexes with organic ligands,[237] and copper-based multinary sulfides (CMSs).[238] Despite progress, existing catalysts are still inefficient for practical applications, with the high cost of noble metal catalysts adding to the challenge

Promising solutions are emerging through catalyst design, aiming to overcome these energy efficiency and selectivity barriers.[239] Catalysts are driving a paradigm shift in CO_2 conversion processes, enabling advancements in areas like electrochemical CO_2RR. Despite significant efforts, the primary obstacle to large-scale CO_2RR implementation remains the lack of highly reactive, selective, and cost-effective electrocatalysts. Therefore, designing and synthesizing high-performance CO_2RR electrocatalysts is crucial. SACs are promising candidates for catalyzing electrochemical CO_2RR due to their maximized atomic utilization. A partial-carbonization approach was proposed by Yanming Cai et al. to alter the electronic structures of single-atom catalysts. This approach led to the development of a carbon dots–based SAC containing CuN_2O_2 sites as shown in Figure 8. The SAC demonstrates a Faradaic efficiency of 78% and selectivity of 99% for CH_4, achieving a current density of 40 mA/cm^2. Their findings also highlighted that the high Faradaic efficiency and selectivity is attributed to the introduction of the oxygen ligand into the catalyst structure which lowered the endothermic energy of the intermediate.[227] Single-atom metal catalysts, such as Me–N–C catalysts with metals like Ni, Fe, Co, Zn, Mn, etc., are unique cases that deviate from the basic properties of metallic materials. These catalysts involve the atomic dispersion and bonding of metal ions to nonmetallic functional groups. They have attracted considerable interest for their ability to selectively produce CO from CO_2 reduction reactions.[43,240] Significantly, single-atom nickel catalysts have shown exceptional efficiency in converting CO_2 to CO, exceeding that of conventional metal-organic-carbon catalysts and even competing with catalysts using noble metals.[241] For instance, at −0.81 V RHE, a Ni–N–C catalyst synthesized by topochemical transformation attained about 100% CO selectivity. This high selectivity is attributed to the protective carbon layer, which effectively promotes topochemical transformation while maintaining the Ni–N_4 structure. Additionally, it prevents the aggregation of Ni atoms into particles, thereby providing a large number of active sites for catalytic reactions.[242] An analogous Ni–N–C catalyst in a gas diffusion electrode setup achieved a CO partial current density over 200 mA cm^{-2} and maintained a consistent CO Faradaic efficiency of around 85%, underscoring its considerable promise for future industrial uses.

Another intriguing SAC in CO_2 conversion is the Cd-based SACs, which interact with CO_2 molecules to initiate various chemical reactions. These reactions often involve reduction pathways leading to the formation of valuable compounds such as CO, formic acid, or methane. The specific reaction mechanisms depend on the unique properties of the Cd atoms, the supporting material, and the reaction conditions.[195,210] Their isolated and active nature enhances catalytic efficiency, making them a significant player in the development of effective carbon capture and conversion strategies[153]

CO_2 reforming of methane

In the dry reforming of methane (DRM), methane and CO_2 are converted into a mixture of CO and H_2 called syngas.[244] However, in this reaction, heterogeneous catalysts employ a broad size distribution of active metals, with only a small portion effectively serving as active sites.[245] To enhance metal utilization efficiency, SACs have been developed.[246] Tang et al.[247] introduced a SAC featuring Ru and Ni atoms on CeO_2 nanorods, showcasing exceptional low-temperature dry DRM activity. These single-atom sites worked synergistically to enhance H_2 production, as confirmed by density functional theory (DFT) calculations. Similarly, noble metal SACs like the Pt/CeO_2 catalyst developed by Shen et al.[248] exhibited improved metal utilization and demonstrated effective DRM reactivity at 350°C, with the Pt–CeO_2 interface playing a crucial role in CH_4 activation and CO_2 dissociation. Other notable SACs include a Rh-$La_2Ti_2O_7$ catalyst, which achieved over 25% conversion of CH_4 and CO_2 at 550°C. This remarkable catalytic performance is attributed to the coexistence of Rh^0 and $Rh^{\delta+}$ species in Rh–$La_2Ti_2O_7$, which enhances electron transport and increases the mobility of active oxygen species.[249] Also, a Ni/HAP SAC by Akri et al.,[190] which displayed significant DRM performance at 750°C with excellent resistance to coke formation. Despite these advantages, SACs face challenges in synthesis and stabilization and have not consistently outperformed traditional heterogeneous catalysts. Additionally, SACs often struggle with stability in fixed-bed reactors for DRM reactions.[190]

A synergistic effect of single-atom Ni_1 and Ru_1 sites on CeO_2 nanorods ($Ce_{0.95}Ni_{0.025}Ru_{0.025}O_2$) has been reported for DRM (CH_4 + CO_2).[247] This catalyst, featuring highly active SACs, achieves a turnover rate of 73.6 H_2 molecules per site per second at 560°C, with 98.5% selectivity to H_2. The Ni_1 and Ru_1 sites remain atomically dispersed and cationic even at temperatures up to 600°C, working together to reduce the activation barrier and enhance H_2 and CO production rates. This performance surpasses that of catalysts containing only Ni_1 or Ru_1 sites. Computational studies reveal that Ni_1 sites activate CH_4 to form CO, while Ru_1 sites dissociate CO_2 to CO, with H_2 forming through H atom coupling on Ru_1 sites. Small active sites at the atomic level often face synthesis challenges and show minimal improvement in catalytic reactivity. For the DRM reaction, nanocluster and nanoparticle level metal sites (larger than 1 nm) are more effective. Recent studies have shown that Ni sites sized 10–20 nm exhibit significant DRM activity and reduced coke formation above 700°C. Below 700°C, Ni sintering effects are less significant, but coke formation increases and catalyst activity decreases, especially for CH_4 activation.[250,251] Therefore, proper sizing of active sites is crucial for achieving high activity and coke resistance in low-temperature DRM reactions. Further research is needed to understand the size effects of active metals and guide the synthesis of cost-effective, highly active catalysts. Kim et al.[252] reported a Pt-NiCe@SiO_2 single-atom alloy (SAA) prepared by the reverse microemulsion method for DRM. Figure 9A shows the TEM image of the reduced $Pt_{0.25}$-NiCe@SiO_2 SAA catalyst. The yolks are well distributed within the SiO_2 shell, with an average cavity diameter of 106.5 nm and a wall thickness of 6.6 nm. Isolated Pt atoms, highlighted in yellow circles, confirm the SAA structure.

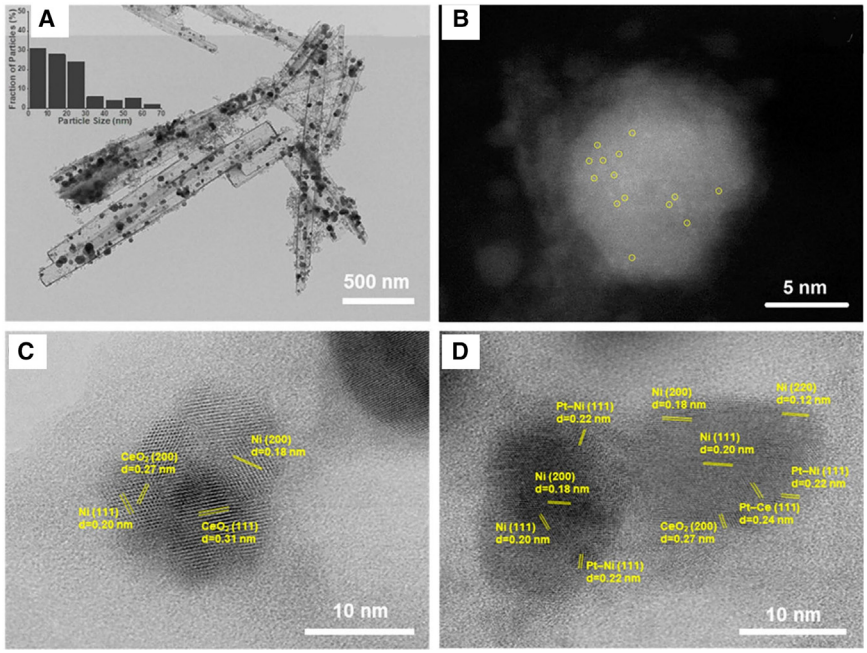

Figure 9. Physical characterization of the ctalayst

(A) TEM, (B) AC-HAADF-STEM, and (C, D) HRTEM images of the reduced nanotubular yolk–shell $Pt_{0.25}$-NiCe@SiO_2 SAA catalyst. Reprinted with permission from.[252]

HRTEM images shown in Figures 9C and 9D reveal lattice fringes of 0.20 nm (Ni (111)), 0.18 nm (Ni (200)), 0.31 nm (CeO_2 (111)), and 0.27 nm (CeO_2 (200)), indicating a Ni–CeO_2 interaction. Pt–Ni alloys are mostly at the yolk edges, suggesting Pt-terminated Pt–Ni catalysts form a stable core–shell structure under reducing conditions. The yolk-shell morphology and Pt–Ni SAA structures prevent carbon formation and enhance catalyst stability. This design facilitates CO desorption and reduces carbon deposition. Adding 0.25 wt % Pt ensures 120 h stability at 500°C during DRM by forming Pt–Ni SAA structures within the SiO_2 shell, enhancing interactions and suppressing carbon formation.

Rao et al.[253] introduced a concept for achieving highly durable DRM at low temperatures by integrating active sites with light irradiation. They successfully developed two types of active sites on CeO_2: Ni–O coordination (Ni_{SA}/CeO_2) and Ni–Ni coordination (Ni_{NP}/CeO_2). These sites enabled two distinct reaction paths to produce the key intermediate CH_3O^*, which helps prevent coke formation. However, under light irradiation, formate

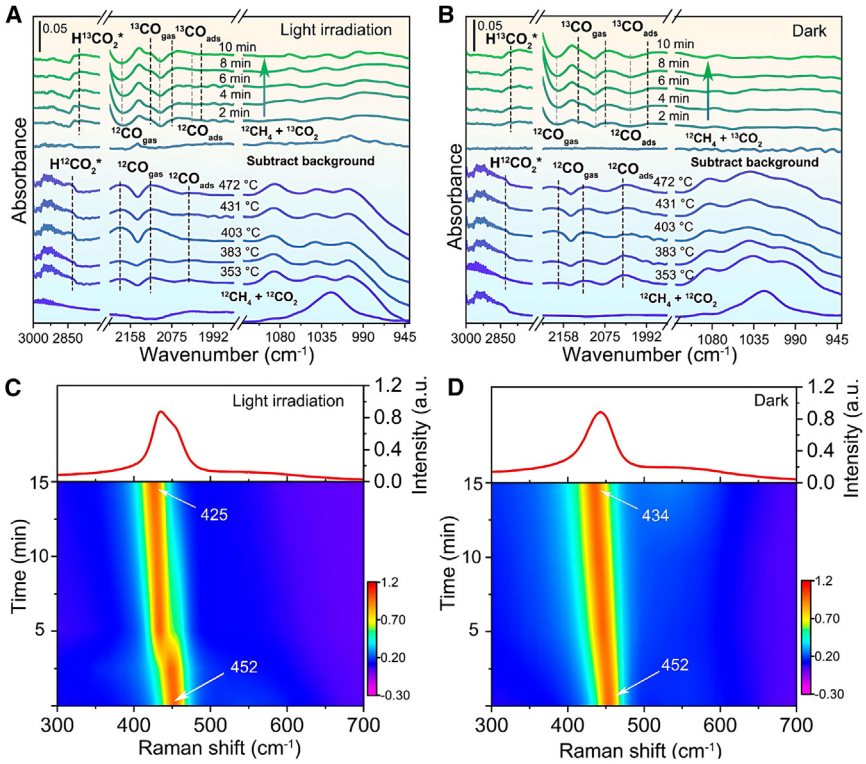

Figure 10. Operando DRIFT-SSITKA in panels (A, B) and panels (C, D) for *in situ* Raman spectra of DRM reaction over NiSA/CeO_2

Reprinted with permission from.[253]

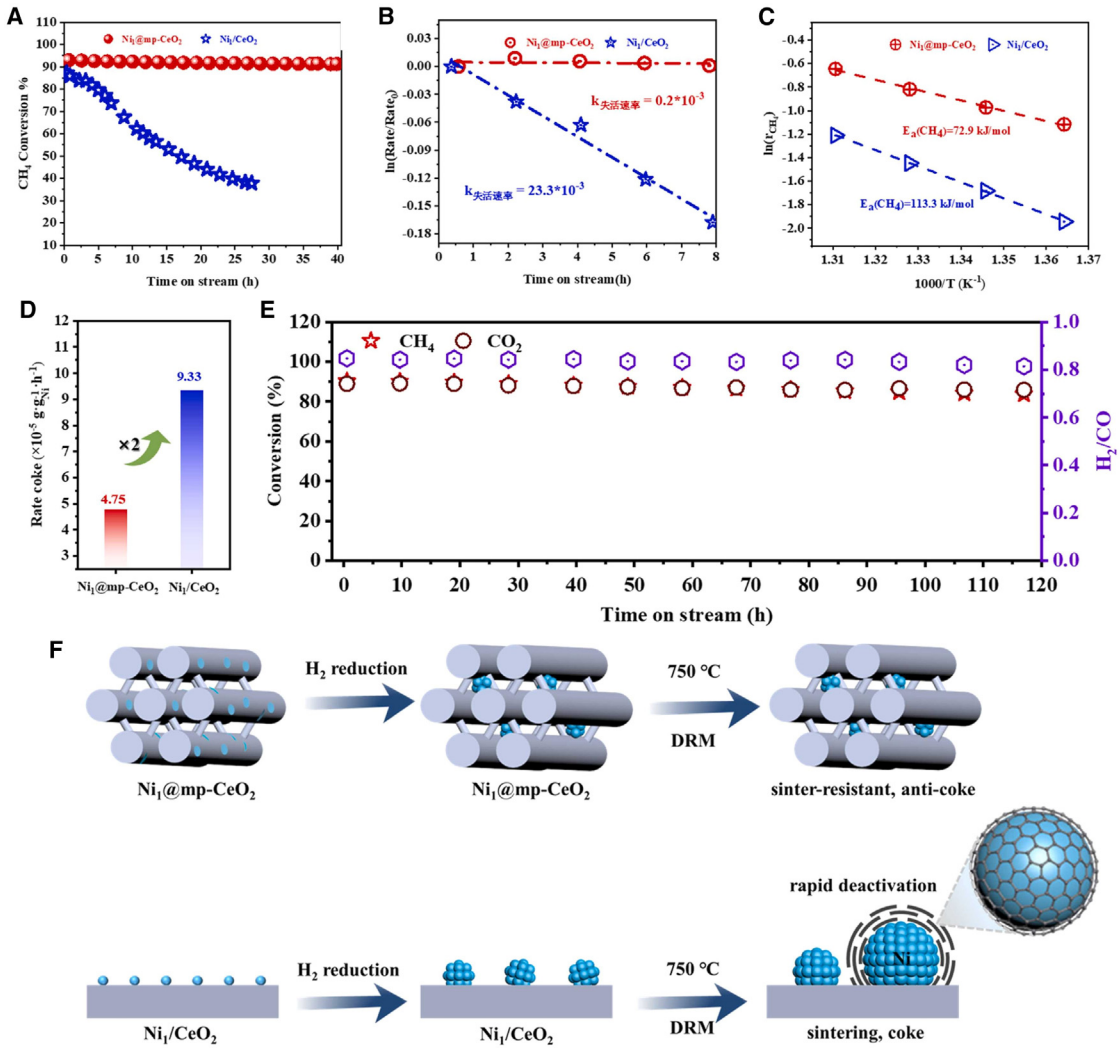

Figure 11. The catalytic performance of the reduced Ni_1@mp-CeO_2 and Ni1/CeO_2 at 750°C

(A) CH_4 conversion.

(B) Corresponding changes of CH_4 rates with respect to the initial rates (r/r0); (C) Arrhenius plot; (D) TGA data of the spent catalysts after reaction.

(E) Stability test of Ni_1@mp-CeO_2 catalyst in continuous DRM for 120 h.

(F and G) Schematic illustration of the structure evolution of the two Ni single atom catalysts supported on bulk CeO_2 and mesoporous CeO_2 during the DRM. Reprinted with permission from.[254]

(HCO_2*) increased, linearly adsorbed CO decreased, and gaseous CO bands became more prominent depicted in Figure 10A. A minimal change occurred in the dark, as shown in Figure 10B. Light enhances Ni_{SA}/CeO_2 activity by accelerating carbonate-to-CO conversion and CO desorption. Switching to $^{13}CO_2/^{12}CH_4$/Ar showed a distinct isotope effect, indicating light speeds up CH_3O* to CO conversion. *In situ* Raman with $C^{18}O_2$ revealed that light significantly accelerates Ce–O ionization and CH_3O* formation, with a shift of 27 cm^{-1} under light compared to 18 cm^{-1} in the dark as shown in Figures 10C and 10D. This study revealed that the CH_3* to CH_3O* path over Ni_{SA}/CeO_2 is crucial for anticoking. Additionally, light irradiation further enhanced this reaction path during DRM, as demonstrated by operando DRIFTS-SSITKA.

Li et al.[254] developed ordered mesoporous ceria (mp-CeO_2) to stabilize Ni single atoms in DRM. As shown in Figure 11, the Ni1@mp-CeO_2 catalyst exhibited superior DRM performance with a lower CO_2 deactivation rate (kd) of 0.1 × 10^{-3} h^{-1}, compared to 9.6 × 10^{-3} h^{-1} for Ni_1/CeO_2. Figure 11D illustrates that catalyst deactivation in DRM is caused by coke deposition and Ni sintering. Remarkably, the Ni_1@mp-CeO_2 catalyst-maintained stability for 120 h without significant deactivation (see Figure 11E), due to its strong metal-support interaction and confinement effect. This demonstrates that Ni single atoms supported on mesoporous CeO_2 offer better stability than those on bulk CeO_2. The Ni1@mp-CeO_2 catalyst, featuring many oxygen vacancies and basic sites, activates CO_2 and removes carbon deposits more effectively than the Ni_1/CeO_2

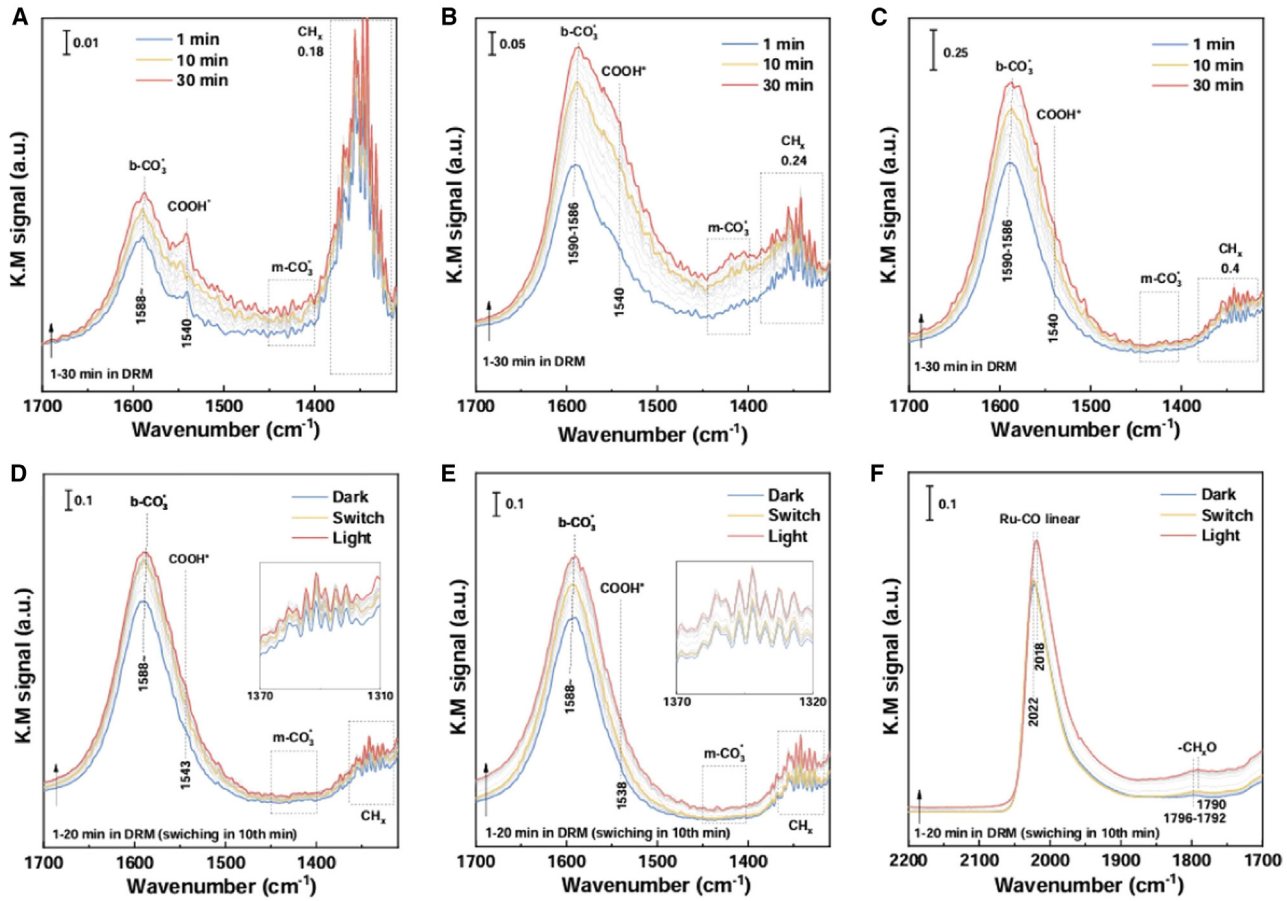

Figure 12. ***In situ*** **DRIFTs spectra and mechanism of DRM reaction**

(A–C) 1310–1700 cm^{-1} spectra over Ru_1/CeO_2-NP, Ru_1/CeO_2-NR and Ru_1/Mg-CeO_2-NR under dark conditions at 450°C; (D) 1310–1700 cm^{-1} spectra over Ru_1/Mg-CeO_2-NR under dark and >650 nm illumination at 450°C; (E) 1310–1700 cm^{-1} spectra over Ru_1/Mg-CeO_2-NR under dark and full spectrum illumination at 450°C and (F) 1700–2200 cm^{-1} spectra over Ru_1/Mg-CeO_2-NR under dark and full spectrum illumination at 450°C; micro-steps of DRM reaction. Reprinted with permission from.[255]

catalyst. The mesoporous structure also prevents Ni cluster sintering, improving stability. This study shows that Ni single atoms can grow into nanoclusters during DRM and using them as precursors helps suppress carbon deposition.

Zhang et al.[255] developed a Ru_1/Mg-CeO_2-NR SAC that exceeded the thermodynamic equilibrium limit for syngas production under photo-thermal catalysis (PTC) conditions, even at high flow rates. The catalyst achieved syngas production rates of 0.56 $molg^{-1}h^{-1}$ for H_2 and 0.85 $molg^{-1}h^{-1}$ for CO at 500°C. Operando experiments demonstrated the Ru-*O*-Ce electron transfer path and its impact on the rate-determining step (RDS) of the DRM. During these experiments, no significant correlation was observed between b-CO_3* or COOH* concentrations and catalyst performance (see Figure 12). However, CH_x concentration was strongly linked to performance in Ru_1/CeO_2-NR and Ru_1/Mg-CeO_2-NR, with the Ru-*O*-Mg structure in Ru_1/Mg-CeO_2-NR enhancing CH_x levels and performance, indicating CH_4 dissociation as the rate-determining step in DRM. UV light boosts CH_4 dissociation, leading to higher H* generation and H_2 production (see Figures 12D and 12E), which improves the H_2/CO ratio and overall performance under photo-thermal conditions. Mg doping and the nanorod structure increase CO_2 adsorption and COOH* conversion (see Figures 12A–12C), further enhancing CO production. Light irradiation also improves CO_2 adsorption (see Figures 12D and 12E), contributing to the superior photo-thermal catalytic performance of Ru_1/Mg-CeO_2-NR.

DRM typically requires high temperatures, leading to the exsolution and redistribution of active sites. However, characterizing these catalysts after cooling and sample preparation often results in the active atoms diffusing back into the bulk. Mekkering et al.[256] investigated the factors influencing the migration dynamics of atoms on the surface and subsurface of supported SACs during the DRM at 700°C–900°C. The catalysts' performance improved with reaction as rhodium atoms migrated from the subsurface to the surface. While the oxidation state of rhodium changed from Rh(III) to Rh(II) or Rh(0) during catalysis, atom migration was the primary factor affecting performance. Multiple processes have been hypothesized for SACs stimulating impact, including stronger interactions with support, the formation of low-coordinated active

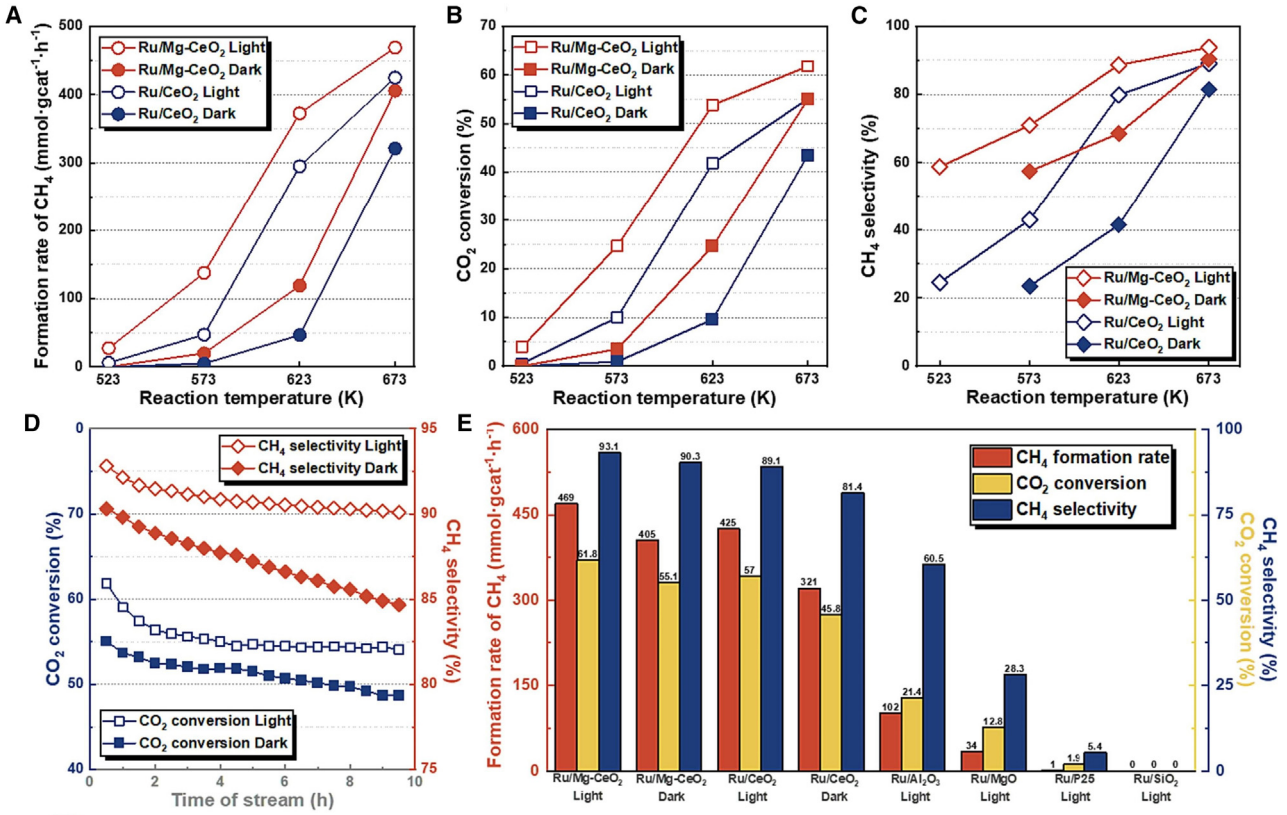

Figure 13. Catalyst performance

Initial (A) CH_4 formation rate, (B) CO_2 conversion and (C) CH_4 selectivity over Ru/CeO_2 and $Ru/Mg\text{-}CeO_2$ under thermal and photo-thermal conditions; (D) CO_2 conversion and CH_4 selectivity during 10 h evaluation test; (E) CH_4 formation rate, CO_2 conversion and CH_4 selectivity over different catalysts. Reprinted with permission from.[268]

sites, and active site-support.[257–259] However, these contributions frequently interact, confusing the understanding of their catalytic nature and impeding rational SAC evolution.[260] Zuo et al.[261] studied single-atom $Ni_1/Mg(100)$ and single-site $Ni_4/Mg(100)$ catalysts in DRM, combining DFT, kinetic Monte Carlo (KMC) simulations, and experiments studies. This approach clarified the reaction mechanisms on SACs, including pathway interplay, conversion, selectivity, carbon deposition/elimination sources, and the roles of Ni sites and MgO support.

CO_2 methanation

CO_2 methanation is an exothermic, thermodynamically favorable reaction. Supported nickel catalysts are effective but face kinetic limitations at lower temperatures. The catalyst's structure greatly influences its activity and selectivity, and understanding the mechanism remains challenging due to structural complexity.[262] Converting CO_2 to CH_4 offers a sustainable alternative to fossil fuels and is useful for syngas production. CH_4 is a crucial raw material for syngas and other chemical products, compatible with existing equipment, and a potential fossil fuel substitute. However, the conversion of CO_2 at lower temperatures is challenging but desirable.[263] Effective catalysts must be stable and active at high pressures and temperatures, often requiring precise tuning.[163] The support material prevents metal agglomeration and maintains activity, while its properties (size, surface area, porosity, acidity, and basicity) impact catalytic performance and selectivity. Supported metal catalysts offer a cost-effective alternative to expensive Ru, Pt, and Pd-based catalysts. By doping 4–6 wt % of precious metal onto a cheaper support, SACs enhance catalytic performance and reduce costs.[264] Atomically dispersed metals provide active sites and maximize efficiency.[265] Similarly, Shi et al.[266] developed an atomic-scale photocatalyst, Pt@Def-CN, for CO_2 methanation with H_2O by embedding single Pt atoms into defect sites of carbon nitride (CN) and adding ^-OH groups. This catalyst achieved high CO_2 reduction activity (6.3 $\mu mol\ g^{-1}\ h^{-1}$ CH_4) and 99% CH_4 selectivity in pure water. The ^-OH groups enhanced CO_2 adsorption, while Pt atoms activated CO_2 to form CH_4 and produced H and O_2 from H_2O. Pt sites reduced the rate-limiting step's energy barrier and improved CH_4 selectivity. Pt@Def-CN was made by first creating primitive CN (P-CN) from melamine, then hydrothermally treating it to form Def-CN with ^-OH groups. Pt was introduced at Def-CN edges and bound through low-temperature calcination. XRD and FTIR confirmed no structural changes to CN, while AC-HAADF-STEM and EDS mapping showed uniform dispersion of atomically isolated Pt.

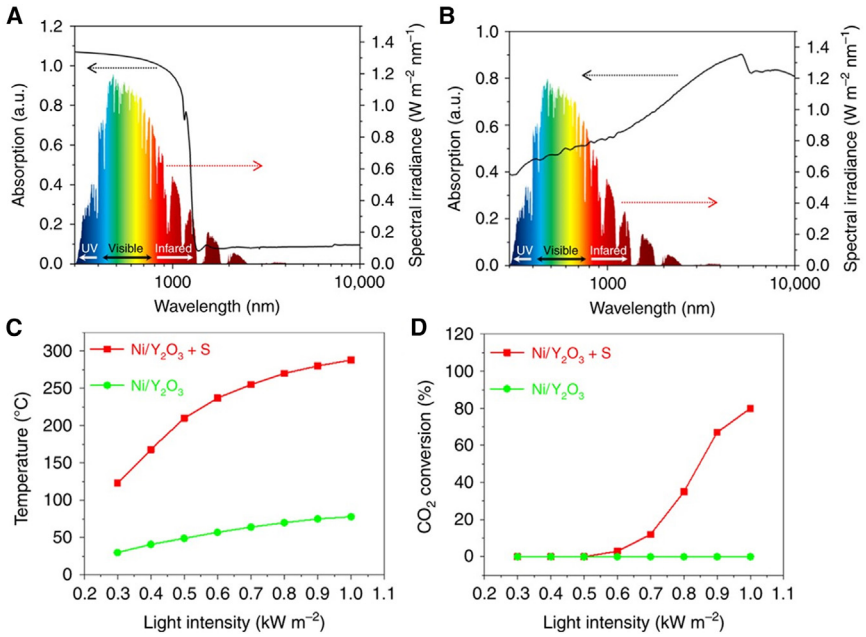

Figure 14. Full solar absorption (300 nm to 2 μm) and high IR absorption

(A) Normalized UV–Vis–IR absorption spectrum of the Ni/Y_2O_3 nanosheets.

(B) Normalized UV–Vis–IR absorption spectrum of the selective light absorber (AlN_x/Al foil).

(C and D) The light-driven temperature and CO_2 conversion rates of the Ni/Y_2O_3 nanosheets with (Ni/Y_2O_3 + S red) and without (Ni/Y_2O_3 green) the selective light absorber-assisted photothermal system, respectively, under different intensities of sunlight irradiation.

Reprinted with permission from.[269]

Vogt et al.[267] employed operando XAS and FT-IR to explore the size effect of SiO_2-supported Ni catalysts for CO_2 methanation. They found that sub-2 nm Ni particles had lower d-band energy, affecting catalytic activity. Smaller Ni particles favored CO production, while larger particles were more methane selective. Single-atom Ni catalysts produced only CO. The size effect in Ni/SiO_2 catalysts was attributed to changes in the electronic structure for particles 1–7 nm, whereas for larger particles (8–21 nm), the effect was due to increased active site abundance. Additionally, Ru/Mg-CeO_2 catalyst was developed based on single-atom and photo-thermal catalysis concepts.[268] It achieved a CH_4 formation rate of 469 mmol g^{-1} h^{-1} at 400°C under photo-thermal conditions, demonstrating good stability. Characterization revealed the advantages of single Ru atoms, the Ru-*O*-Ce structure, and alkaline metal doping. ISI-XPS experiments confirmed electron migration from Ce and Mg to Ru via Ru-*O*-Ce and Ru-*O*-Mg paths under photo-thermal catalysis. As shown in Figures 13A and 13B, the Ru/Mg-CeO_2 catalyst achieved higher CH_4 formation rates and CO_2 conversion compared to Ru/CeO_2, demonstrating that Mg doping enhances reaction performance. The Mg-doped catalyst also lowered the initial CO_2 methanation temperature and showed noticeable CO_2 conversion at 573 K. Additionally, Mg doping improved methane selectivity as shown in Figures 13C–13E, likely due to increased H_2 dissociation capacity from enhanced activation of H_2 at Ru sites, facilitated by electron migration from low-valence metals. Furthermore, Li et al.[269] developed a photothermal system using a selective light absorber to achieve temperatures up to 288°C under ineffective solar irradiation (1 kW m^{-2}), three times higher than traditional systems. They synthesized ultrathin amorphous Y_2O_3 nanosheets with single Ni atoms (SA Ni/Y_2O_3), which showed excellent CO_2 methanation performance. The system achieved 80% CO_2 conversion and a CH_4 production rate of 7.5 L m^{-2} h^{-1} under solar irradiation (0.52–0.7 kW m^{-2}), demonstrating its effectiveness for converting CO_2 to valuable chemicals using dispersed solar energy. The UV–Vis–IR spectrum Figure 14A shows full solar absorption (300 nm–2 μm) and high IR absorption (2–10 μm), leading to heat dissipation and limiting temperatures to 78°C under 1 kW m^{-2} (see Figure 14C). The selective light absorber absorbs 300–1300 nm (~100% of the solar spectrum) with minimal IR absorption (see Figure 14B. The radiative heat loss from the absorber is 0.21 kW m^{-2} at 200°C, much lower than that of Ni/Y_2O_3. The photothermal system with the selective light absorber on a quartz tube enhances temperatures. Ni/Y_2O_3 nanosheets reach 288°C under 1 kW m^{-2}, which is 3.7 times higher than direct irradiation (see Figure 14C). The system achieves 80% CO_2 methanation efficiency, outperforming Ni/Al_2O_3 systems that only reach 81°C, as illustrated in Figure 14D.[269]

CO_2 formylation with aniline

Converting CO_2 into valuable products using efficient and reusable catalysts is crucial for mitigating carbon emissions.[270,271] Developing a catalyst that effectively promotes the N-formylation reaction under mild conditions is highly desirable. N-Formamides serve as crucial intermediates in the production of numerous pharmaceuticals and function as protective agents for amines. Additionally, they catalyze various chemical reactions.[272] SAC offer exceptional potential due to their optimal atom utilization and remarkable catalytic activity.[38,273] Various fabrication methods for utilizing SACs in N-formylation have been documented. including atomic layer deposition,[274] wet chemistry[52] and MOF derivative.[275] However, these methods often demand harsh conditions, such as high temperature, high pressure, acids, or complex reaction procedures. facilitating large-scale industrial applications, developing straightforward and efficient methods for producing SACs is crucial. Qiang Cao et al. developed a highly efficient zinc-based SAC for converting CO_2 into valuable N-formanilide under mild conditions. their catalyst exhibits exceptional activity and recyclability, offering a promising approach to CO_2 utilization and environmental sustainability.[276] The effective synthesis of a single-atom zinc catalyst based on a porous organic polymer was achieved by Yingjun Li et al. Under moderate reaction conditions, this catalyst demonstrated outstanding efficiency in transforming CO_2 into

valuable N-formanilide. Their finding highlighted that the exceptional catalyst activity and selectivity can be ascribed to the uniform distribution of zinc single atoms and the permeable structure of the support material. Crucially, this catalyst can be reused several times without a substantial decrease in activity, showcasing its promise for practical usage in CO_2 valorization systems[277]

CO_2 hydrogenation

The production of higher alcohols has gained significant attention due to their versatile applications as solvents and fuel additives in various industries.[278–281] Given the natural process of photosynthesis, where fossil fuels originated from carbon and hydrogen, artificially combining CO_2 and H_2 to recreate hydrocarbon fuels presents a promising approach to sustainability.[282,283] Converting CO_2 into valuable products through direct hydrogenation presents challenges due to CO_2's stability. However, significant advancements have been made in producing single-carbon compounds like formic acid, carbon monoxide, methane, and methanol using this method.[283,284] Both direct hydrogen reduction and chemical reduction in water have been explored to achieve these products.[285–290] The conversion of CO_2 into methane through thermocatalysis is a relatively straightforward process that can be achieved under mild conditions. This method has demonstrated high efficiency in converting CO_2 to methane. Additionally, producing carbon monoxide from CO_2 can be accomplished through the reverse water-gas shift reaction. Furthermore, the industrial-scale production of methanol from CO_2 has already been realized in Iceland, utilizing geothermal energy and catalytic processes.[291–293]

Kothandaraman et al.[292] developed a highly efficient homogeneous catalytic system for converting CO_2 into CH_3OH. This system utilizes pentaethylenehexamine and Ru-Macho-BH (1) as catalysts, operating at temperatures between 125°C and 165°C in an ethereal solvent. It achieves an initial turnover frequency of 70 h^{-1} at 145°C and maintains robustness over five cycles with a turnover number exceeding 2000. The system can process CO_2 from various sources, including air with its low concentration of 400 ppm CO_2. Remarkably, this represents the first successful demonstration of direct methanol production from air-captured CO_2, achieving a yield of 79%. Also, Sugiyama et al. introduced[294,295] a PdMo intermetallic catalyst that enables low-temperature CO_2 hydrogenation. Synthesized via the simple ammonolysis of an oxide precursor, this catalyst shows excellent stability in both air and reaction environments, significantly boosting catalytic activity for converting CO_2 to methanol and CO compared to a Pd catalyst. A turnover frequency of 0.15 h^{-1} for methanol synthesis was achieved at 0.9 MPa and 25°C, matching or surpassing state-of-the-art heterogeneous catalysts operating under higher pressures (4–5 MPa). Table 1 summarizes key advancements in SACs for CO_2 utilization, emphasizing improvements in catalytic performance, selectivity, and stability. It provides an overview of various SACs, their synthesis methods, active sites, and their effectiveness in electrocatalytic or thermocatalytic CO_2 reduction. Notable trends include the development of SACs with well-defined metal-N-C structures, which enhance CO_2 adsorption and activation. Recent research focuses on tuning electronic structures through coordination engineering to improve selectivity toward C_{2+}products.

COMPUTATIONAL WORKS

In the quest for efficient CO_2 conversion using SACs, DFT methods have emerged as indispensable tools for deciphering the underlying molecular mechanisms and catalytic pathways. DFT offers a computational framework to explore the intricate electronic and structural changes during CO_2 conversion, providing insights into reaction energetics, intermediate species, and reaction kinetics. From traditional functionals like local density approximation (LDA) and generalized gradient approximation (GGA) to more advanced hybrid and dispersion-corrected functionals, DFT methods offer a spectrum of accuracy and computational efficiency.[240,322] Additionally, approaches such as van der Waals-corrected DFT and advanced spin-orbit coupling calculations allow researchers to capture subtle interactions and electronic properties essential in CO_2 conversion. This introduction highlights the spectrum of DFT methods employed in elucidating CO_2 conversion mechanisms by SACs, showcasing their pivotal role in guiding experimental design, optimizing catalysts, and advancing the field toward sustainable and selective carbon transformation technologies.[323,324] For example, Jiao et al., used DFT calculations to illustrate the effect of adsorption configuration on the activation energy, which has an impact on the selectivity and stability under the applied potential. Their results indicated that the Cu_{10}–Cu_{1x+} site in an atom-pair catalyst (APC) promotes CO_2 activation via a 'biatomic activating bimolecular' mechanism. This offers an ideal model of interface design at the atomic level, because the afforded APC features two different atomic centers to absorb two different molecules. However, the concept of APC is an effective and competent supplement to SAC and will afford numerous new opportunities for atomic-level dispersed catalysts to be applied in more complex catalytic reactions.[325] An adsorption design reduces the activation energy, leading to enhanced activity, selectivity, as well as stability at comparatively low potentials. In a different report,[158] DFT computations demonstrated that N/O coordinated Cu decoration sites enhance CH_4 selectivity by stabilizing the adsorption of *CHO and *O key intermediates as shown in Figure 15. This strategy achieved a CH_4 FE of 71% at a current density of 100 mA cm^{-2} and a CH_4 energy efficiency (EE) of 21%. The produced CH_4 has 50% the energy intensity of that produced in the best prior electrolyzers.[158]

In addition to experimental methods, several computational tools are employed to study the DRM mechanism and evaluate the impact of experimental variables on the response.[326,327] DFT modeling and microkinetic modeling are used to investigate the fundamental chemical processes in the breakdown of methane and CO_2 on different metal surfaces.[327–329] Lea Gašparič et al.,[326] utilized the fundamental chemical processes of dry reforming of methane (DRM) on Ni(111) and NiO(100) using DFT simulations as models for metallic and oxidized nickel catalysts. The results indicate that although DRM may be achieved on metallic Ni at elevated temperatures, a notable challenge arises from the occurrence of coke production, which coincides with the same activation barriers for C* creation and DRM

Table 1. Recent advances in SACs for CO_2 utilization

Catalyst	Synthesis methods	Applications	Catalytic efficiency	Key product	Key findings	Reference
Pd-Cu Pt-Cu SACs	Galvanic displacement	CO_2RR	60% C_{2+} products	C_2H_4 and CH_4	Atomically dispersed platinum group metal (PGM) species on copper surfaces suppress HER and promote CO_2 reduction by facilitating CO* hydrogenation and CO-CHO* coupling via Pd-Cu dual-site pathways, enabling selective CH_4 and C_2H_4 production.	Chhetri et al.[192]
Cu-N/O single sites	Spray the decoration on commercial catalyst	CO_2RR	71% C_1	CH_4	A coordination strategy using EDTA stabilizes Cu ions, forming Cu-N/O single sites and regulating Cu cluster size, achieving 71% CH_4 selectivity (Faradaic efficiency) under acidic CO_2 reduction with minimal CO_2 loss (<3%). The process halves energy intensity compared to conventional methods, enhancing efficiency.	Fan et al.,[158]
p-block Al SAC	pyrolysis	CO_2RR	98.76% C_1	CO, HCOOH	The Al–NC single-atom catalyst with Al–N_4 sites overcomes transition metal limitations in CO_2RR by balancing *COOH formation and *CO desorption, achieving 98.76% CO Faradaic efficiency and a turnover frequency of 3.60 s^{-1}. It delivers high CO partial currents (309 mA cm^{-2} in a flow cell, 605 mA in an MEA) with exceptional efficiency.	Ma et al.,[296]
Ni single atoms	Pyrolysis	CO_2RR	100% C_1	CO	A scalable Ni single-atom catalyst on carbon black achieves >100 mA cm^{-2} current density with nearly 100% CO selectivity and minimal hydrogen evolution in a gas-phase reactor. Scaled to a 10 × 10 cm^2 cell, it delivers 8 A current and 3.34 L h^{-1} CO production, though limited Ni site density affects the 60% CO selectivity.	Zheng et al.,[297]

(*Continued on next page*)

Table 1. *Continued*

Catalyst	Synthesis methods	Applications	Catalytic efficiency	Key product	Key findings	Reference
BiCu-SAA	*in situ* electrochemical reconstruction	CO_2RR	73.4% C_{2+}	C_2H_4	The BiCu-SAA electrocatalyst enhances CO_2 reduction to C_{2+} products with a 73.4% Faradaic efficiency by promoting C–C coupling, outperforming conventional Cu-based catalysts. It maintains high structural stability and performance at 400 mA cm^{-2} in a flow cell system.	Cao et al.,[298]
Cu–Ag	spatially dispersed	CO_2RR	69.9% C_{2+}	C_2H_5OH	A coordination-controlled Ag–Cu alloy catalyst with spatially dispersed Cu clusters enhances *CO binding through Cu–Cu and Cu–Ag interactions, shifting CO_2 reduction selectivity from ethylene (69.6% FE) to ethanol (40.4% FE).	Kim et al.,[299]
Cu surfaces and Cu(i) species	Electrodeposition	CO_2RR	76% C_{2+}	C_2H_5OH	Single-atom Cu (Cu_1) catalysts lack intrinsic activity for C_{2+} product generation due to insufficient active sites for *CO hydrogenation and CO–CO coupling, but small Cu clusters formed via aggregation enable efficient CO–CO coupling. The C_{2+} performance of these Cu clusters is substrate-dependent, offering guidance for catalyst optimization.	Zhang et al.,[300]
F-doped Cu SACs	one-step solid-state pyrolysis	CO_2RR	7.03 mmol h^{-1} mgper Cu^{-1} C_{2+}	C_2H_4	A fluorine doping strategy enables the reconstruction of isolated Cu atoms into Cu nanocrystals with stable Cu^+ species, achieving high C_{2+} product generation with exceptional Cu utilization. *In situ* Raman spectroscopy and DFT confirm fluorine's role in enhancing structural evolution and catalytic performance.	Jia et al.,[301]

(*Continued on next page*)

Table 1. *Continued*

Catalyst	Synthesis methods	Applications	Catalytic efficiency	Key product	Key findings	Reference
Sn single atom	two-step stabilization strategy	CO_2RR	92.4% C_1	HCOOH	High-density Sn SACs achieve efficient acidic CO_2 reduction to formic acid (Faradaic efficiency: 90.8%, current density: −178.5 mA cm^{-2}) by creating a favorable alkaline microenvironment and optimizing the pH-dependent *CO_2- intermediate adsorption strength, suppressing HER competition.	Sun et al.,[302]
Single-atom Cu/ZrO_2	impregnation	Hydrogenation	100% C_1	CH_3OH	A single-atom Cu–Zr catalyst with Cu_1–O_3 units enables selective CO_2 hydrogenation to methanol at 180°C, while Cu clusters or nanoparticles favor CO by-product formation. The migration of Cu_1–O_3 units to the surface enhances catalytic activity, offering insights for designing efficient copper-based catalysts.	Zhao et al.,[303]
Single-atom Rh embedded on Ti-doped CeO_2	impregnating	Hydrogenation	99.1% C_{2+}	C_2H_5OH	The Rh_1/CeTiOx single-atom catalyst exhibits ultra-high ethanol selectivity (≈99.1%) and turnover frequency (493.1 h^{-1}), with excellent stability. Synergistic Ti-doping and monoatomic Rh enhance CO_2 activation and C−C coupling, contributing to outstanding catalytic performance.	Zheng et al.,[304]
Ir_1–In_2O_3 single-atom	precipitation method.	Hydrogenation	99%	C_2H_5OH	The Ir_1−In_2O_3 single-atom catalyst achieves >99% ethanol selectivity and high turnover frequency (481 h^{-1}) by utilizing a bifunctional design with isolated Ir atoms and adjacent oxygen vacancies. Synergistic activation of CO_2 and C−C bond formation via a Lewis acid-base pair enhances its catalytic efficiency.	Ye et al.,[305]

(*Continued on next page*)

Table 1. *Continued*

Catalyst	Synthesis methods	Applications	Catalytic efficiency	Key product	Key findings	Reference
Rh_1/ZrO_2 SAC	impregnating	Hydrogenation	9.4 molCO gRh^{-1} h^{-1}	CO	The Rh_1/ZrO_2 single-atom catalyst enables efficient switching from CH_4 to CO with >99% CO selectivity in CO_2 hydrogenation, achieving high activity (9.4 mol $CO \cdot gRh^{-1} \cdot h^{-1}$) and stability by tuning both Rh_1 atoms and alkali ions. The alkali ions alter the reaction pathway and improve catalyst stability by reinforcing Rh_1-support interactions.	Li et al.,[306]
Pd-promoted $ZnZrO_x$	coprecipitation method	Hydrogenation	85%	CH_3OH	The Pd-ZnZrOx catalyst exhibits enhanced methanol production and stability by atomically dispersing Pd in the ZnZrOx matrix, which increases oxygen vacancies and facilitates H_2 dissociation. This promotes CO_2 hydrogenation on adjacent Zn sites, resulting in high activity and robustness.	Lee et al.,[307]
FeK/Co–NC SAC	atomically dispersing	Hydrogenation	42.2% C_{5+}	C_{5+}	The FeK/Co–NC catalyst shows efficient CO_2 conversion to long-chain hydrocarbons with up to 42.4% C_{5+} selectivity, stable performance over 100 h, and reduced methane formation, thanks to Fe–Co alloy formation on the Co–NC support.	Hwang et al.,[308]

(*Continued on next page*)

Table 1. *Continued*

Catalyst	Synthesis methods	Applications	Catalytic efficiency	Key product	Key findings	Reference
Na–$CoFe_2O_4$/CNT SAC	Pyrolysis	Hydrogenation	39% C_1	CH_4	The Na–$CoFe_2O_4$/CNT catalyst exhibits high CO_2 conversion (~34%) and selectivity toward light olefins (~39%) by forming a stable bimetallic alloy carbide (Fe1–xCox) 5C2, outperforming single-metal and mixed-metal catalysts.	Kim et al.,[309]
Rh_1/TiO_2 SAC	depositing functionalized	Hydrogenation	80%	CO	The Rh1/TiO_2 catalyst, modified with amine-functionalized phosphonic acid monolayers, shows an ~8× increase in CO_2 reduction turnover frequency at 150°C and improved on-stream stability. The modification enhances CO selectivity and CO_2 hydrogenation activity by positioning amine groups near Rh1 sites.	Jenkins et al.,[310]
Rh_1/CeO_2	ispersing Rh atoms onto CeO_2	Dry reforming	>80%	H_2/CO	The Rh1/CeO_2 single-atom catalyst undergoes product-driven restructuring, transitioning from single Rh atoms to nanoparticles and clusters, which affects its catalytic performance in methane reforming by CO_2, highlighting the dynamic nature of single-atom catalysts under reaction conditions.	Tang et al.,[311]

(*Continued on next page*)

Table 1. *Continued*

Catalyst	Synthesis methods	Applications	Catalytic efficiency	Key product	Key findings	Reference
Yolk–Shell Pt-NiCe@SiO_2	Core-shell synthesis	Dry reforming	45%	H_2/CO	The Pt-NiCe@SiO_2 single-atom-alloy (SAA) catalyst exhibits exceptional carbon resistance and stability in dry reforming of methane (DRM) due to its yolk–shell structure and Pt–Ni SAA, which prevent carbon formation and enhance reducibility at 500°C for 120 h.	Kim et al.,[252]
RuNi SAC	Thermal reduction	Dry reforming	0.44 mmol $g^{-1} \cdot min^{-1}$	H_2/CO	The RuNi-SAA catalyst supported on Al_2O_3 enhances CO and H_2 production in solar-driven dry reforming of methane (DRM), achieving high rates under photothermal conditions.	Yin et al.,[312]
Ni-Ce SAC	Pyrolysis	Dry reforming	60,000 mL g_{cat}^{-1} h^{-1}	H_2/CO	Ce-doped HAP supports Ni single atoms, preventing coking and sintering during dry reforming of methane (DRM), enhancing catalyst stability and selectivity for methane activation, leading to high activity and stability over 100 h.	Akri et al.,[190]
Ni–Mo SAC	Pyrolysis	Dry reforming	60%	H_2/CO	The molybdenum-doped nickel nanocatalyst stabilized at the edges of a single-crystalline MgO support shows no coking or sintering, with stable operation for over 850 h during dry reforming of methane, achieving continuous synthesis gas production.	Song et al.,[313]

(*Continued on next page*)

Table 1. *Continued*

Catalyst	Synthesis methods	Applications	Catalytic efficiency	Key product	Key findings	Reference
Pt-TiO_2 SAC	spatial confinement	Dry reforming	34.41 mol g_{Pt}^{-1} h^{-1}	H_2/CO	The catalyst developed using spatial confinement on TiO2 surfaces effectively controls platinum species from single atoms to nanoclusters, optimizing syngas production with high activity and stability. It achieves an outstanding syngas generation rate of 34.41 mol gPt^{-1} h^{-1} and a high turnover frequency of 1289 h^{-1}.	He et al.,[314]
Ir@CeO_{2-x}	hydrothermal method	Dry reforming	973 μmol_{CH_4} g_{cat}^{-1} s^{-1}	H_2/CO	The 0.6% Ir/CeO_2−x catalyst achieves high CH_4 (∼72%) and CO_2 (∼82%) conversion with a CH4 reaction rate of ∼973 $\mu molCH_4$ $g_{cat^{-1}}$ s^{-1}, maintaining stability for 100 h at 700°C. The metal-support interface structure facilitates CH_4 dissociation and prevents coke formation, ensuring long-term performance.	Wang et al.,[315]
Ru1/3L-TiO_2	DFT-D3 method	CO_2 methanation	80%	CH_4	The process of hydrogenation of CO* → HCO* is recognized as the rate-limiting step. The methanation process occurring on the Ru1/3L-TiO_2 realized a lower activation energy and was accompanied by a significantly reduced endothermic heat, in contrast to the reactions on the Ru1/2L-TiO_2.	Lei et al.,[316]

(*Continued on next page*)

Table 1. *Continued*

Catalyst	Synthesis methods	Applications	Catalytic efficiency	Key product	Key findings	Reference
1% Ni SAs-Bi_3O_4Br	Wet chemical method	Hydrogenation	100% selectivity for HCOO	HCOOH	The defect self-regulation mechanism enables photo-induced reconstruction, wherein Ni single atoms inhibit the migration of oxygen species to the oxygen vacancy surface, thereby preventing deactivation and guaranteeing prolonged catalytic stability.	Meng et al.,[317]
Co doped copper catalyst	electroreduction of a Co-Cu precursor	CO_2 methanation	exceeding 60%	CH_4	Mechanistic studies showed that the inclusion of individual Co atoms facilitates the activation and dissociation of H_2O molecules, therefore reducing the energy barrier for the hydrogenation of *CO intermediates.	Li et al.,[318]
Ru1Ni/SiO_2	Hydrothermal synthesis	CO_2 methanation	100%	CH_4	Both *in situ* experiments as well as theoretical calculations validate that the interface sites of Ru1Ni-SAA serve as the intrinsic active sites, facilitating the direct dissociation of CO_2 and reducing the energy barrier for the hydrogenation of the CO* intermediate, thus directing and augmenting the hydrogenation of CO_2 to CH_4.	Zhang et al.,[319]
Ru_1Ni/CeO_2	Hydrothermal synthesis	CO_2 methanation	~90% CO_2 conversion and ~99% CH_4 selectivity at	CH_4	The cohabitation of Ru and Ni sites substantially enhances the reaction compared to their individual active component catalysts.	Zhang et al.,[320]
Pt−CN catalyst	Hydrothermal synthesis	CO_2 methanation	99%	CH_4	The Pt sites were not significantly involved in H_2 development due to the distinctive environment established by −OH groups and adsorbed CO_2.	Shi et al.,[266]

(*Continued on next page*)

Table 1. *Continued*

Catalyst	Synthesis methods	Applications	Catalytic efficiency	Key product	Key findings	Reference
Cu/C–Al_2O_3 SAC	Hydrothermal synthesis	Electrochemical CO_2 methanation	62%	CH_4	The results indicate that the hydrogenation of CO_2 to methane is enhanced on Lewis's acid oxide-supported Cu single atoms.	Chen et al.,[163]
Zn-TpPa	Wet chemical method	N-formylation of amines	TOF 17,155 h^{-1} amon	N-methylaniline	Out of all the catalysts that were available, Zn-TpPa demonstrated the greatest TOF, promoting the N-formylation of N-methylaniline with CO_2 and hydrosilanes that were highly recyclable.	Cao et al.,[276]
$Zn(OAc)_2$@P(BiPy-DVB)-1	Copolymerization	N-formylation of amines	94%	N-methylformanilide	Under moderate circumstances, the ideal single-atom Zn catalyst had the greatest TOF among all recorded heterogeneous catalysts.	Li et al.,[277]
Ru-POM-ILs/BMImOAc	Wet chemical method	N-formylation of amines	96.0%	formamides	The current catalyst can be recycled without noticeable loss of activity and has improved long-term storage stability even in the air.	Ma et al.,[321]

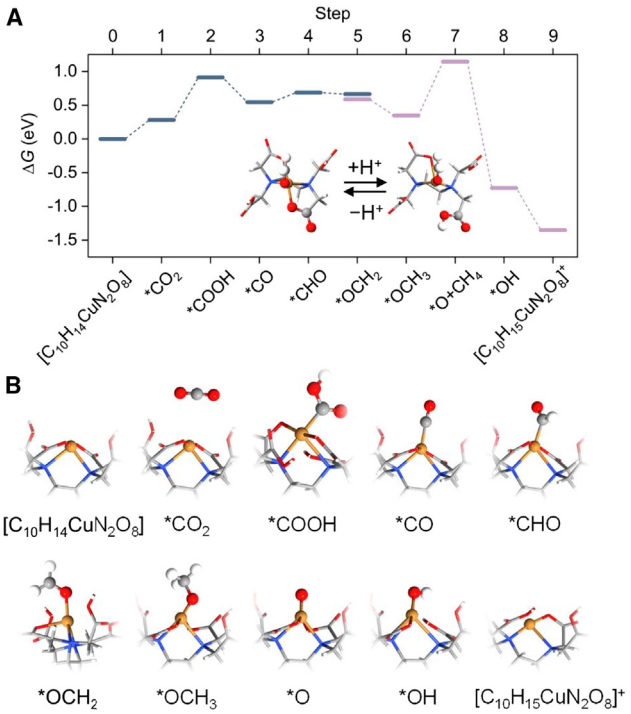

Figure 15. DFT calculations on CO_2 protonation to CH_4, where (A) is an energy profile and (B) is different intermediate. Reprinted with permission from.[158]

product synthesis. Although nickel oxide prevents the production of coke, it is not very efficient as a catalyst due to its high activation energy and sluggish surface diffusion of H*. This research also elucidates the observed disparities in DRM efficiency between Ni catalysts based on undoped CeO_3 (Ni/CeO_3) and CeO_3 doped with MnO (Ni/$MnCeO_3$). The lack of the 2020 cm^{+1} vibrational peak on the Ni/$MnCeO_2$ catalyst is due to the absence of carbon monoxide adsorbed on the top surface of metallic Ni, which is commonly found on Ni/CeO_2 catalyst. The existence of this peak on Ni/CeO_2 suggested that nickel particles possess a high degree of metallicity and are susceptible to carbon poisoning. In contrast, the lack of the peak on Ni/$MnCeO_2$ indicates that Ni particles have undergone sufficient oxidation to reduce carbon poisoning, while still enabling DRM. This explains why Ni/$MnCeO_2$ is a superior DRM catalyst compared to Ni/CeO_2 as in shown Figure 16.

Despite numerous experimental studies aimed at characterizing the reaction mechanism on single-alloy catalysts, the underlying reasons for the observed promoting effects remain unclear. This has shifted the focus toward guiding the experimental design of more effective single alloy catalysts for methanol synthesis. In the realm of catalyst design, theoretical calculations provide a highly advantageous methodology for the identification of reaction routes, intermediates, and active sites. By combining empirical and theoretical investigations, scholars can acquire a more profound understanding of CO_2 hydrogenation, thereby facilitating the advancement of more effective catalysts for methanol production.[330,331] Lingna Liu et al.[332] used DFT calculations to investigate the adsorption properties and reaction process of CO_2 hydrogenation to CH_3OH on a copper-based catalyst with varying Ir doping ratios. Throughout the reverse water-gas shift (RWGS) pathway, CO_2 initially hydrogenates to *trans*-COOH, which then isomerizes to *cis*-COOH and subsequently dissociates into CO + OH. CO further hydrogenates sequentially to form HCO, H_2CO, H_3CO, and the final product, H_3COH. The results reveal that the rate-determining step for the Ir_6Cu_3(111) surface is the formation of CO + OH, while for Ir_6Cu_3(111) and IrMLCu(111), it is the formation of HCO, with energy barriers of 1.21 eV, 1.35 eV, and 1.34 eV, respectively. Additionally, H_2 dissociation is nearly spontaneous on IrCu(111) surfaces, providing ample hydrogen for the reaction. The study highlights the significant influence of Ir doping ratios on the hydrogenation process, particularly on the IrMLCu(111) surface. These findings offer valuable insights for designing and optimizing Ir-doped Cu-based catalysts for CO_2 hydrogenation to methanol as in illustrated Figure 17.

IMPACT OF MACHINE LEARNING IN DEVELOPING THE PROCESS

In the advancement of renewable energy transformation technology, catalysts play a pivotal role.[333] These solutions offer a sustainable and environmentally friendly approach to tackle the energy problem as well as global climate change concerns.[334] Conventional heterogeneous catalysts typically comprise multiple metal particles of varying sizes, with only a small fraction of metal atoms acting as catalytic active species.[335] Additionally, the presence of multiple active sites with different selectivities leads to variations in product distributions, reducing metal utilization efficiency and selectivity.[336]

SACs, along with double-atom catalysts (DACs) and triple-atom catalysts (TACs), bridge the gap between homogeneous and heterogeneous catalysis. However, designing highly efficient SACs is challenging due to the extensive combinatorial design space. The combination of 44 metals with various substrate supports could lead to millions of possible SACs.[337] Traditional experimental and computational methods, including DFT, face significant time and cost constraints, making purely trial-and-error approaches infeasible.

ML, a rapidly evolving artificial intelligence technique, has transitioned from theoretical research to practical applications in materials science. ML is widely used to analyze complex datasets, detect structural flow abnormalities in disordered materials,[338] and investigate relationships between physical characteristics and catalytic performance.[339,340] Specifically, ML has been instrumental in understanding the adsorption energy of reaction intermediates and the maximum adsorption capacities of SACs supported on graphene-based solid-state electrolytes.[341] Various ML algorithms, including K-nearest neighbor regression (KNR),[342] random forest regression,[343] support vector regression (SVR),[344] gradient boosting regression (GBR),[345] extreme gradient boosting regression (XGBR), deep neural networks (DNN),[346] and Gaussian process regression (GPR)[347] have been employed for SAC design (see Figure 18), are now being employed for the design of SAC.[347] Among these, RFR, GBR, DNN, and GPR have shown promising results in catalyst optimization.[348]

ML has been instrumental in advancing CO_2 electroreduction,[349] which relies on CO as a key intermediate for generating

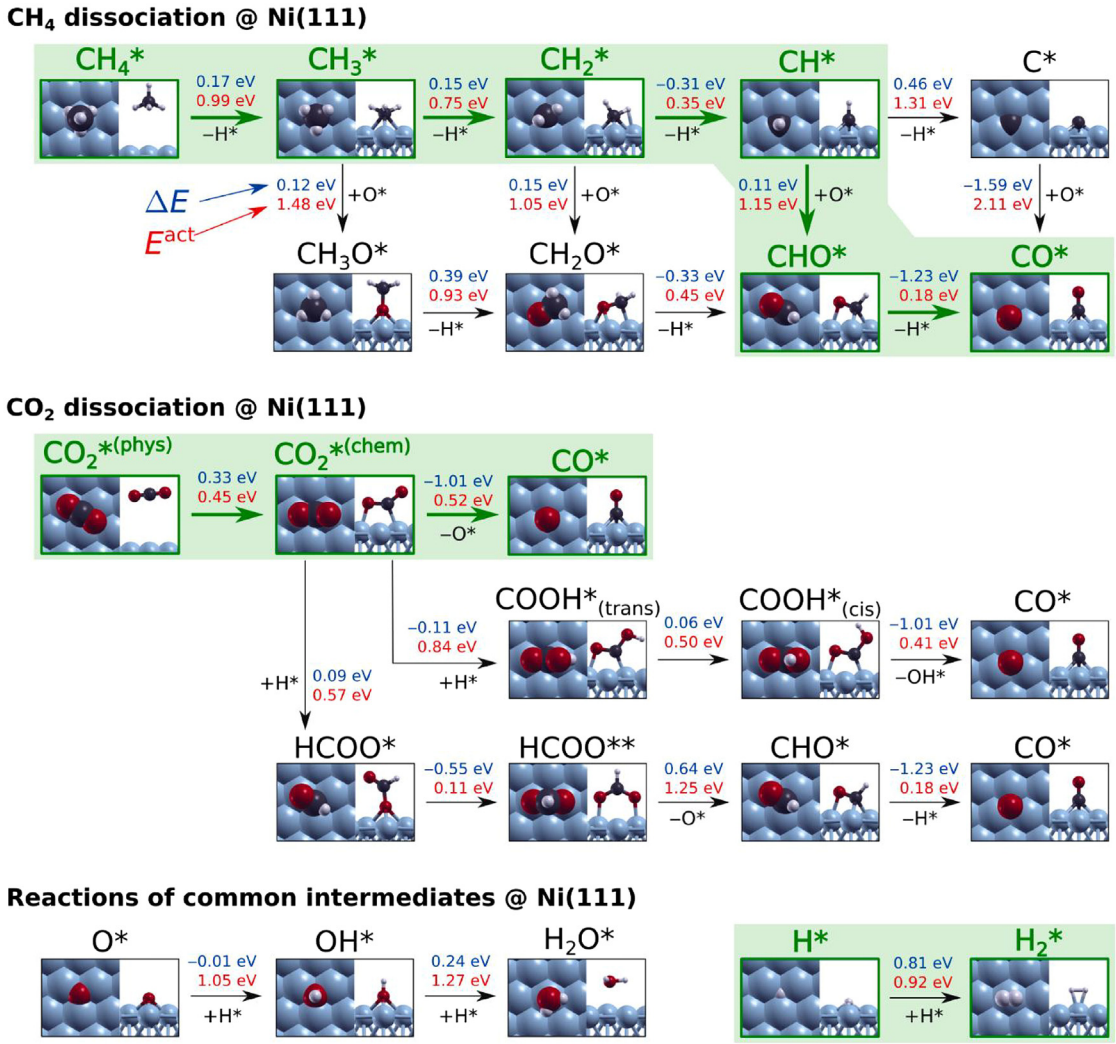

Figure 16. The snapshots and computed reaction (ΔE, blue) plus activation (Eact, red) energies of the primary steps in the breakdown of CH_4 and CO_2, as well as the production of water and hydrogen molecules, on Ni(111) are presented

For each reaction, the reaction pathways that include the primary steps with the smallest activation barriers are depicted in green. All computed reaction energy pathways and their matching IS, TS, and FS structures are displayed. Reprinted with permission from.[326]

multi-carbon hydrocarbons and oxygenates. Traditional catalyst evaluation often depends on a single assessment criterion, which may lead to biased outcomes. To address this, an XGBR-based predictive model was developed, using RFR, GBR, KNR, and SVR as training algorithms for comparison. The final XGBR model demonstrated the highest prediction accuracy, integrating a DFT database with ML techniques to rapidly screen potential catalysts for CO_2 electroreduction.[228] This framework identified 94 prospective SACs for CO_2 electroreduction by overlaying results from CO_2 reduction and hydrogen evolution reaction (HER) studies. By employing feature engineering and high-throughput screening, ML-based models enable researchers to efficiently identify promising catalysts before conducting detailed experimental investigations.[228]

Additionally, ML has been applied in DRM to mitigate catalyst deactivation due to coke formation and sintering at high reaction temperatures.[350–352] Traditional DRM catalyst development relies on expensive trial-and-error approaches, but ML models have facilitated the prediction of key performance parameters such as methane and CO_2 conversion rates, syngas ratios, and carbon deposition.[353–356] Jiwon Roh et al.[357] proposed an interpretable ML framework that reduces computational costs while offering valuable insights into catalyst performance. Their framework utilized Shapley additive explanations and partial dependence values for enhanced data preparation and analysis, achieving an R^2 value of 0.96. Experimental validation confirmed its potential to accelerate catalyst discovery. The effectiveness of this framework was validated through experimental tests focused on the dry reforming of methane, confirming its potential to significantly accelerate the rational design of catalysts as shown in Figure 19.

ML has also emerged as a powerful tool in CO_2 hydrogenation, particularly in methanol synthesis. Direct catalytic hydrogenation

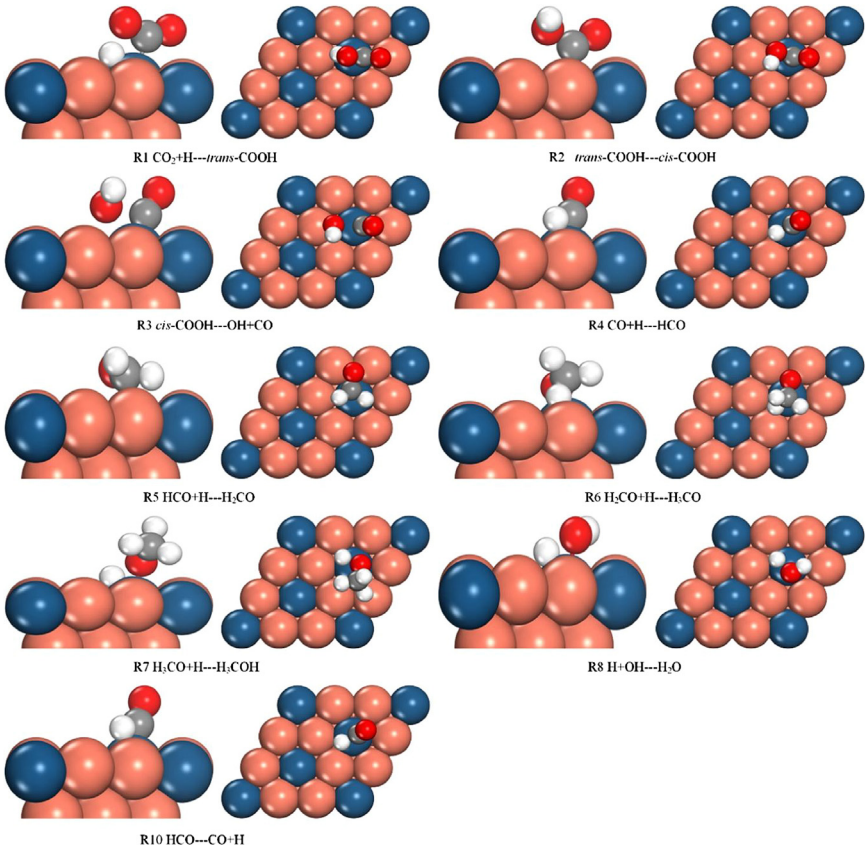

Figure 17. The transition states of the primary steps involved in carbon dioxide hydrogenation on Ir_3Cu_6(111) surface

Red, Oxygen atom; White, Hydrogen atom; gray, Carbon atom. Reprinted with permission from.[332]

of CO_2 is a promising strategy to meet growing fuel demands while reducing anthropogenic CO_2 emissions.[358] However, the reaction's thermodynamic constraints necessitate catalysts with high selectivity to minimize unwanted byproducts.[359] Several ML models, including multilinear regression, LASSO, ridge regression, SVR, GPR, RFR, GBR, and artificial neural networks (ANNs), have been developed to predict CO_2 conversion efficiency and methanol selectivity. Using 698 experimental data points from fixed-bed reactors (2010–2020), Vanjari et al.[360] demonstrated that GBRT and ANN exhibited superior predictive accuracy, with R^2 values of ~0.95. Their analysis highlighted catalyst composition and calcination temperature as key factors influencing performance as illustrated in Figure 20.

The integration of ML into catalyst research has significantly advanced materials discovery, enabling rapid screening and optimization of catalysts for CO_2 electroreduction, DRM, and hydrogenation processes. By leveraging ML-based predictive models, researchers can efficiently explore large design spaces, reducing reliance on traditional, resource-intensive methods. As ML techniques continue to evolve, they will play an increasingly vital role in accelerating the development of next-generation catalysts for sustainable energy applications.

CHALLENGES AND PROSPECTS

Addressing the challenges associated with general CO_2 conversion requires a multidisciplinary approach that leverages SACs, cascade systems, and machine learning. These challenges can be represented in terms of low selectivity and yield. Conventional CO_2 utilization methods, including CO_2 conversion, dry reforming, and hydrogenation applications, often suffer from low selectivity and yield, leading to inefficient carbon transformation.[361] This is primarily due to the complex nature of CO_2 and the multitude of competing reactions. Additionally, catalyst deactivation poses a significant challenge, limiting the effectiveness and sustainability of CO_2 conversion processes.[362] Traditional catalysts are prone to deactivation over time, resulting in reduced performance and increased operational costs. In addition, the kinetics of CO_2 conversion reactions are often slow, hindering the overall efficiency of the process.[363] Overcoming these kinetic limitations is crucial for the development of economically viable CO_2 utilization technologies.[364–367] Furthermore, achieving desired product distributions is challenging, as CO_2 conversion often results in a mixture of products with varying carbon chain lengths.[367,368] This hampers the production of specific high value multicarbon compounds.

SACs offer an innovative method for addressing difficulties of several applications of CO_2 conversion.[368] SACs provide enhanced catalytic activity,[369] precise control over selectivity,[162] decreased metal consumption,[370] increased stability,[371] easier mass transfer,[372] and adjustable reactivity by incorporating isolated metal atoms onto a supporting material.[373] The combination of these traits together enhances the performance of SACs in converting CO_2, leading to increased efficiency, long-term stability, and cost-effectiveness. Moreover, the combination of SACs with robust support materials and the knowledge obtained from computational studies highlights their potential as crucial elements in sustainable technologies.[374] This presents a hopeful opportunity to tackle environmental issues by converting CO_2 into valuable products.

Implementing cascade systems is a strategic approach to address challenges associated with different applications such as CO_2RR, DRM, and hydrogenation. using SACs. Several catalysts are sequentially integrated in a cascade system to increase selectivity and overall efficiency.[375] Using a cascade system may start with SACs that have metal atoms tuned for activating CO_2, then go on to catalysts that convert intermediate products into the fuels or required chemicals in different applications for CO_2

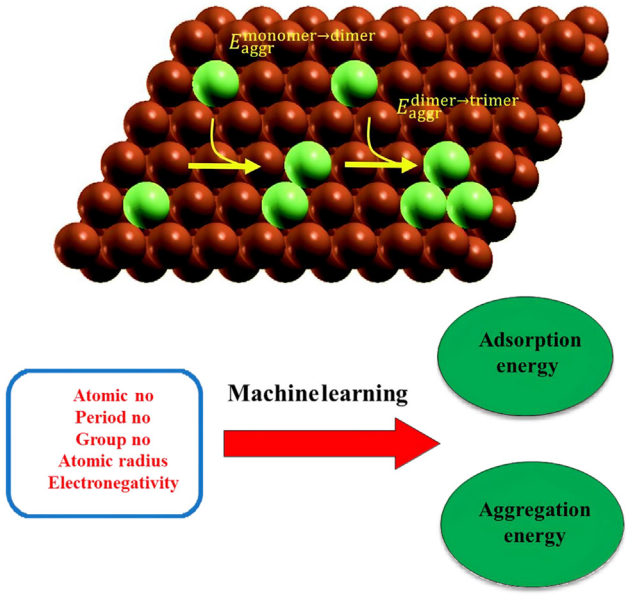

Figure 18. Modeling the aggregation energy of SA-bimetallic catalysts with both clean and O* adsorbed surfaces using machine learning algorithms
Reprinted with modification form.[347]

conversion.[151] The sequential design facilitates a more extensive exploitation of the CO_2 reduction route, therefore addressing problems such as inadequate product selection and incomplete conversion. Through the strategic integration of SACs with other catalysts in a cascade, it is feasible to enhance the overall process, optimize reaction kinetics, and attain increased yields of valuable products from different CO_2 conversion applications.[376] Furthermore, one of the strategies is to incorporate ML techniques that show great promise in optimizing and accelerating the development of efficient catalysts for CO_2 general conversion applications.[377] ML algorithms can analyze vast datasets, predict catalytic activity, and identify novel catalyst compositions, accelerating the discovery process. Additionally, ML can aid in understanding complex reaction mechanisms, leading to the design of catalysts with improved selectivity and performance. The integration of ML in CO_2 conversion and utilization research also enables the identification of structure-property relationships, facilitating the rational design of catalysts tailored for specific CO_2 conversion pathways.[378]

In technologies of CO_2 utilization, it is imperative to recommend strategic measures for future progress. First, fostering interdisciplinary research collaboration between scholars specializing in catalysis, materials science, and ML is crucial for the seamless integration of SACs, cascade systems, and ML methodologies in the domain of CO_2 utilization. Such interdisciplinary collaboration holds significant potential for pushing the boundaries of innovation in this field. Second, rigorous experimental validation is underscored. Despite the value of theoretical models and simulations, robust confirmation of the efficacy of proposed approaches through extensive real-world testing is indispensable. This validation process is crucial for elucidating the scalability and practical applicability of the envisaged technologies. Lastly, advocating for policy support and industry adoption is emphasized. Government policies and incentives are identified as pivotal drivers for the widespread adoption of innovative CO_2 utilization technologies, and collaborative efforts with industries are essential for the effective and expansive implementation of these advancements, ensuring a substantial and meaningful environmental impact.

FUTURE DIRECTIONS

The exploration of SACs represents a significant advancement in catalysis, presenting unique opportunities and challenges.[379] Based on the existing literature, several promising future directions can be identified to enhance the understanding, synthesis, and application of SACs in various catalytic processes. While current synthesis methods such as pyrolysis, wet chemistry, and coordination confinement have yielded promising results, the development of more precise and scalable synthesis techniques is crucial.[380] Future research should focus on high-throughput synthesis, employing automation and machine learning to optimize synthesis parameters rapidly, refining electrochemical deposition to achieve better control over the dispersion and stability of single atoms on support materials, and developing *in situ* synthesis methods that allow for the formation of SACs directly under reaction conditions, potentially leading to more active and stable catalysts.[381]

Advances in characterization techniques are essential for a deeper understanding of SACs' structure–property relationship.[382] Future efforts should aim to enhance atomic-level resolution using state-of-the-art electron microscopy and spectroscopy methods to achieve better visualization and identification of single atoms, developing techniques to observe the behavior of SACs under actual reaction conditions in real time, and leveraging AI and machine learning to analyze large datasets from characterization studies, identifying patterns and correlations that may not be immediately evident.[383]

A comprehensive understanding of the mechanisms underlying SACs catalytic activity is necessary to guide the rational design of new catalysts.[384] In addition, future research should focus on first-principles calculations using DFT and other computational methods to predict the activity and stability of SACs, developing detailed kinetic models to describe the behavior of SACs in various catalytic processes, and applying machine learning algorithms to predict the performance of SACs based on their structural and electronic properties.[385]

While significant progress has been made in using SACs for CO_2 conversion, addressing the current challenge of low CO_2 conversion efficiency and selectivity is crucial. Future research should focus on overcoming this challenge through hybrid catalyst systems, such as combining SACs with other catalytic materials or using tandem reaction systems, which will enable multi-step CO_2 reduction and enhance product yields. Additionally, applying machine learning algorithms to predict optimal reaction conditions, coupled with real-time data from the system, will increase the efficiency and precision of CO_2 conversion.

Also, future research should explore other potential applications such as renewable energy, investigating the use of SACs

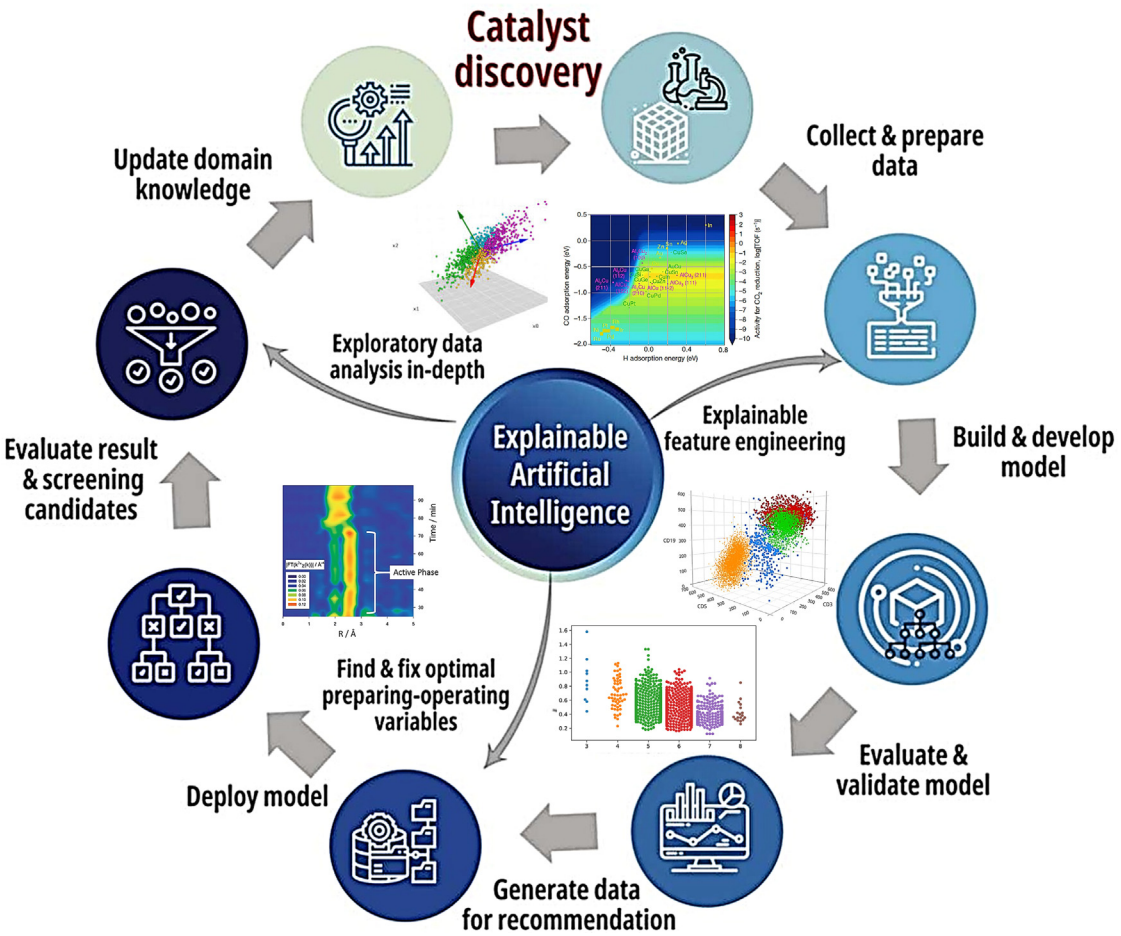

Figure 19. Workflow of explainable artificial intelligence in catalyst discovery
Reprinted with modification form.[357]

in hydrogen production, fuel cells, and battery technologies, environmental remediation, exploring the potential of SACs in pollutant degradation and water treatment, and chemical synthesis, extending the application of SACs to the synthesis of fine chemicals and pharmaceuticals.[386] The integration of SACs with emerging technologies can lead to breakthroughs in catalytic performance by combining SACs with nanostructured materials to enhance their activity and selectivity, investigating the potential of SACs in photocatalytic processes for solar energy conversion and environmental applications, and exploring the use of SACs in electrocatalytic processes for energy storage and conversion.[217,386]

Also, addressing the scalability and sustainability of SACs is essential. Developing environmentally friendly and sustainable synthesis routes, investigating the use of earth-abundant and non-toxic materials, and addressing the challenges associated with scaling up SAC production for industrial applications are key research goals.[386] The future of SACs is promising, with numerous opportunities for advancements in synthesis, characterization, mechanistic understanding, and applications. By leveraging cutting-edge technologies and interdisciplinary approaches, researchers can overcome current challenges and unlock the full potential of SACs in various catalytic processes, contributing to a sustainable and efficient chemical industry.

CONCLUSION

In conclusion, this review provided an in-depth analysis of the significant advancements and the current state of SACs. The historical evolution of SACs highlights their transition from theoretical concepts to practical applications, driven by advancements in synthesis methods such as pyrolysis, wet chemistry, and coordination confinement. These methods have enabled the precise control of SAC structures, crucial for their unique catalytic properties. Comprehensive characterizations using techniques like high-resolution transmission electron microscopy (HR-TEM), XAS, and atomic force microscopy (AFM) have provided detailed insights into the atomic distribution and electronic environment of SACs, furthering our understanding and optimization of these catalysts. The review also emphasizes the versatility of SAC-derived materials, including Cu-based, Fe-based, Ni-based, and Cd-based catalysts, as well as more complex structures like yolk shell Pd@Fe and MOF-based SACs. Each of these materials demonstrates specific advantages in various catalytic reactions,

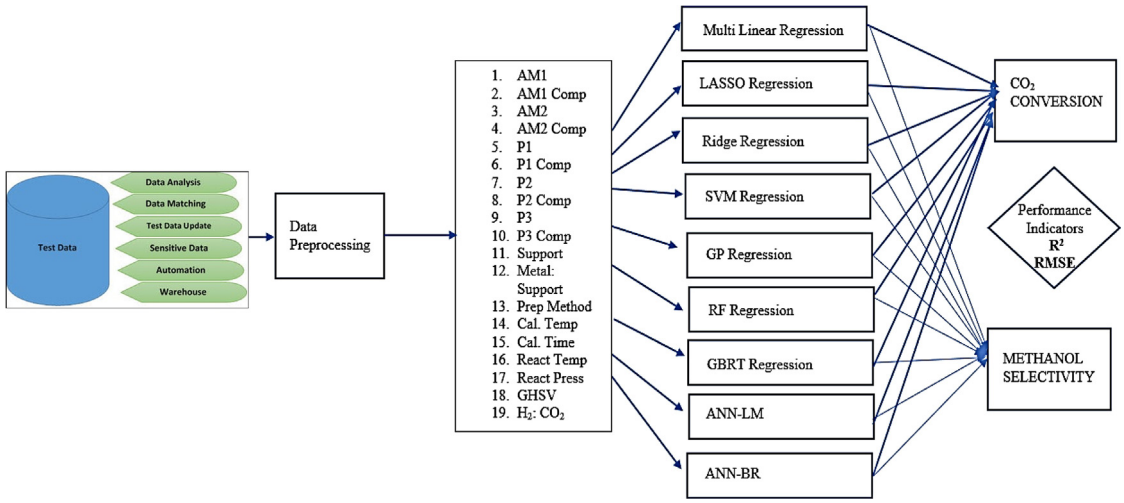

Figure 20. Methodology for development of ML models
Reprinted with modification form.[360]

underscoring the broad applicability of SACs. Particularly noteworthy is their role in CO_2 conversion applications, where SACs facilitate processes such as electrochemical reduction, hydrogenation, reforming of CH_4, methanation, cycloaddition with epoxides, and polymer production. These applications not only contribute to mitigating CO_2 emissions but also offer pathways for generating valuable chemicals and materials, highlighting the environmental and economic benefits of SACs. The integration of machine learning and computational methods has significantly impacted the field, enabling the optimization of synthesis processes and the prediction of catalyst performance. Computational studies, including DFT calculations, provide atomic-level insights into the mechanisms of SACs, guiding experimental research and accelerating the discovery of new catalysts. Despite these advancements, challenges such as scalability, stability, and cost-effectiveness remain. Addressing these issues is critical for the broader industrial adoption of SACs, and future research must focus on developing more robust supports, optimizing atom-support interactions, and reducing production costs. The future of SACs lies in interdisciplinary approaches that combine advancements in materials science, chemistry, and computational technologies. Collaborative efforts across academia, industry, and government will be essential to drive innovation and tackle global challenges. Continued exploration of SACs for emerging applications, particularly in renewable energy and environmental remediation, will be crucial. This review underscores the transformative potential of SACs in catalysis, offering unparalleled opportunities for scientific discovery and practical applications. With ongoing research and technological advancements, SACs are poised to play a pivotal role in shaping a sustainable future, revolutionizing catalytic processes, reducing environmental impact, and contributing to the development of green technologies.

ACKNOWLEDGMENTS

The author(s) would like to acknowledge the research support provided by the interdisciplinary research center for refining and advanced chemicals through INRC2406. The financial support provided by Renewable Energy Technical incubator (RETI) by the national industrial development and logistics program under the interdisciplinary research center for sustainable energy systems at King Fahd University of Petroleum & Minerals, through Project No. CREP2522 is also acknowledged.

AUTHOR CONTRIBUTIONS

E.K.: Conceptualization, data curation, writing– original draft preparation; M.M.A.: methodology and analysis; M.U.: reviewing and editing; O.A.T.: reviewing and editing; I.H.: supervision, reviewing, and editing; S.I.A.: writing–original draft preparation, data interpretation, and discussion; K.A.: supervision, reviewing, and editing; S.A.G.: supervision, reviewing, and editing.

DECLARATION OF INTERESTS

The authors declare that they have no competing financial or personal interests that could have influenced the work reported in this manuscript.

REFERENCES

1. Sharma, J., Kumar, S.S., Bishnoi, N.R., and Pugazhendhi, A. (2018). Enhancement of lipid production from algal biomass through various growth parameters. J. Mol. Liq. *269*, 712–720.
2. Kumar, V., Nanda, M., Joshi, H.C., Singh, A., Sharma, S., and Verma, M. (2018). Production of biodiesel and bioethanol using algal biomass harvested from fresh water river. Renew. Energy *116*, 606–612.
3. Vooradi, R., Anne, S.B., Tula, A.K., Eden, M.R., and Gani, R. (2019). Energy and CO2 management for chemical and related industries: issues, opportunities and challenges. BMC Chem. Eng. *1*, 7. https://doi.org/10.1186/s42480-019-0008-6.
4. Lai, W., Ma, Z., Zhang, J., Yuan, Y., Qiao, Y., and Huang, H. (2022). Dynamic Evolution of Active Sites in Electrocatalytic CO2 Reduction Reaction: Fundamental Understanding and Recent Progress (Preprint at John Wiley and Sons Inc). https://doi.org/10.1002/adfm.202111193.
5. Aghbashlo, M., Tabatabaei, M., Hosseini, S.S., B. Dashti, B., and Mojarab Soufiyan, M. (2018). Performance assessment of a wind power plant using standard exergy and extended exergy accounting (EEA) approaches. J. Clean. Prod. *171*, 127–136. https://doi.org/10.1016/j.jclepro.2017.09.263.

6. Chang, B., Pang, H., Raziq, F., Wang, S., Huang, K.W., Ye, J., and Zhang, H. (2023). Electrochemical reduction of carbon dioxide to multicarbon (C2+) products: challenges and perspectives. Energy Environ. Sci. *16*, 4714–4758. https://doi.org/10.1039/d3ee00964e.

7. Ouda, O.K.M., Raza, S.A., Nizami, A.S., Rehan, M., Al-Waked, R., and Korres, N.E. (2016). Waste to Energy Potential: A Case Study of Saudi Arabia (Preprint at Elsevier Ltd). https://doi.org/10.1016/j.rser.2016.04.005.

8. Chen, H., Liang, X., Liu, Y., Ai, X., Asefa, T., and Zou, X. (2020). Active Site Engineering in Porous Electrocatalysts (Preprint at Wiley-VCH Verlag). https://doi.org/10.1002/adma.202002435.

9. Ahmed Taialla, O., Mustapha, U., Hakam Shafiu Abdullahi, A., Kotob, E., Mosaad Awad, M., Musa Alhassan, A., Hussain, I., Omer, K., Ganiyu, S.A., and Alhooshani, K. (2024). Unlocking the Potential of ZIF-Based Electrocatalysts for Electrochemical Reduction of CO2: Recent Advances, Current Trends, and Machine Learnings (Preprint at Elsevier B.V.). https://doi.org/10.1016/j.ccr.2024.215669.

10. Ellabban, O., Abu-Rub, H., and Blaabjerg, F. (2014). Renewable Energy Resources: Current Status, Future Prospects and Their Enabling Technology (Preprint at Elsevier Ltd). https://doi.org/10.1016/j.rser.2014.07.113.

11. Fan, Q., Hou, P., Choi, C., Wu, T.S., Hong, S., Li, F., Soo, Y.L., Kang, P., Jung, Y., and Sun, Z. (2020). Activation of Ni Particles into Single Ni–N Atoms for Efficient Electrochemical Reduction of CO2. Adv. Energy Mater. *10*, 20201903068. https://doi.org/10.1002/aenm.201903068.

12. Sargeant, E., and Rodríguez, P. (2023). Electrochemical Conversion of CO2 in Non-conventional Electrolytes: Recent Achievements and Future Challenges (Preprint at John Wiley and Sons Inc). https://doi.org/10.1002/elsa.202100178.

13. Mac Dowell, N., Fennell, P.S., Shah, N., and Maitland, G.C. (2017). The role of CO2 capture and utilization in mitigating climate change (Preprint at Nature Publishing Group). https://doi.org/10.1038/nclimate3231.

14. Zhan, X., Fan, X., Li, W., Tan, X., Robertson, A. W., Muhammad, U., and Sun, Z. (2024). Coupled metal atomic pairs for synergistic electrocatalytic CO2 reduction. Matter *7*, 4206–4232. https://doi.org/10.1016/j.matt.2024.09.013.

15. Galanakis, N., and Tuckerman, M.E. (2024). Rapid prediction of molecular crystal structures using simple topological and physical descriptors. Nat. Commun. *15*, 9757. https://doi.org/10.1038/s41467-024-53596-5.

16. Koytsoumpa, E.I., Bergins, C., and Kakaras, E. (2018). The CO2 Economy: Review of CO2 Capture and Reuse Technologies (Preprint at Elsevier B.V.). https://doi.org/10.1016/j.supflu.2017.07.029.

17. Anwar, M.N., Fayyaz, A., Sohail, N.F., Khokhar, M.F., Baqar, M., Khan, W.D., Rasool, K., Rehan, M., and Nizami, A.S. (2018). CO2 capture and storage: A way forward for sustainable environment. J. Environ. Manag. *226*, 131–144. https://doi.org/10.1016/j.jenvman.2018.08.009.

18. Wang, G., Chen, X., Zhang, Z., and Niu, C. (2015). Influencing factors of energy-related CO2 emissions in China: A decomposition analysis. Sustainability *7*, 14408–14426. https://doi.org/10.3390/su71014408.

19. Pérez-Fortes, M., Schöneberger, J.C., Boulamanti, A., and Tzimas, E. (2016). Methanol synthesis using captured CO2 as raw material: Techno-economic and environmental assessment. Appl. Energy *161*, 718–732. https://doi.org/10.1016/j.apenergy.2015.07.067.

20. Madduluri, V.R., Marella, R.K., Hanafiah, M.M., Lakkaboyana, S.K., and Suresh babu, G. (2020). CO2 utilization as a soft oxidant for the synthesis of styrene from ethylbenzene over Co3O4 supported on magnesium aluminate spinel: role of spinel activation temperature. Sci. Rep. *10*, 22170. https://doi.org/10.1038/s41598-020-79188-z.

21. Karimaie, H., Nazarian, B., Aurdal, T., Nøkleby, P.H., and Hansen, O. (2017). Simulation Study of CO2 EOR and Storage Potential in a North Sea Reservoir. In Energy Procedia (Elsevier Ltd), pp. 7018–7032. https://doi.org/10.1016/j.egypro.2017.03.1843.

22. Umar, M., Aljezan, M.Y., Abdulazeez, I., Amao, A.O., Ganiyu, S.A., and Alhooshani, K. (2024). Modulating the electrocatalytic reduction of CO2 to CO via surface reconstruction of ZnO nanoshapes. J. Sci.: Advanced Materials and Devices *9*, 100748. https://doi.org/10.1016/j.jsamd.2024.100748.

23. Zhang, F., Chen, W., and Li, W. (2023). Recent advances in the catalytic conversion of CO2 to chemicals and demonstration projects in China. Mol. Catal. *541*, 113093. https://doi.org/10.1016/j.mcat.2023.113093.

24. Sibi, M.G., Verma, D., and Kim, J. (2024). Direct conversion of CO2 into aromatics over multifunctional heterogeneous catalysts. Catal. Rev. Sci. Eng. *66*, 863–922. https://doi.org/10.1080/01614940.2022.2099058.

25. Hamby, H., Li, B., Shinopoulos, K.E., Keller, H.R., Elliott, S.J., and Dukovic, G. (2020). Light-driven carbon−carbon bond formation via CO_2 reduction catalyzed by complexes of CdS nanorods and a 2-oxoacid oxidoreductase. Proc. Natl. Acad. Sci. USA *117*, 135–140. https://doi.org/10.1073/pnas.1903948116.

26. Ruiz-López, E., Gandara-Loe, J., Baena-Moreno, F., Reina, T.R., and Odriozola, J.A. (2022). Electrocatalytic CO2 Conversion to C2 Products: Catalysts Design, Market Perspectives and Techno-Economic Aspects (Preprint at Elsevier Ltd). https://doi.org/10.1016/j.rser.2022.112329.

27. Habisreutinger, S.N., Schmidt-Mende, L., and Stolarczyk, J.K. (2013). Photocatalytic reduction of CO2 on TiO2 and other semiconductors. Angew Chem. Int. Ed. Engl. *52*, 7372–7408. https://doi.org/10.1002/anie.201207199.

28. Grodkowski, J., and Neta, P. (2001). Copper-catalyzed radiolytic reduction of CO2 to CO in aqueous solutions. J. Phys. Chem. B *105*, 4967–4972. https://doi.org/10.1021/jp004567d.

29. Wang, W., Wang, S., Ma, X., and Gong, J. (2011). Recent advances in catalytic hydrogenation of carbon dioxide. Chem. Soc. Rev. *40*, 3703–3727. https://doi.org/10.1039/c1cs15008a.

30. Guo, F., Cao, W., Wang, L., Zhang, Q., and Xu, J. (2023). High activity and strong coke resistance of nickel CO2-CH4 reforming catalyst promoted by different plasma treated modes. Mol. Catal. *535*, 112821. https://doi.org/10.1016/j.mcat.2022.112821.

31. Mustapha, U., Nnadiekwe, C.C., Alhaboudal, M.A., Yunusa, U., Abdullahi, A.H.S., Abdulazeez, I., Hussain, I., Ganiyu, S.A., Al-Saadi, A.A., and Alhooshani, K. (2023). The Role of Morphology on the Electrochemical CO2 Reduction Performance of Transition Metal-Based Catalysts (Preprint at Elsevier B.V.). https://doi.org/10.1016/j.jechem.2023.06.010.

32. Varela, A.S., Ju, W., Bagger, A., Franco, P., Rossmeisl, J., and Strasser, P. (2019). Electrochemical Reduction of CO2 on Metal-Nitrogen-Doped Carbon Catalysts. ACS Catal. *9*, 7270–7284. https://doi.org/10.1021/acscatal.9b01405.

33. Gawande, M.B., Fornasiero, P., and Zbořil, R. (2020). Carbon-Based Single-Atom Catalysts for Advanced Applications. ACS Catal. *10*, 2231–2259. https://doi.org/10.1021/acscatal.9b04217.

34. Chen, Y., Ji, S., Chen, C., Peng, Q., Wang, D., and Li, Y. (2018). Single-Atom Catalysts: Synthetic Strategies and Electrochemical Applications. Joule *2*, 1242–1264. https://doi.org/10.1016/j.joule.2018.06.019.

35. Yang, X.F., Wang, A., Qiao, B., Li, J., Liu, J., and Zhang, T. (2013). Single-atom catalysts: A new frontier in heterogeneous catalysis. Acc. Chem. Res. *46*, 1740–1748. https://doi.org/10.1021/ar300361m.

36. Bao, H., Qiu, Y., Peng, X., Wang, J.A., Mi, Y., Zhao, S., Liu, X., Liu, Y., Cao, R., Zhuo, L., et al. (2021). Isolated copper single sites for high-performance electroreduction of carbon monoxide to multicarbon products. Nat. Commun. *12*, 238. https://doi.org/10.1038/s41467-020-20336-4.

37. Wang, A., Li, J., and Zhang, T. (2018). Heterogeneous Single-Atom Catalysis (Preprint at Nature Publishing Group). https://doi.org/10.1038/s41570-018-0010-1.

38. Ji, S., Chen, Y., Wang, X., Zhang, Z., Wang, D., and Li, Y. (2020). Chemical Synthesis of Single Atomic Site Catalysts. Chem. Rev. *120*, 11900–11955. https://doi.org/10.1021/acs.chemrev.9b00818.

39. Meshitsuka, S., Ichikawa, M., and Tamaru, K. (1974). Electrocatalysis by metal phthalocyanines in the reduction of carbon dioxide. J. Chem. Soc. Chem. Commun., 158–159. https://doi.org/10.1039/C39740000158.

40. Han, N., Wang, Y., Ma, L., Wen, J., Li, J., Zheng, H., Nie, K., Wang, X., Zhao, F., Li, Y., et al. (2017). Supported Cobalt Polyphthalocyanine for High-Performance Electrocatalytic CO2 Reduction. Chem *3*, 652–664. https://doi.org/10.1016/j.chempr.2017.08.002.

41. Zhang, Z., Xiao, J., Chen, X., Yu, S., Yu, L., Si, R., Wang, Y., Wang, S., Meng, X., Wang, Y., et al. (2018). Reaction Mechanisms of Well-Defined Metal–N 4 Sites in Electrocatalytic CO 2 Reduction. Angew. Chem. *130*, 16577–16580. https://doi.org/10.1002/ange.201808593.

42. Zhang, X., Wu, Z., Zhang, X., Li, L., Li, Y., Xu, H., Li, X., Yu, X., Zhang, Z., Liang, Y., and Wang, H. (2017). Highly selective and active CO2 reduction electrocatalysts based on cobalt phthalocyanine/carbon nanotube hybrid structures. Nat. Commun. *8*, 14675. https://doi.org/10.1038/ncomms14675.

43. Varela, A.S., Ranjbar Sahraie, N., Steinberg, J., Ju, W., Oh, H., and Strasser, P. (2015). Metal-Doped Nitrogenated Carbon as an Efficient Catalyst for Direct CO 2 Electroreduction to CO and Hydrocarbons. Angew. Chem. *127*, 10908–10912. https://doi.org/10.1002/ange.201502099.

44. Meng, Y., Huang, H., Zhang, Y., Cao, Y., Lu, H., and Li, X. (2023). Recent Advances in the Theoretical Studies on the Electrocatalytic CO2 Reduction Based on Single and Double Atoms (Preprint at Frontiers Media S.A). https://doi.org/10.3389/fchem.2023.1172146.

45. Abbet, S., Sanchez, A., Heiz, U., Schneider, W.D., Ferrari, A.M., Pacchioni, G., and Rösch, N. (2000). Acetylene cyclotrimerization on supported size-selected Pd(n) clusters ($1 \leq n \leq 30$): One atom is enough. J. Am. Chem. Soc. *122*, 3453–3457. https://doi.org/10.1021/ja9922476.

46. Qin, Q., Heil, T., Antonietti, M., and Oschatz, M. (2018). Single-Site Gold Catalysts on Hierarchical N-Doped Porous Noble Carbon for Enhanced Electrochemical Reduction of Nitrogen. Small Methods *2*, 20181800202. https://doi.org/10.1002/smtd.201800202.

47. Pan, F., Zhang, H., Liu, K., Cullen, D., More, K., Wang, M., Feng, Z., Wang, G., Wu, G., and Li, Y. (2018). Unveiling Active Sites of CO2 Reduction on Nitrogen-Coordinated and Atomically Dispersed Iron and Cobalt Catalysts. ACS Catal. *8*, 3116–3122. https://doi.org/10.1021/acscatal.8b00398.

48. Yan, X., Liu, D., Cao, H., Hou, F., Liang, J., and Dou, S.X. (2019). Nitrogen Reduction to Ammonia on Atomic-Scale Active Sites under Mild Conditions (Preprint at John Wiley and Sons Inc.). https://doi.org/10.1002/smtd.201800501.

49. Mitchell, S., and Pérez-Ramírez, J. (2020). Single atom catalysis: a decade of stunning progress and the promise for a bright future. Nat. Commun. *11*, 4302. https://doi.org/10.1038/s41467-020-18182-5.

50. Fu, Q., Saltsburg, H., and Flytzani-Stephanopoulos, M. (2003). Active Nonmetallic Au and Pt Species on Ceria-Based Water-Gas Shift. Catal. Sci. *301*, 935–938. https://doi.org/10.1126/science.1085721.

51. Bashyam, R., and Zelenay, P. (2006). A class of non-precious metal composite catalysts for fuel cells. Nature *443*, 63–66. https://doi.org/10.1038/nature05118.

52. Qiao, B., Wang, A., Yang, X., Allard, L.F., Jiang, Z., Cui, Y., Liu, J., Li, J., and Zhang, T. (2011). Single-atom catalysis of CO oxidation using Pt1/FeOx. Nat. Chem. *3*, 634–641. https://doi.org/10.1038/nchem.1095.

53. Kyriakou, G., Boucher, M.B., Jewell, A.D., Lewis, E.A., Lawton, T.J., Baber, A.E., Tierney, H.L., Flytzani-Stephanopoulos, M., Charles, E., Sykes, H., et al. (2012). Isolated Metal Atom Geometries as a Strategy for Selective Heterogeneous Hydrogenations. Science *335*, 1209–1212. https://doi.org/10.1126/science.1215864.

54. Mitchell, S., Vorobyeva, E., and Pérez-Ramírez, J. (2018). Die facettenreiche Reaktivität heterogener Einzelatom-Katalysatoren. Angew. Chem. *130*, 15538–15552. https://doi.org/10.1002/ange.201806936.

55. Li, X., Yang, X., Zhang, J., Huang, Y., and Liu, B. (2019). In Situ/Operando Techniques for Characterization of Single-Atom Catalysts. ACS Catal. *9*, 2521–2531. https://doi.org/10.1021/acscatal.8b04937.

56. Fei, H., Dong, J., Arellano-Jiménez, M.J., Ye, G., Dong Kim, N., Samuel, E.L.G., Peng, Z., Zhu, Z., Qin, F., Bao, J., et al. (2015). Atomic cobalt on nitrogen-doped graphene for hydrogen generation. Nat. Commun. *6*, 8668. https://doi.org/10.1038/ncomms9668.

57. Yang, H.B., Hung, S.F., Liu, S., Yuan, K., Miao, S., Zhang, L., Huang, X., Wang, H.Y., Cai, W., Chen, R., et al. (2018). Atomically dispersed Ni(i) as the active site for electrochemical CO2 reduction. Nat. Energy *3*, 140–147. https://doi.org/10.1038/s41560-017-0078-8.

58. Li, X., Bi, W., Zhang, L., Tao, S., Chu, W., Zhang, Q., Luo, Y., Wu, C., and Xie, Y. (2016). Single-Atom Pt as Co-Catalyst for Enhanced Photocatalytic H2Evolution. Adv. Mater. *28*, 2427–2431. https://doi.org/10.1002/adma.201505281.

59. He, T., Puente-Santiago, A.R., Xia, S., Ahsan, M.A., Xu, G., and Luque, R. (2022). Experimental and Theoretical Advances on Single Atom and Atomic Cluster-Decorated Low-Dimensional Platforms towards Superior Electrocatalysts. Adv. Energy Mater. *12*, 20222200493. https://doi.org/10.1002/aenm.202200493.

60. Wang, F., Li, J., Zhao, J., Yang, Y., Su, C., Zhong, Y.L., Yang, Q.H., and Lu, J. (2020). Single-atom electrocatalysts for lithium sulfur batteries: Progress, opportunities, and challenges. ACS Mater. Lett. *2*, 1450–1463. https://doi.org/10.1021/acsmaterialslett.0c00396.

61. Zhao, L., Zhang, Y., Huang, L.B., Liu, X.Z., Zhang, Q.H., He, C., Wu, Z.Y., Zhang, L.J., Wu, J., Yang, W., et al. (2019). Cascade anchoring strategy for general mass production of high-loading single-atomic metal-nitrogen catalysts. Nat. Commun. *10*, 1278. https://doi.org/10.1038/s41467-019-09290-y.

62. Liu, L., and Corma, A. (2018). Metal Catalysts for Heterogeneous Catalysis: From Single Atoms to Nanoclusters and Nanoparticles. Chem. Rev. *118*, 4981–5079. https://doi.org/10.1021/acs.chemrev.7b00776.

63. Uzun, A., Ortalan, V., Browning, N.D., and Gates, B.C. (2010). A site-isolated mononuclear iridium complex catalyst supported on MgO: Characterization by spectroscopy and aberration-corrected scanning transmission electron microscopy. J. Catal. *269*, 318–328. https://doi.org/10.1016/j.jcat.2009.11.017.

64. Böldl, M., and Fleischer, I. (2019). Homogeneous nickel-catalyzed hydrogenations. In Homogeneous Hydrogenation with Non-Precious Catalysts (wiley), pp. 63–86. https://doi.org/10.1002/9783527814237.ch3.

65. Choi, H., Oh, S., Trung Tran, S.B., and Park, J.Y. (2019). Size-controlled model Ni catalysts on Ga2O3 for CO2 hydrogenation to methanol. J. Catal. *376*, 68–76. https://doi.org/10.1016/j.jcat.2019.06.051.

66. Wang, S., Wang, L., Wang, D., and Li, Y. (2023). Recent advances of single-atom catalysts in CO2 conversion. Energy Environ. Sci. *16*, 2759–2803. https://doi.org/10.1039/d3ee00037k.

67. Kim, K., Wagner, P., Wagner, K., and Mozer, A.J. (2022). Electrochemical CO2Reduction Catalyzed by Copper Molecular Complexes: The Influence of Ligand Structure. Energy Fuels *36*, 4653–4676. https://doi.org/10.1021/acs.energyfuels.2c00400.

68. Lee, H., Wu, X., and Sun, L. (2020). Copper-based homogeneous and heterogeneous catalysts for electrochemical water oxidation. Nanoscale *12*, 4187–4218. https://doi.org/10.1039/c9nr10437b.

69. Scotti, N., Bossola, F., Zaccheria, F., and Ravasio, N. (2020). Copper–zirconia catalysts: Powerful multifunctional catalytic tools to approach sustainable processes. Catalysts *10*, 168. https://doi.org/10.3390/catal10020168.

70. Syal, B., Kumar, P., and Gupta, P. (2023). Recent Advancements in the Preparation and Application of Copper Single-Atom Catalysts. ACS Appl. Nano Mater. *6*, 4987–5041. https://doi.org/10.1021/acsanm.2c05295.

71. Zhang, Z., Yang, Z., Liu, L., Wang, Y., and Kawi, S. (2023). Catalytic CO2 Conversion to C1 Chemicals over Single-Atom Catalysts (Preprint at John Wiley and Sons Inc). https://doi.org/10.1002/aenm.202301852.

72. Yang, T., Mao, X., Zhang, Y., Wu, X., Wang, L., Chu, M., Pao, C.W., Yang, S., Xu, Y., and Huang, X. (2021). Coordination tailoring of Cu single sites on C3N4 realizes selective CO2 hydrogenation at low temperature. Nat. Commun. *12*, 6022. https://doi.org/10.1038/s41467-021-26316-6.

73. Gao, R., Zhang, Q., Wang, H., Wang, F., Ren, J., Wang, X., Ma, X., and Wang, R. (2023). Synergic effect of covalent and chemical sulfur fixation enhancing the immobilization-conversion of polysulfides in lithium-sulfur batteries. J. Energy Chem. *79*, 1–11. https://doi.org/10.1016/j.jechem.2022.12.042.

74. Peng, M., Dong, C., Gao, R., Xiao, D., Liu, H., and Ma, D. (2021). Fully exposed cluster catalyst (FECC): Toward rich surface sites and full atom utilization efficiency. ACS Cent. Sci. *7*, 262–273. https://doi.org/10.1021/acscentsci.0c01486.

75. Hu, Q., Gao, K., Wang, X., Zheng, H., Cao, J., Mi, L., Huo, Q., Yang, H., Liu, J., and He, C. (2022). Subnanometric Ru clusters with upshifted D band center improve performance for alkaline hydrogen evolution reaction. Nat. Commun. *13*, 3958. https://doi.org/10.1038/s41467-022-31660-2.

76. Wu, Y., Wei, W., Yu, R., Xia, L., Hong, X., Zhu, J., Li, J., Lv, L., Chen, W., Zhao, Y., et al. (2022). Anchoring Sub-Nanometer Pt Clusters on Crumpled Paper-Like MXene Enables High Hydrogen Evolution Mass Activity. Adv. Funct. Mater. *32*, 20222110910. https://doi.org/10.1002/adfm.202110910.

77. Fang, L., Seifert, S., Winans, R.E., and Li, T. (2021). Operando XAS/SAXS: Guiding Design of Single-Atom and Subnanocluster Catalysts (Preprint at John Wiley and Sons Inc). https://doi.org/10.1002/smtd.202001194.

78. Dong, C., Li, Y., Cheng, D., Zhang, M., Liu, J., Wang, Y.G., Xiao, D., and Ma, D. (2020). Supported Metal Clusters: Fabrication and Application in Heterogeneous Catalysis. ACS Catal. *10*, 11011–11045. https://doi.org/10.1021/acscatal.0c02818.

79. Roduner, E. (2006). Size matters: Why nanomaterials are different. Chem. Soc. Rev. *35*, 583–592. https://doi.org/10.1039/b502142c.

80. Ishida, T., Murayama, T., Taketoshi, A., and Haruta, M. (2020). Importance of Size and Contact Structure of Gold Nanoparticles for the Genesis of Unique Catalytic Processes. Chem. Rev. *120*, 464–525. https://doi.org/10.1021/acs.chemrev.9b00551.

81. Beniya, A., and Higashi, S. (2019). Towards dense single-atom catalysts for future automotive applications. Nat. Catal. *2*, 590–602. https://doi.org/10.1038/s41929-019-0282-y.

82. van Deelen, T.W., Hernández Mejía, C., and de Jong, K.P. (2019). Control of Metal-Support Interactions in Heterogeneous Catalysts to Enhance Activity and Selectivity (Preprint at Nature Publishing Group). https://doi.org/10.1038/s41929-019-0364-x.

83. Yan, Q.Q., Wu, D.X., Chu, S.Q., Chen, Z.Q., Lin, Y., Chen, M.X., Zhang, J., Wu, X.J., and Liang, H.W. (2019). Reversing the charge transfer between platinum and sulfur-doped carbon support for electrocatalytic hydrogen evolution. Nat. Commun. *10*, 4977. https://doi.org/10.1038/s41467-019-12851-w.

84. Judai, K., Abbet, S., Wörz, A.S., Heiz, U., and Henry, C.R. (2004). Low-Temperature Cluster Catalysis. J. Am. Chem. Soc. *126*, 2732–2737. https://doi.org/10.1021/ja039037k.

85. Li, Z., Ji, S., Liu, Y., Cao, X., Tian, S., Chen, Y., Niu, Z., and Li, Y. (2020). Well-Defined Materials for Heterogeneous Catalysis: From Nanoparticles to Isolated Single-Atom Sites. Chem. Rev. *120*, 623–682. https://doi.org/10.1021/acs.chemrev.9b00311.

86. Gao, D., Zhou, H., Wang, J., Miao, S., Yang, F., Wang, G., Wang, J., and Bao, X. (2015). Size-Dependent Electrocatalytic Reduction of CO2 over Pd Nanoparticles. J. Am. Chem. Soc. *137*, 4288–4291. https://doi.org/10.1021/jacs.5b00046.

87. Chen, W., Ji, J., Feng, X., Duan, X., Qian, G., Li, P., Zhou, X., Chen, D., and Yuan, W. (2014). Mechanistic insight into size-dependent activity and durability in Pt/CNT catalyzed hydrolytic dehydrogenation of ammonia borane. J. Am. Chem. Soc. *136*, 16736–16739. https://doi.org/10.1021/ja509778y.

88. Qi, P., Wang, J., Djitcheu, X., He, D., Liu, H., and Zhang, Q. (2022). Techniques for the Characterization of Single Atom Catalysts (Preprint at Royal Society of Chemistry). https://doi.org/10.1039/d1ra07799f.

89. Uzun, A., Ortalan, V., Hao, Y., Browning, N.D., and Gates, B.C. (2009). Nanoclusters of gold on a high-area support: Almost uniform nanoclusters imaged by scanning transmission electron microscopy. ACS Nano *3*, 3691–3695. https://doi.org/10.1021/nn9008142.

90. Herzing, A.A., Kiely, C.J., Carley, A.F., Landon, P., and Hutchings, G.J. (2008). Identification of active gold nanoclusters on iron oxide supports for CO oxidation. Science *321*, 1331–1335. https://doi.org/10.1126/science.1159639.

91. Kaden, W.E., Wu, T., Kunkel, W.A., and Anderson, S.L. (2009). Electronic structure controls reactivity of size-selected pd clusters adsorbed on tio2 surfaces. Science *326*, 826–829. https://doi.org/10.1126/science.1180297.

92. Böhme, D.K., and Schwarz, H. (2005). Gas-phase catalysis by atomic and cluster metal ions: The ultimate single-site catalysts. Angew Chem. Int. Ed. Engl. *44*, 2336–2354. https://doi.org/10.1002/anie.200461698.

93. Song, B., Zhou, Y., Yang, H.M., Liao, J.H., Yang, L.M., Yang, X.B., and Ganz, E. (2019). Two-dimensional anti-Van't Hoff/Le Bel array AlB 6 with high stability, unique motif, triple dirac cones, and superconductivity. J. Am. Chem. Soc. *141*, 3630–3640. https://doi.org/10.1021/jacs.8b13075.

94. Yang, L.M., Bačić, V., Popov, I.A., Boldyrev, A.I., Heine, T., Frauenheim, T., and Ganz, E. (2015). Two-dimensional Cu2Si monolayer with planar hexacoordinate copper and silicon bonding. J. Am. Chem. Soc. *137*, 2757–2762. https://doi.org/10.1021/ja513209c.

95. Liu, J.H., Yang, L.M., and Ganz, E. (2018). Efficient and Selective Electroreduction of CO2 by Single-Atom Catalyst Two-Dimensional TM-Pc Monolayers. ACS Sustain. Chem. Eng. *6*, 15494–15502. https://doi.org/10.1021/acssuschemeng.8b03945.

96. Liu, J.H., Yang, L.M., and Ganz, E. (2019). Electrochemical reduction of CO 2 by single atom catalyst TM-TCNQ monolayers. J. Mater. Chem. A Mater. *7*, 3805–3814. https://doi.org/10.1039/c8ta08677j.

97. Liu, J.H., Yang, L.M., and Ganz, E. (2019). Electrocatalytic reduction of CO2 by two-dimensional transition metal porphyrin sheets. J. Mater. Chem. A Mater. *7*, 11944–11952. https://doi.org/10.1039/c9ta01188a.

98. Liu, J.H., Yang, L.M., and Ganz, E. (2019). Efficient electrocatalytic reduction of carbon dioxide by metal-doped β12-borophene monolayers. RSC Adv. *9*, 27710–27719. https://doi.org/10.1039/c9ra04135d.

99. Liu, J.H., Yang, L.M., and Ganz, E. (2019). Two-Dimensional Organometallic TM3–C12S12 Monolayers for Electrocatalytic Reduction of CO2. Energy &. Environ. Materials *2*, 193–200. https://doi.org/10.1002/eem2.12048.

100. Naguib, M., Kurtoglu, M., Presser, V., Lu, J., Niu, J., Heon, M., Hultman, L., Gogotsi, Y., and Barsoum, M.W. (2011). Two-dimensional nanocrystals produced by exfoliation of Ti 3AlC 2. Adv. Mater. *23*, 4248–4253. https://doi.org/10.1002/adma.201102306.

101. Alhabeb, M., Maleski, K., Anasori, B., Lelyukh, P., Clark, L., Sin, S., and Gogotsi, Y. (2017). Guidelines for Synthesis and Processing of Two-Dimensional Titanium Carbide (Ti3C2Tx MXene). Chem. Mater. *29*, 7633–7644. https://doi.org/10.1021/acs.chemmater.7b02847.

102. Chen, M.S., and Goodman, D.W. (2004). The structure of catalytically active gold on titania. Science *306*, 252–255. https://doi.org/10.1126/science.1102420.

103. Matthey, D., Wang, J.G., Wendt, S., Matthiesen, J., Schaub, R., Laegsgaard, E., Hammer, B., and Besenbacher, F. (2007). Enhanced Bonding

of Gold Nanoparticles on Oxidized TiO_2(110). Science *315*, 1692–1696. https://doi.org/10.1126/science.1135752.

104. Peng, Y., Ellis, B.D., Wang, X., Fettinger, J.C., and Power, P.P. (2009). Reversible reactions of ethylene with distannynes under ambient conditions. Science *325*, 1668–1670. https://doi.org/10.1126/science.1176443.

105. Thomas, J.M., Saghi, Z., and Gai, P.L. (2011). Can a single atom serve as the active site in some heterogeneous catalysts? Top. Catal. *54*, 588–594. https://doi.org/10.1007/s11244-011-9677-y.

106. Wang, Y., Mao, J., Meng, X., Yu, L., Deng, D., and Bao, X. (2019). Catalysis with Two-Dimensional Materials Confining Single Atoms: Concept, Design, and Applications. Chem. Rev. *119*, 1806–1854. https://doi.org/10.1021/acs.chemrev.8b00501.

107. Zhang, B.W., Wang, Y.X., Chou, S.L., Liu, H.K., and Dou, S.X. (2019). Fabrication of Superior Single-Atom Catalysts toward Diverse Electrochemical Reactions (Preprint at John Wiley and Sons Inc.). https://doi.org/10.1002/smtd.201800497.

108. Lü, F., Zhao, S., Guo, R., He, J., Peng, X., Bao, H., Fu, J., Han, L., Qi, G., Luo, J., et al. (2019). Nitrogen-coordinated single Fe sites for efficient electrocatalytic N2 fixation in neutral media. Nano Energy *61*, 420–427. https://doi.org/10.1016/j.nanoen.2019.04.092.

109. Lü, F., Bao, H., Mi, Y., Liu, Y., Sun, J., Peng, X., Qiu, Y., Zhuo, L., Liu, X., and Luo, J. (2020). Electrochemical CO2 reduction: From nanoclusters to single atom catalysts. Sustain. Energy Fuels *4*, 1012–1028. https://doi.org/10.1039/c9se00776h.

110. Yang, H., Wu, Y., Li, G., Lin, Q., Hu, Q., Zhang, Q., Liu, J., and He, C. (2019). Scalable Production of Efficient Single-Atom Copper Decorated Carbon Membranes for CO2 Electroreduction to Methanol. J. Am. Chem. Soc. *141*, 12717–12723. https://doi.org/10.1021/jacs.9b04907.

111. Thomas, J.M., Raja, R., Gai, P.L., Grönbeck, H., and Hernández-Garrido, J.C. (2010). Exceptionally Active Single-Site Nanocluster Multifunctional Catalysts for Cascade Reactions. ChemCatChem *2*, 402–406. https://doi.org/10.1002/cctc.200900258.

112. Gurudayal, G., Perone, D., Malani, S., Lum, Y., Haussener, S., and Ager, J.W. (2019). Sequential Cascade Electrocatalytic Conversion of Carbon Dioxide to C-C Coupled Products. ACS Appl. Energy Mater. *2*, 4551–4559. https://doi.org/10.1021/acsaem.9b00791.

113. Haas, T., Krause, R., Weber, R., Demler, M., and Schmid, G. (2018). Technical photosynthesis involving CO2 electrolysis and fermentation. Nat. Catal. *1*, 32–39. https://doi.org/10.1038/s41929-017-0005-1.

114. Cai, T., Sun, H., Qiao, J., Zhu, L., Zhang, F., Zhang, J., Tang, Z., Wei, X., Yang, J., Yuan, Q., et al. (2021). Cell-free chemoenzymatic starch synthesis from carbon dioxide. Science *373*, 1523–1527. https://doi.org/10.1126/science.abh4049.

115. Xie, Z., Xu, Y., Xie, M., Chen, X., Lee, J.H., Stavitski, E., Kattel, S., and Chen, J.G. (2020). Reactions of CO2 and ethane enable CO bond insertion for production of C3 oxygenates. Nat. Commun. *11*, 1887. https://doi.org/10.1038/s41467-020-15849-x.

116. Ye, R.P., Ding, J., Gong, W., Argyle, M.D., Zhong, Q., Wang, Y., Russell, C.K., Xu, Z., Russell, A.G., Li, Q., et al. (2019). CO2 hydrogenation to high-value products via heterogeneous catalysis. Nat. Commun. *10*, 5698. https://doi.org/10.1038/s41467-019-13638-9.

117. Cui, M., Qian, Q., Zhang, J., Wang, Y., Asare Bediako, B.B., Liu, H., and Han, B. (2021). Liquid fuel synthesis via CO2 hydrogenation by coupling homogeneous and heterogeneous catalysis. Chem *7*, 726–737. https://doi.org/10.1016/j.chempr.2020.12.005.

118. Gomez, E., Kattel, S., Yan, B., Yao, S., Liu, P., and Chen, J.G. (2018). Combining CO2 reduction with propane oxidative dehydrogenation over bimetallic catalysts. Nat. Commun. *9*, 1398. https://doi.org/10.1038/s41467-018-03793-w.

119. Ramirez, A., Gong, X., Caglayan, M., Nastase, S.A.F., Abou-Hamad, E., Gevers, L., Cavallo, L., Dutta Chowdhury, A., and Gascon, J. (2021). Selectivity descriptors for the direct hydrogenation of CO2 to hydrocarbons during zeolite-mediated bifunctional catalysis. Nat. Commun. *12*, 5914. https://doi.org/10.1038/s41467-021-26090-5.

120. Cui, X., Gao, P., Li, S., Yang, C., Liu, Z., Wang, H., Zhong, L., and Sun, Y. (2019). Selective Production of Aromatics Directly from Carbon Dioxide Hydrogenation. ACS Catal. *9*, 3866–3876. https://doi.org/10.1021/acscatal.9b00640.

121. Wei, J., Yao, R., Ge, Q., Wen, Z., Ji, X., Fang, C., Zhang, J., Xu, H., and Sun, J. (2018). Catalytic Hydrogenation of CO2 to Isoparaffins over Fe-Based Multifunctional Catalysts. ACS Catal. *8*, 9958–9967. https://doi.org/10.1021/acscatal.8b02267.

122. Agirrezabal-Telleria, I., Luz, I., Ortuño, M.A., Oregui-Bengoechea, M., Gandarias, I., López, N., Lail, M.A., and Soukri, M. (2019). Gas reactions under intrapore condensation regime within tailored metal–organic framework catalysts. Nat. Commun. *10*, 2076. https://doi.org/10.1038/s41467-019-10013-6.

123. Lee, S., Kim, D., and Lee, J. (2015). Electrocatalytic Production of C3-C4 Compounds by Conversion of CO 2 on a Chloride-Induced Bi-Phasic Cu 2 O-Cu Catalyst. Angew. Chem. *127*, 14914–14918. https://doi.org/10.1002/ange.201505730.

124. Ting, L.R.L., García-Muelas, R., Martín, A.J., Veenstra, F.L.P., Chen, S.T.J., Peng, Y., Per, E.Y.X., Pablo-García, S., López, N., Pérez-Ramírez, J., and Yeo, B.S. (2020). Electrochemical Reduction of Carbon Dioxide to 1-Butanol on Oxide-Derived Copper. Angew. Chem. Int. Ed. *59*, 21072–21079. https://doi.org/10.1002/anie.202008289.

125. Metzger, E.D., Brozek, C.K., Comito, R.J., and Dincă, M. (2016). Selective dimerization of ethylene to 1-butene with a porous catalyst. ACS Cent. Sci. *2*, 148–153. https://doi.org/10.1021/acscentsci.6b00012.

126. Ehrmaier, A., Liu, Y., Peitz, S., Jentys, A., Chin, Y.H.C., Sanchez-Sanchez, M., Bermejo-Deval, R., and Lercher, J. (2019). Dimerization of Linear Butenes on Zeolite-Supported Ni 2+. ACS Catal. *9*, 315–324. https://doi.org/10.1021/acscatal.8b03095.

127. Du, C., Mills, J.P., Yohannes, A.G., Wei, W., Wang, L., Lu, S., Lian, J.X., Wang, M., Guo, T., Wang, X., et al. (2023). Cascade electrocatalysis via AgCu single-atom alloy and Ag nanoparticles in CO2 electroreduction toward multicarbon products. Nat. Commun. *14*, 6142. https://doi.org/10.1038/s41467-023-41871-w.

128. Lee, S., Fan, C., Wu, T., and Anderson, S.L. (2004). CO Oxidation on Aun/TiO2 Catalysts Produced by Size-Selected Cluster Deposition. J. Am. Chem. Soc. *126*, 5682–5683. https://doi.org/10.1021/ja049436v.

129. Liu, L., Díaz, U., Arenal, R., Agostini, G., Concepción, P., and Corma, A. (2017). Generation of subnanometric platinum with high stability during transformation of a 2D zeolite into 3D. Nat. Mater. *16*, 132–138. https://doi.org/10.1038/nmat4757.

130. Choi, C.H., Kim, M., Kwon, H.C., Cho, S.J., Yun, S., Kim, H.T., Mayrhofer, K.J.J., Kim, H., and Choi, M. (2016). Tuning selectivity of electrochemical reactions by atomically dispersed platinum catalyst. Nat. Commun. *7*, 10922. https://doi.org/10.1038/ncomms10922.

131. Lee, M.G., Kandambeth, S., Li, X.Y., Shekhah, O., Ozden, A., Wicks, J., Ou, P., Wang, S., Dorakhan, R., Park, S., et al. (2024). Bimetallic Metal Sites in Metal-Organic Frameworks Facilitate the Production of 1-Butene from Electrosynthesized Ethylene. J. Am. Chem. Soc. *146*, 14267–14277. https://doi.org/10.1021/jacs.4c03806.

132. Kim, H., Shin, D., Yang, W., Won, D.H., Oh, H.S., Chung, M.W., Jeong, D., Kim, S.H., Chae, K.H., Ryu, J.Y., et al. (2021). Identification of Single-Atom Ni Site Active toward Electrochemical CO2Conversion to CO. J. Am. Chem. Soc. *143*, 925–933. https://doi.org/10.1021/jacs.0c11008.

133. Xie, H., Wang, T., Liang, J., Li, Q., and Sun, S. (2018). Cu-based Nanocatalysts for Electrochemical Reduction of CO2 (Preprint at Elsevier B.V.). https://doi.org/10.1016/j.nantod.2018.05.001.

134. Duan, X., Xu, J., Wei, Z., Ma, J., Guo, S., Wang, S., Liu, H., and Dou, S. (2017). Metal-Free Carbon Materials for CO2 Electrochemical

Reduction (Preprint at Wiley-VCH Verlag). https://doi.org/10.1002/adma.201701784.

135. Liu, Y., Su, X., Ding, J., Zhou, J., Liu, Z., Wei, X., Yang, H.B., and Liu, B. (2024). Progress and challenges in structural, in situ and operando characterization of single-atom catalysts by X-ray based synchrotron radiation techniques. Chem. Soc. Rev. *53*, 11850–11887. https://doi.org/10.1039/d3cs00967j.

136. Kottwitz, M., Li, Y., Wang, H., Frenkel, A.I., and Nuzzo, R.G. (2021). Single Atom Catalysts: A Review of Characterization Methods (Preprint at John Wiley and Sons Inc). https://doi.org/10.1002/cmtd.202100020.

137. Li, Q., Zhu, W., Fu, J., Zhang, H., Wu, G., and Sun, S. (2016). Controlled assembly of Cu nanoparticles on pyridinic-N rich graphene for electrochemical reduction of CO2 to ethylene. Nano Energy *24*, 1–9. https://doi.org/10.1016/j.nanoen.2016.03.024.

138. Fang, Y., and Flake, J.C. (2017). Electrochemical Reduction of CO2 at Functionalized Au Electrodes. J. Am. Chem. Soc. *139*, 3399–3405. https://doi.org/10.1021/jacs.6b11023.

139. Moura de Salles Pupo, M., and Kortlever, R. (2019). Electrolyte Effects on the Electrochemical Reduction of CO2 (Preprint at Wiley-VCH Verlag). https://doi.org/10.1002/cphc.201900680.

140. Huang, H., Jia, H., Liu, Z., Gao, P., Zhao, J., Luo, Z., Yang, J., and Zeng, J. (2017). Understanding of Strain Effects in the Electrochemical Reduction of CO 2 : Using Pd Nanostructures as an Ideal Platform. Angew. Chem. *129*, 3648–3652. https://doi.org/10.1002/ange.201612617.

141. Millet, M.M., Algara-Siller, G., Wrabetz, S., Mazheika, A., Girgsdies, F., Teschner, D., Seitz, F., Tarasov, A., Levchenko, S.V., Schlögl, R., and Frei, E. (2019). Ni Single Atom Catalysts for CO2Activation. J. Am. Chem. Soc. *141*, 2451–2461. https://doi.org/10.1021/jacs.8b11729.

142. Dongare, S., Singh, N., Bhunia, H., and Bajpai, P.K. (2021). Electrochemical reduction of CO2 using oxide based Cu and Zn bimetallic catalyst. Electrochim. Acta *392*, 138988. https://doi.org/10.1016/j.electacta.2021.138988.

143. Hsu, C.S., Wang, J., Chu, Y.C., Chen, J.H., Chien, C.Y., Lin, K.H., Tsai, L.D., Chen, H.C., Liao, Y.F., Hiraoka, N., et al. (2023). Activating dynamic atomic-configuration for single-site electrocatalyst in electrochemical CO2 reduction. Nat. Commun. *14*, 5245. https://doi.org/10.1038/s41467-023-40970-y.

144. Wang, M., Yao, Y., Tian, Y., Yuan, Y., Wang, L., Yang, F., Ren, J., Hu, X., Wu, F., Zhang, S., et al. (2023). Atomically Dispersed Manganese on Carbon Substrate for Aqueous and Aprotic CO2 Electrochemical Reduction. Adv. Mater. *35*, e2210658. https://doi.org/10.1002/adma.202210658.

145. Khan, H., Yerramilli, A.S., D'Oliveira, A., Alford, T.L., Boffito, D.C., and Patience, G.S. (2020). Experimental Methods in Chemical Engineering: X-Ray Diffraction Spectroscopy—XRD (Preprint at Wiley-Liss Inc.). https://doi.org/10.1002/cjce.23747.

146. Permyakova, A.A., Herranz, J., El Kazzi, M., Diercks, J.S., Povia, M., Mangani, L.R., Horisberger, M., Pătru, A., and Schmidt, T.J. (2019). On the Oxidation State of Cu2O upon Electrochemical CO2 Reduction: An XPS Study. ChemPhysChem *20*, 3120–3127. https://doi.org/10.1002/cphc.201900468.

147. Li, W., Seredych, M., Rodríguez-Castellón, E., and Bandosz, T.J. (2016). Metal-free Nanoporous Carbon as a Catalyst for Electrochemical Reduction of CO2 to CO and CH4. ChemSusChem *9*, 606–616. https://doi.org/10.1002/cssc.201501575.

148. Dutta, A., Rahaman, M., Hecker, B., Drnec, J., Kiran, K., Zelocualtecatl Montiel, I., Jochen Weber, D., Zanetti, A., Cedeño López, A., Martens, I., et al. (2020). CO2 electrolysis – Complementary operando XRD, XAS and Raman spectroscopy study on the stability of CuxO foam catalysts. J. Catal. *389*, 592–603. https://doi.org/10.1016/j.jcat.2020.06.024.

149. Amirbeigiarab, R., Tian, J., Herzog, A., Qiu, C., Bergmann, A., Roldan Cuenya, B., and Magnussen, O.M. (2023). Atomic-scale surface restructuring of copper electrodes under CO2 electroreduction conditions. Nat. Catal. *6*, 837–846. https://doi.org/10.1038/s41929-023-01009-z.

150. Chen, C., Li, J., Tan, X., Zhang, Y., Li, Y., He, C., Xu, Z., Zhang, C., and Chen, C. (2024). Harnessing single-atom catalysts for CO 2 electroreduction: a review of recent advances. EES Catal. *2*, 71–93. https://doi.org/10.1039/d3ey00150d.

151. Guo, W., Wang, Z., Wang, X., and Wu, Y. (2021). General Design Concept for Single-Atom Catalysts toward Heterogeneous Catalysis (Preprint at John Wiley and Sons Inc). https://doi.org/10.1002/adma.202004287.

152. Sun, Q., Jia, C., Zhao, Y., and Zhao, C. (2022). Single atom-based catalysts for electrochemical CO2 reduction. Preprint at Science Press *43*, 1547–1597. https://doi.org/10.1016/S1872-2067(21)64000-7.

153. Shang, X., Yang, X., Liu, G., Zhang, T., and Su, X. (2024). A molecular view of single-atom catalysis toward carbon dioxide conversion. Chem. Sci. *15*, 4631–4708. https://doi.org/10.1039/d3sc06863c.

154. Su, X., Yang, X.F., Huang, Y., Liu, B., and Zhang, T. (2019). Single-Atom Catalysis toward Efficient CO 2 Conversion to CO and Formate Products. Acc. Chem. Res. *52*, 656–664. https://doi.org/10.1021/acs.accounts.8b00478.

155. He, C., Gong, Y., Li, S., Wu, J., Lu, Z., Li, Q., Wang, L., Wu, S., and Zhang, J. (2024). Single-Atom Alloys Materials for CO2 and CH4 Catalytic Conversion (Preprint at John Wiley and Sons Inc). https://doi.org/10.1002/adma.202311628.

156. Loy, A.C.M., Teng, S.Y., How, B.S., Zhang, X., Cheah, K.W., Butera, V., Leong, W.D., Chin, B.L.F., Yiin, C.L., Taylor, M.J., et al. (2023). Elucidation of Single Atom Catalysts for Energy and Sustainable Chemical Production: Synthesis, Characterization and Frontier Science (Preprint at Elsevier Ltd). https://doi.org/10.1016/j.pecs.2023.101074.

157. Wang, H., Zhan, G., Tang, C., Yang, D., Liu, W., Wang, D., Wu, Y., Wang, H., Liu, K., Li, J., et al. (2023). Scalable Edge-Oriented Metallic Two-Dimensional Layered Cu2Te Arrays for Electrocatalytic CO2 Methanation. ACS Nano *17*, 4790–4799. https://doi.org/10.1021/acsnano.2c11227.

158. Fan, M., Miao, R.K., Ou, P., Xu, Y., Lin, Z.Y., Lee, T.J., Hung, S.F., Xie, K., Huang, J.E., Ni, W., et al. (2023). Single-site decorated copper enables energy- and carbon-efficient CO2 methanation in acidic conditions. Nat. Commun. *14*, 3314. https://doi.org/10.1038/s41467-023-38935-2.

159. Wang, Y., Zhu, Y., Zhu, X., Shi, J., Ren, X., Zhang, L., and Li, S. (2023). Selective Hydrogenation of CO2 to CH3OH on a Dynamically Magic Single-Cluster Catalyst: Cu3/MoS2/Ag(111). ACS Catal. *13*, 714–724. https://doi.org/10.1021/acscatal.2c05072.

160. Song, Q.W., Zhou, Z.H., and He, L.N. (2017). Efficient, Selective and Sustainable Catalysis of Carbon Dioxide (Preprint at Royal Society of Chemistry). https://doi.org/10.1039/c7gc00199a.

161. Zhang, H., Jin, X., Lee, J.M., and Wang, X. (2022). Tailoring of Active Sites from Single to Dual Atom Sites for Highly Efficient Electrocatalysis. ACS Nano *16*, 17572–17592. https://doi.org/10.1021/acsnano.2c06827.

162. Li, M., Wang, H., Luo, W., Sherrell, P.C., Chen, J., and Yang, J. (2020). Heterogeneous Single-Atom Catalysts for Electrochemical CO2 Reduction Reaction (Preprint at Wiley-VCH Verlag). https://doi.org/10.1002/adma.202001848.

163. Chen, S., Wang, B., Zhu, J., Wang, L., Ou, H., Zhang, Z., Liang, X., Zheng, L., Zhou, L., Su, Y.Q., et al. (2021). Lewis Acid Site-Promoted Single-Atomic Cu Catalyzes Electrochemical CO2Methanation. Nano Lett. *21*, 7325–7331. https://doi.org/10.1021/acs.nanolett.1c02502.

164. Naguib, M., Mochalin, V.N., Barsoum, M.W., and Gogotsi, Y. (2014). 25th anniversary article: MXenes: A new family of two-dimensional materials. Adv. Mater. *26*, 992–1005. https://doi.org/10.1002/adma.201304138.

165. Zhao, Q., Zhang, C., Hu, R., Du, Z., Gu, J., Cui, Y., Chen, X., Xu, W., Cheng, Z., Li, S., et al. (2021). Selective Etching Quaternary MAX Phase toward Single Atom Copper Immobilized MXene (Ti3C2Clx) for Efficient CO2Electroreduction to Methanol. ACS Nano *15*, 4927–4936. https://doi.org/10.1021/acsnano.0c09755.

166. Zhao, D., Chen, Z., Yang, W., Liu, S., Zhang, X., Yu, Y., Cheong, W.C., Zheng, L., Ren, F., Ying, G., et al. (2019). MXene (Ti 3 C 2)

Vacancy-Confined Single-Atom Catalyst for Efficient Functionalization of CO 2. J. Am. Chem. Soc. *141*, 4086–4093. https://doi.org/10.1021/jacs.8b13579.

167. Zhao, S., Wen, Y., Peng, X., Mi, Y., Liu, X., Liu, Y., Zhuo, L., Hu, G., Luo, J., and Tang, X. (2020). Isolated single-atom Pt sites for highly selective electrocatalytic hydrogenation of formaldehyde to methanol. J. Mater. Chem. A Mater. *8*, 8913–8919. https://doi.org/10.1039/d0ta00190b.

168. Chang, B., Wu, S., Wang, Y., Sun, T., and Cheng, Z. (2022). Emerging single-atom iron catalysts for advanced catalytic systems. Nanoscale Horiz. *7*, 1340–1387. https://doi.org/10.1039/d2nh00362g.

169. Yan, Y., Cheng, H., Qu, Z., Yu, R., Liu, F., Ma, Q., Zhao, S., Hu, H., Cheng, Y., Yang, C., et al. (2021). Recent progress on the synthesis and oxygen reduction applications of Fe-based single-atom and double-atom catalysts. J. Mater. Chem. A *9*, 19489–19507. https://doi.org/10.1039/d1ta02769g.

170. Qi, K., Chhowalla, M., and Voiry, D. (2020). Single Atom Is Not Alone: Metal–Support Interactions in Single-Atom Catalysis (Preprint at Elsevier B.V.). https://doi.org/10.1016/j.mattod.2020.07.002.

171. Hossain, M.N., Zhang, L., Neagu, R., and Rassachack, E. (2024). Free-Standing Single-Atom Catalyst-Based Electrodes for CO2 Reduction. Preprint at Springer *7*, 5. https://doi.org/10.1007/s41918-023-00193-7.

172. Liu, Q., Wang, Y., Hu, Z., and Zhang, Z. (2021). Iron-based single-atom electrocatalysts: synthetic strategies and applications. RSC Adv. *11*, 3079–3095. https://doi.org/10.1039/d0ra08223f.

173. Li, Y., Li, Y., Sun, H., Gao, L., Jin, X., Li, Y., LV, Z., Xu, L., Liu, W., and Sun, X. (2024). Current Status and Perspectives of Dual-Atom Catalysts towards Sustainable Energy Utilization (Preprint at Springer Science and Business Media B.V). https://doi.org/10.1007/s40820-024-01347-y.

174. Takele Menisa, L., Cheng, P., Qiu, X., Zheng, Y., Huang, X., Gao, Y., and Tang, Z. (2022). Single atomic Fe-N4 active sites and neighboring graphitic nitrogen for efficient and stable electrochemical CO2 reduction. Nanoscale Horiz. *7*, 916–923. https://doi.org/10.1039/d2nh00143h.

175. Li, Z., Jiang, J., Liu, X., Zhu, Z., Wang, J., He, Q., Kong, Q., Niu, X., Chen, J.S., Wang, J., and Wu, R. (2022). Coupling Atomically Dispersed Fe–N5 Sites with Defective N-Doped Carbon Boosts CO2 Electroreduction. Small *18*, e2203495. https://doi.org/10.1002/smll.202203495.

176. Pan, F., Li, B., Sarnello, E., Fei, Y., Gang, Y., Xiang, X., Du, Z., Zhang, P., Wang, G., Nguyen, H.T., et al. (2020). Atomically Dispersed Iron-Nitrogen Sites on Hierarchically Mesoporous Carbon Nanotube and Graphene Nanoribbon Networks for CO2 Reduction. ACS Nano *14*, 5506–5516. https://doi.org/10.1021/acsnano.9b09658.

177. Gu, J., Hsu, C.-S., Bai, L., Ming Chen, H., and Hu, X. (2019). Atomically dispersed Fe^{3+} sites catalyze efficient CO_2 electroreduction to CO. Science *364*, 1091–1094. https://doi.org/10.1126/science.aaw7515.

178. Sharma, P.P., Wu, J., Yadav, R.M., Liu, M., Wright, C.J., Tiwary, C.S., Yakobson, B.I., Lou, J., Ajayan, P.M., and Zhou, X. (2015). Nitrogen-Doped Carbon Nanotube Arrays for High-Efficiency Electrochemical Reduction of CO 2 : On the Understanding of Defects, Defect Density, and Selectivity. Angew. Chem. *127*, 13905–13909. https://doi.org/10.1002/ange.201506062.

179. Vajda, S., Pellin, M.J., Greeley, J.P., Marshall, C.L., Curtiss, L.A., Ballentine, G.A., Elam, J.W., Catillon-Mucherie, S., Redfern, P.C., Mehmood, F., and Zapol, P. (2009). Subnanometre platinum clusters as highly active and selective catalysts for the oxidative dehydrogenation of propane. Nat. Mater. *8*, 213–216. https://doi.org/10.1038/nmat2384.

180. Umar, M., Abdulazeez, I., Tanimu, A., Ganiyu, S.A., and Alhooshani, K. (2024). Synergistic effect of CexOy and Zn ion within the ZIF-zni framework for enhanced electrocatalytic reduction of CO2. J. Environ. Chem. Eng. *12*, 112899. https://doi.org/10.1016/j.jece.2024.112899.

181. Jiao, L., and Jiang, H.L. (2019). Metal-Organic-Framework-Based Single-Atom Catalysts for Energy Applications (Preprint at Elsevier Inc). https://doi.org/10.1016/j.chempr.2018.12.011.

182. Huang, H., Shen, K., Chen, F., and Li, Y. (2020). Metal-organic frameworks as a good platform for the fabrication of single-atom catalysts. ACS Catal. *10*, 6579–6586. https://doi.org/10.1021/acscatal.0c01459.

183. Wang, D., and Zhao, Y. (2021). Single-atom Engineering of Metal-Organic Frameworks toward Healthcare (Preprint at Elsevier Inc.). https://doi.org/10.1016/j.chempr.2021.08.020.

184. Zhou, D., Li, X., Shang, H., Qin, F., and Chen, W. (2021). Atomic regulation of metal-organic framework derived carbon-based single-atom catalysts for the electrochemical CO2reduction reaction. J. Mater. Chem. A *9*, 23382–23418. https://doi.org/10.1039/d1ta06915b.

185. Nwosu, U., and Siahrostami, S. (2023). Copper-based metal-organic frameworks for CO2 reduction: selectivity trends, design paradigms, and perspectives. Catal. Sci. Technol. *13*, 3740–3761. https://doi.org/10.1039/d3cy00408b.

186. Feng, D., Zhou, L., White, T.J., Cheetham, A.K., Ma, T., and Wei, F. (2023). Nanoengineering Metal–Organic Frameworks and Derivatives for Electrosynthesis of Ammonia (Preprint at Springer Science and Business Media B.V). https://doi.org/10.1007/s40820-023-01169-4.

187. Li, C., Ji, Y., Wang, Y., Liu, C., Chen, Z., Tang, J., Hong, Y., Li, X., Zheng, T., Jiang, Q., et al. (2023). Applications of Metal–Organic Frameworks and Their Derivatives in Electrochemical CO2 Reduction (Preprint at Springer Science and Business Media B.V). https://doi.org/10.1007/s40820-023-01092-8.

188. Li, C., Zhang, H., Liu, M., Lang, F.-F., Pang, J., and Bu, X.-H. (2023). Recent progress in metal–organic frameworks (MOFs) for electrocatalysis. Ind. Chem. Mater. *1*, 9–38. https://doi.org/10.1039/d2im00063f.

189. Zhou, Y., Zhou, Q., Liu, H., Xu, W., Wang, Z., Qiao, S., Ding, H., Chen, D., Zhu, J., Qi, Z., et al. (2023). Asymmetric dinitrogen-coordinated nickel single-atomic sites for efficient CO2 electroreduction. Nat. Commun. *14*, 3776. https://doi.org/10.1038/s41467-023-39505-2.

190. Akri, M., Zhao, S., Li, X., Zang, K., Lee, A.F., Isaacs, M.A., Xi, W., Gangarajula, Y., Luo, J., Ren, Y., et al. (2019). Atomically dispersed nickel as coke-resistant active sites for methane dry reforming. Nat. Commun. *10*, 5181. https://doi.org/10.1038/s41467-019-12843-w.

191. Jiao, J., Yuan, Q., Tan, M., Han, X., Gao, M., Zhang, C., Yang, X., Shi, Z., Ma, Y., Xiao, H., et al. (2023). Constructing asymmetric double-atomic sites for synergistic catalysis of electrochemical CO2 reduction. Nat. Commun. *14*, 6164. https://doi.org/10.1038/s41467-023-41863-w.

192. Chhetri, M., Wan, M., Jin, Z., Yeager, J., Sandor, C., Rapp, C., Wang, H., Lee, S., Bodenschatz, C.J., Zachman, M.J., et al. (2023). Dual-site catalysts featuring platinum-group-metal atoms on copper shapes boost hydrocarbon formations in electrocatalytic CO2 reduction. Nat. Commun. *14*, 3075. https://doi.org/10.1038/s41467-023-38777-y.

193. Wang, H., Kang, X., and Han, B. (2024). Rare-earth Element-Based Electrocatalysts Designed for CO2 Electro-Reduction (Preprint at John Wiley and Sons Inc). https://doi.org/10.1002/cssc.202301539.

194. Hu, C., Bai, S., Gao, L., Liang, S., Yang, J., Cheng, S.D., Mi, S.B., and Qiu, J. (2019). Porosity-Induced High Selectivity for CO2 Electroreduction to CO on Fe-Doped ZIF-Derived Carbon Catalysts. ACS Catal. *9*, 11579–11588. https://doi.org/10.1021/acscatal.9b03175.

195. Zhang, X., Guo, S.X., Gandionco, K.A., Bond, A.M., and Zhang, J. (2020). Electrocatalytic Carbon Dioxide Reduction: From Fundamental Principles to Catalyst Design (Preprint at Elsevier Ltd). https://doi.org/10.1016/j.mtadv.2020.100074.

196. Yang, Y., and Liu, S. (2024). Theoretical Insights into Dual-Atomic Catalysts for Electrochemical CO2 Reduction. J. Phys. Chem. C *128*, 6269–6279. https://doi.org/10.1021/acs.jpcc.3c08289.

197. Wang, X., Xu, L., Li, C., Zhang, C., Yao, H., Xu, R., Cui, P., Zheng, X., Gu, M., Lee, J., et al. (2023). Developing a class of dual atom materials for multifunctional catalytic reactions. Nat. Commun. *14*, 7210. https://doi.org/10.1038/s41467-023-42756-8.

198. Hao, Q., Zhong, H.x., Wang, J.z., Liu, K.h., Yan, J.m., Ren, Z.h., Zhou, N., Zhao, X., Zhang, H., Liu, D.x., et al. (2022). Nickel dual-atom sites for

electrochemical carbon dioxide reduction. Nat. Synth. *1*, 719–728. https://doi.org/10.1038/s44160-022-00138-w.

199. Zhang, Y., Liu, T., Wang, X., Dang, Q., Zhang, M., Zhang, S., Li, X., Tang, S., and Jiang, J. (2022). Dual-Atom Metal and Nonmetal Site Catalyst on a Single Nickel Atom Supported on a Hybridized BCN Nanosheet for Electrochemical CO2Reduction to Methane: Combining High Activity and Selectivity. ACS Appl. Mater. Interfaces *14*, 9073–9083. https://doi.org/10.1021/acsami.1c22761.

200. Liu, X.-H., Jia, X.-L., Zhao, Y.-L., Zheng, R.-X., Meng, Q.-L., Liu, C.-P., Xing, W., and Xiao, M.-L. (2023). Recent advances in nickel-based catalysts for electrochemical reduction of carbon dioxide. Advanced Sensor and Energy Materials *2*, 100073. https://doi.org/10.1016/j.asems.2023.100073.

201. Daiyan, R., Zhu, X., Tong, Z., Gong, L., Razmjou, A., Liu, R.S., Xia, Z., Lu, X., Dai, L., and Amal, R. (2020). Transforming active sites in nickel–nitrogen–carbon catalysts for efficient electrochemical CO2 reduction to CO. Nano Energy *78*, 105213. https://doi.org/10.1016/j.nanoen.2020.105213.

202. Zhang, H., Lu, X.F., Wu, Z.P., and Lou, X.W.D. (2020). Emerging Multifunctional Single-Atom Catalysts/Nanozymes. ACS Cent. Sci. *6*, 1288–1301. https://doi.org/10.1021/acscentsci.0c00512.

203. Yu, Y., Zhu, Z., and Huang, H. (2024). Surface Engineered Single-Atom Systems for Energy Conversion (Preprint at John Wiley and Sons Inc). https://doi.org/10.1002/adma.202311148.

204. Zhou, L.L., Liu, P.X., Ding, Y., Xi, J.R., Liu, L.J., Wang, W.K., and Xu, J. (2022). Hierarchically porous structure of two-dimensional nano-flakes assembled flower-like NiO promotes the formation of surface-activated complex during persulfate activation. Chem. Eng. J. *430*, 133134. https://doi.org/10.1016/j.cej.2021.133134.

205. Cho, Y.S., and Kang, J. (2024). Two-dimensional materials as catalysts, interfaces, and electrodes for an efficient hydrogen evolution reaction. Nanoscale *16*, 3936–3950. https://doi.org/10.1039/d4nr00147h.

206. Gandionco, K.A., Kim, J., Bekaert, L., Hubin, A., and Lim, J. (2024). Single-atom Catalysts for the Electrochemical Reduction of Carbon Dioxide into Hydrocarbons and Oxygenates (Preprint at John Wiley and Sons Inc). https://doi.org/10.1002/cey2.410.

207. Wang, J., and Luo, X. (2024). Theoretical Investigation of the BCN Monolayer and Their Derivatives for Metal-free CO2 Photocatalysis, Capture, and Utilization. ACS Omega *9*, 3772–3780. https://doi.org/10.1021/acsomega.3c07795.

208. Yang, M., Qin, B., Si, C., Sun, X.Y., and Li, B. (2023). Electrochemical Reactions Catalyzed by Carbon Dots from Computational Investigations: Functional Groups, Dopants, and Defects (Preprint at Royal Society of Chemistry). https://doi.org/10.1039/d3ta06361e.

209. Nguyen, D.L.T., Kim, Y., Hwang, Y.J., and Won, D.H. (2020). Progress in Development of Electrocatalyst for CO2 Conversion to Selective CO Production (Preprint at Blackwell Publishing Inc.). https://doi.org/10.1002/cey2.27.

210. Wu, Y., Chen, C., Yan, X., Sun, X., Zhu, Q., Li, P., Li, Y., Liu, S., Ma, J., Huang, Y., and Han, B. (2021). Boosting CO2 Electroreduction over a Cadmium Single-Atom Catalyst by Tuning of the Axial Coordination Structure. Angew Chem. Int. Ed. Engl. *60*, 20803–20810. https://doi.org/10.1002/anie.202105263.

211. Li, J., Chen, C., Xu, L., Zhang, Y., Wei, W., Zhao, E., Wu, Y., and Chen, C. (2023). Challenges and Perspectives of Single-Atom-Based Catalysts for Electrochemical Reactions. JACS Au *3*, 736–755. https://doi.org/10.1021/jacsau.3c00001.

212. Wang, S., Zhou, P., Zhou, L., Lv, F., Sun, Y., Zhang, Q., Gu, L., Yang, H., and Guo, S. (2021). A Unique Gas-Migration, Trapping, and Emitting Strategy for High-Loading Single Atomic Cd Sites for Carbon Dioxide Electroreduction. Nano Lett. *21*, 4262–4269. https://doi.org/10.1021/acs.nanolett.1c00432.

213. Harthi, A., Abri, M.A., Younus, H.A., and Hajri, R.A. (2024). Criteria and cutting-edge catalysts for CO_2 electrochemical reduction at the industrial scale. J. CO2 Util. *83*, 102819. https://doi.org/10.1016/j.jcou.2024.102819.

214. Peter, S.C. (2018). Reduction of CO2 to Chemicals and Fuels: A Solution to Global Warming and Energy Crisis. ACS Energy Lett. *3*, 1557–1561. https://doi.org/10.1021/acsenergylett.8b00878.

215. Li, X., Wu, X., Lv, X., Wang, J., and Wu, H.B. (2022). Recent Advances in Metal-Based Electrocatalysts with Hetero-Interfaces for CO2 Reduction Reaction (Preprint at Elsevier Inc.). https://doi.org/10.1016/j.checat.2021.10.015.

216. Fan, W.K., and Tahir, M. (2021). Recent trends in developments of active metals and heterogenous materials for catalytic CO2hydrogenation to renewable methane: A review. J. Environ. Chem. Eng. *9*, 105460. https://doi.org/10.1016/j.jece.2021.105460.

217. Yin, H., Pan, R., Zou, M., Ge, X., Shi, C., Yuan, J., Huang, C., and Xie, H. (2024). Recent Advances in Carbon-Based Single-Atom Catalysts for Electrochemical Oxygen Reduction to Hydrogen Peroxide in Acidic Media. Nanomaterials *14*, 835. https://doi.org/10.3390/nano14100835.

218. Gong, Q., Ding, P., Xu, M., Zhu, X., Wang, M., Deng, J., Ma, Q., Han, N., Zhu, Y., Lu, J., et al. (2019). Structural defects on converted bismuth oxide nanotubes enable highly active electrocatalysis of carbon dioxide reduction. Nat. Commun. *10*, 2807. https://doi.org/10.1038/s41467-019-10819-4.

219. Wicks, J., Jue, M.L., Beck, V.A., Oakdale, J.S., Dudukovic, N.A., Clemens, A.L., Liang, S., Ellis, M.E., Lee, G., Baker, S.E., et al. (2021). 3D-Printable Fluoropolymer Gas Diffusion Layers for CO2 Electroreduction. Adv. Mater. *33*, e2003855. https://doi.org/10.1002/adma.202003855.

220. Zhu, Z., Jiang, T., Ali, M., Meng, Y., Jin, Y., Cui, Y., and Chen, W. (2022). Rechargeable Batteries for Grid Scale Energy Storage. Chem. Rev. *122*, 16610–16751. https://doi.org/10.1021/acs.chemrev.2c00289.

221. Kibria, M.G., Edwards, J.P., Gabardo, C.M., Dinh, C.T., Seifitokaldani, A., Sinton, D., and Sargent, E.H. (2019). Electrochemical CO2 Reduction into Chemical Feedstocks: From Mechanistic Electrocatalysis Models to System Design (Preprint at Wiley-VCH Verlag). https://doi.org/10.1002/adma.201807166.

222. Ahmad, T., Liu, S., Sajid, M., Li, K., Ali, M., Liu, L., and Chen, W. (2022). Electrochemical CO2 Reduction to C2+ Products Using Cu-Based Electrocatalysts: A Review (Preprint at Tsinghua University Press). https://doi.org/10.26599/NRE.2022.9120021.

223. Dresselhaus, M.S. (2001). Solid State Physics, Part IV: Superconducting Properties of Solids. 6.732, Fall. World J. Condens. Matt. Phys. *5*. https://www.scirp.org/reference/referencespapers?referenceid=1532973.

224. Whipple, D.T., and Kenis, P.J.A. (2010). Prospects of CO2 utilization via direct heterogeneous electrochemical reduction. J. Phys. Chem. Lett. *1*, 3451–3458. https://doi.org/10.1021/jz1012627.

225. Olah, G.A., Prakash, G.K.S., and Goeppert, A. (2011). Anthropogenic chemical carbon cycle for a sustainable future. J. Am. Chem. Soc. *133*, 12881–12898. https://doi.org/10.1021/ja202642y.

226. Zhang, Y.J., Sethuraman, V., Michalsky, R., and Peterson, A.A. (2014). Competition between CO2 reduction and H2 evolution on transition-metal electrocatalysts. ACS Catal. *4*, 3742–3748. https://doi.org/10.1021/cs5012298.

227. Zhu, D.D., Liu, J.L., and Qiao, S.Z. (2016). Recent Advances in Inorganic Heterogeneous Electrocatalysts for Reduction of Carbon Dioxide (Preprint at Wiley-VCH Verlag). https://doi.org/10.1002/adma.201504766.

228. Zhang, L., Zhao, Z., and Gong, J. (2017). Nanostrukturierte Materialien für die elektrokatalytische CO 2 -Reduktion und ihre Reaktionsmechanismen. Angew. Chem. *129*, 11482–11511. https://doi.org/10.1002/ange.201612214.

229. Cheng, Q., Wang, M., Ni, J., Zhang, L., Cheng, Y., Zhou, X., Cao, Y., Qian, T., and Yan, C. (2023). Comprehensive Understanding and Rational Regulation of Microenvironment for Gas-Involving Electrochemical

Reactions (Preprint at John Wiley and Sons Inc). https://doi.org/10.1002/cey2.307.

230. Liu, M., Pang, Y., Zhang, B., De Luna, P., Voznyy, O., Xu, J., Zheng, X., Dinh, C.T., Fan, F., Cao, C., et al. (2016). Enhanced electrocatalytic CO2 reduction via field-induced reagent concentration. Nature *537*, 382–386. https://doi.org/10.1038/nature19060.

231. Ham, Y.S., Choe, S., Kim, M.J., Lim, T., Kim, S.K., and Kim, J.J. (2017). Electrodeposited Ag catalysts for the electrochemical reduction of CO2 to CO. Appl. Catal., B *208*, 35–43. https://doi.org/10.1016/j.apcatb.2017.02.040.

232. Lei, F., Liu, W., Sun, Y., Xu, J., Liu, K., Liang, L., Yao, T., Pan, B., Wei, S., and Xie, Y. (2016). Metallic tin quantum sheets confined in graphene toward high-efficiency carbon dioxide electroreduction. Nat. Commun. *7*, 12697. https://doi.org/10.1038/ncomms12697.

233. Yan, C., Lin, L., Gao, D., Wang, G., and Bao, X. (2018). Selective CO2 electroreduction over an oxide-derived gallium catalyst. J. Mater. Chem. A Mater. *6*, 19743–19749. https://doi.org/10.1039/c8ta08613c.

234. Klinkova, A., De Luna, P., Dinh, C.T., Voznyy, O., Larin, E.M., Kumacheva, E., and Sargent, E.H. (2016). Rational Design of Efficient Palladium Catalysts for Electroreduction of Carbon Dioxide to Formate. ACS Catal. *6*, 8115–8120. https://doi.org/10.1021/acscatal.6b01719.

235. Handoko, A.D., Steinmann, S.N., and Seh, Z.W. (2019). Theory-guided Materials Design: Two-Dimensional MXenes in Electro- and Photocatalysis (Preprint at Royal Society of Chemistry). https://doi.org/10.1039/c9nh00100j.

236. Lim, K.R.G., Handoko, A.D., Nemani, S.K., Wyatt, B., Jiang, H.Y., Tang, J., Anasori, B., and Seh, Z.W. (2020). Rational Design of Two-Dimensional Transition Metal Carbide/Nitride (MXene) Hybrids and Nanocomposites for Catalytic Energy Storage and Conversion. ACS Nano *14*, 10834–10864. https://doi.org/10.1021/acsnano.0c05482.

237. Zhang, S., Fan, Q., Xia, R., and Meyer, T.J. (2020). CO2 Reduction: From Homogeneous to Heterogeneous Electrocatalysis. Acc. Chem. Res. *53*, 255–264. https://doi.org/10.1021/acs.accounts.9b00496.

238. Regulacio, M.D., Wang, Y., Seh, Z.W., and Han, M.Y. (2018). Tailoring Porosity in Copper-Based Multinary Sulfide Nanostructures for Energy, Biomedical, Catalytic, and Sensing Applications. ACS Appl. Nano Mater. *1*, 3042–3062. https://doi.org/10.1021/acsanm.8b00639.

239. Zhang, Z., Li, S., Zhang, Z., Chen, Z., Wang, H., Meng, X., Cui, W., Qi, X., and Wang, J. (2024). A Review on Electrocatalytic CO2 Conversion via C–C and C–N Coupling (Preprint at John Wiley and Sons Inc). https://doi.org/10.1002/cey2.513.

240. Wang, Z., Wang, F., Peng, Y., Zheng, Z., and Han, Y. (2012). Imaging the homogeneous nucleation during the melting of superheated colloidal crystals. Science *338*, 87–90. https://doi.org/10.1126/science.1224763.

241. Liu, S., Yang, H.B., Hung, S., Ding, J., Cai, W., Liu, L., Gao, J., Li, X., Ren, X., Kuang, Z., et al. (2020). Elucidating the Electrocatalytic CO 2 Reduction Reaction over a Model Single-Atom Nickel Catalyst. Angew. Chem. *132*, 808–813. https://doi.org/10.1002/ange.201911995.

242. Li, X., Bi, W., Chen, M., Sun, Y., Ju, H., Yan, W., Zhu, J., Wu, X., Chu, W., Wu, C., and Xie, Y. (2017). Exclusive Ni-N4 Sites Realize Near-Unity CO Selectivity for Electrochemical CO2 Reduction. J. Am. Chem. Soc. *139*, 14889–14892. https://doi.org/10.1021/jacs.7b09074.

243. Cai, Y., Fu, J., Zhou, Y., Chang, Y.C., Min, Q., Zhu, J.J., Lin, Y., and Zhu, W. (2021). Insights on forming N,O-coordinated Cu single-atom catalysts for electrochemical reduction CO2 to methane. Nat. Commun. *12*, 586. https://doi.org/10.1038/s41467-020-20769-x.

244. Mosaad Awad, M., Hussain, I., Ahmed Taialla, O., Ganiyu, S.A., and Alhooshani, K. (2024). Unveiling the catalytic performance of unique core-fibrous shell silica-lanthanum oxide with different nickel loadings for dry reforming of methane. Energy Convers. Manag. *311*, 118508. https://doi.org/10.1016/j.enconman.2024.118508.

245. Mosaad Awad, M., Hussain, I., Mustapha, U., Ahmed Taialla, O., Musa Alhassan, A., Kotob, E., Shafiu Abdullahi, A., Ganiyu, S.A., and Alhooshani, K. (2023). A critical review of recent advancements in catalytic dry reforming of methane: Physicochemical properties, Current Challenges, and Informetric Insights. Chemistry *19*, e202300641. https://doi.org/10.1002/asia.202300641.

246. Kaiser, S.K., Chen, Z., Faust Akl, D., Mitchell, S., and Pérez-Ramírez, J. (2020). Single-Atom Catalysts across the Periodic Table. Chem. Rev. *120*, 11703–11809. https://doi.org/10.1021/acs.chemrev.0c00576.

247. Tang, Y., Wei, Y., Wang, Z., Zhang, S., Li, Y., Nguyen, L., Li, Y., Zhou, Y., Shen, W., Tao, F.F., and Hu, P. (2019). Synergy of single-atom Ni1 and Ru1 sites on CeO2 for dry reforming of CH4. J. Am. Chem. Soc. *141*, 7283–7293. https://doi.org/10.1021/jacs.8b10910.

248. Shen, D., Li, Z., Shan, J., Yu, G., Wang, X., Zhang, Y., Liu, C., Lyu, S., Li, J., and Li, L. (2022). Synergistic Pt-CeO2 interface boosting low temperature dry reforming of methane. Appl. Catal., B *318*, 121809. https://doi.org/10.1016/j.apcatb.2022.121809.

249. Wu, J., Qiao, L.Y., Zhou, Z.F., Cui, G.J., Zong, S.S., Xu, D.J., Ye, R.P., Chen, R.P., Si, R., and Yao, Y.G. (2019). Revealing the Synergistic Effects of Rh and Substituted La 2 B 2 O 7 (B = Zr or Ti) for Preserving the Reactivity of Catalyst in Dry Reforming of Methane. ACS Catal. *9*, 932–945. https://doi.org/10.1021/acscatal.8b03319.

250. Zhou, R., Mohamedali, M., Ren, Y., Lu, Q., and Mahinpey, N. (2022). Facile synthesis of multi-layered nanostructured Ni/CeO2 catalyst plus in-situ pre-treatment for efficient dry reforming of methane. Appl. Catal., B *316*, 121696. https://doi.org/10.1016/j.apcatb.2022.121696.

251. Song, Y., Ozdemir, E., Ramesh, S., Adishev, A., Subramanian, S., Harale, A., Albuali, M., Fadhel, B.A., Jamal, A., Moon, D., et al. (2020). Dry reforming of methane by stable Ni–Mo nanocatalysts on single-crystalline MgO. Science *367*, 777–781. https://doi.org/10.1126/science.aav2412.

252. Kim, S., Lauterbach, J., and Sasmaz, E. (2021). Yolk-Shell Pt-NiCe@SiO2Single-Atom-Alloy Catalysts for Low-Temperature Dry Reforming of Methane. ACS Catal. *11*, 8247–8260. https://doi.org/10.1021/acscatal.1c01223.

253. Rao, Z., Wang, K., Cao, Y., Feng, Y., Huang, Z., Chen, Y., Wei, S., Liu, L., Gong, Z., Cui, Y., et al. (2023). Light-Reinforced Key Intermediate for Anticoking To Boost Highly Durable Methane Dry Reforming over Single Atom Ni Active Sites on CeO2. J. Am. Chem. Soc. *145*, 24625–24635. https://doi.org/10.1021/jacs.3c07077.

254. Li, J., Du, C., Feng, Q., Zhao, Y., Liu, S., Xu, J., Hu, M., Zeng, Z., Zhang, Z., Shen, H., et al. (2024). Evolution and performances of Ni single atoms trapped by mesoporous ceria in Dry Reforming of Methane. Appl. Catal., B *354*, 124069. https://doi.org/10.1016/j.apcatb.2024.124069.

255. Zhang, Z.Y., Huang, Z.X., Yu, X.Y., Chen, L., Ou, H.H., Tang, Z.Y., Li, T., Xu, B.Y., He, Y.L., and Xie, T. (2024). Photo-thermal coupled single-atom catalysis boosting dry reforming of methane beyond thermodynamic limits over high equivalent flow. Nano Energy *123*, 109401. https://doi.org/10.1016/j.nanoen.2024.109401.

256. Mekkering, M.J., Biemolt, J., de Graaf, J., Lin, Y.A., van Leest, N.P., Troglia, A., Bliem, R., de Bruin, B., Rothenberg, G., and Yan, N. (2023). Dry reforming of methane over single-atom Rh/Al2O3 catalysts prepared by exsolution. Catal. Sci. Technol. *13*, 2255–2260. https://doi.org/10.1039/d2cy02126a.

257. Malta, G., Kondrat, S.A., Freakley, S.J., Davies, C.J., Lu, L., Dawson, S., Thetford, A., Gibson, E.K., Morgan, D.J., Jones, W., et al. (2017). Identification of single-site gold catalysis in acetylene hydrochlorination. Science *355*, 1399–1403. https://doi.org/10.1126/science.aal3439.

258. Marcinkowski, M.D., Darby, M.T., Liu, J., Wimble, J.M., Lucci, F.R., Lee, S., Michaelides, A., Flytzani-Stephanopoulos, M., Stamatakis, M., and Sykes, E.C.H. (2018). Pt/Cu single-atom alloys as coke-resistant catalysts for efficient C-H activation. Nat. Chem. *10*, 325–332. https://doi.org/10.1038/NCHEM.2915.

259. Negreiros, F.R., Halder, A., Yin, C., Singh, A., Barcaro, G., Sementa, L., Tyo, E.C., Pellin, M.J., Bartling, S., Meiwes-Broer, K., et al. (2018). Bimetallic Ag-Pt Sub-nanometer Supported Clusters as Highly Efficient and

Robust Oxidation Catalysts. Angew. Chem. *130*, 1223–1227. https://doi.org/10.1002/ange.201709784.

260. Zhang, S., Tang, Y., Nguyen, L., Zhao, Y.F., Wu, Z., Goh, T.W., Liu, J.J., Li, Y., Zhu, T., Huang, W., et al. (2018). Catalysis on Singly Dispersed Rh Atoms Anchored on an Inert Support. ACS Catal. *8*, 110–121. https://doi.org/10.1021/acscatal.7b01788.

261. Zuo, Z., Liu, S., Wang, Z., Liu, C., Huang, W., Huang, J., and Liu, P. (2018). Dry Reforming of Methane on Single-Site Ni/MgO Catalysts: Importance of Site Confinement. ACS Catal. *8*, 9821–9835. https://doi.org/10.1021/acscatal.8b02277.

262. Zhang, Z., Shen, C., Sun, K., Jia, X., Ye, J., and Liu, C.J. (2022). Advances in studies of the structural effects of supported Ni catalysts for CO2 hydrogenation: from nanoparticle to single atom catalyst. J. Mater. Chem. A *10*, 5792–5812. https://doi.org/10.1039/d1ta09914k.

263. Zhou, K.L., Wang, Z., Han, C.B., Ke, X., Wang, C., Jin, Y., Zhang, Q., Liu, J., Wang, H., and Yan, H. (2021). Platinum single-atom catalyst coupled with transition metal/metal oxide heterostructure for accelerating alkaline hydrogen evolution reaction. Nat. Commun. *12*, 3783. https://doi.org/10.1038/s41467-021-24079-8.

264. Kim, J., Kim, H.E., and Lee, H. (2018). Single-Atom Catalysts of Precious Metals for Electrochemical Reactions (Preprint at Wiley-VCH Verlag). https://doi.org/10.1002/cssc.201701306.

265. Wei, L., Grénman, H., Haije, W., Kumar, N., Aho, A., Eränen, K., Wei, L., and de Jong, W. (2021). Sub-nanometer ceria-promoted Ni 13X zeolite catalyst for CO2 methanation. Appl. Catal. Gen. *612*, 118012. https://doi.org/10.1016/j.apcata.2021.118012.

266. Shi, X., Huang, Y., Bo, Y., Duan, D., Wang, Z., Cao, J., Zhu, G., Ho, W., Wang, L., Huang, T., and Xiong, Y. (2022). Highly Selective Photocatalytic CO2 Methanation with Water Vapor on Single-Atom Platinum-Decorated Defective Carbon Nitride. Angew Chem. Int. Ed. Engl. *61*, e202203063. https://doi.org/10.1002/anie.202203063.

267. Vogt, C., Groeneveld, E., Kamsma, G., Nachtegaal, M., Lu, L., Kiely, C.J., Berben, P.H., Meirer, F., and Weckhuysen, B.M. (2018). Publisher Correction: Unravelling structure sensitivity in CO2 hydrogenation over nickel. Nat. Catal. *1*, 163. https://doi.org/10.1038/s41929-018-0036-2.

268. Zhang, Z.Y., Li, T., Sun, X.L., Luo, D.C., Yao, J.L., Yang, G.D., and Xie, T. (2024). Efficient photo-thermal catalytic CO2 methanation and dynamic structural evolution over Ru/Mg-CeO2 single-atom catalyst. J. Catal. *430*, 115303. https://doi.org/10.1016/j.jcat.2024.115303.

269. Li, Y., Hao, J., Song, H., Zhang, F., Bai, X., Meng, X., Zhang, H., Wang, S., Hu, Y., and Ye, J. (2019). Selective light absorber-assisted single nickel atom catalysts for ambient sunlight-driven CO2 methanation. Nat. Commun. *10*, 2359. https://doi.org/10.1038/s41467-019-10304-y.

270. Das, S.K., Chatterjee, S., Bhunia, S., Mondal, A., Mitra, P., Kumari, V., Pradhan, A., and Bhaumik, A. (2017). A new strongly paramagnetic cerium-containing microporous MOF for CO2 fixation under ambient conditions. Dalton Trans. *46*, 13783–13792. https://doi.org/10.1039/c7dt02040f.

271. Molla, R.A., Bhanja, P., Ghosh, K., Islam, S.S., Bhaumik, A., and Islam, S.M. (2017). Pd Nanoparticles Decorated on Hypercrosslinked Microporous Polymer: A Highly Efficient Catalyst for the Formylation of Amines through Carbon Dioxide Fixation. ChemCatChem *9*, 1939–1946. https://doi.org/10.1002/cctc.201700069.

272. Omar, Y.M., Mohamed, N.G., Boshra, A.N., and Abdel-Aal, A.B.M. (2020). Solvent-Free N-Formylation: An Experimental Application of Basic Concepts and Techniques of Organic Chemistry. J. Chem. Educ. *97*, 1134–1138. https://doi.org/10.1021/acs.jchemed.9b00983.

273. Bai, S., Liu, F., Huang, B., Li, F., Lin, H., Wu, T., Sun, M., Wu, J., Shao, Q., Xu, Y., and Huang, X. (2020). High-efficiency direct methane conversion to oxygenates on a cerium dioxide nanowires supported rhodium single-atom catalyst. Nat. Commun. *11*, 954. https://doi.org/10.1038/s41467-020-14742-x.

274. Cheng, N., Stambula, S., Wang, D., Banis, M.N., Liu, J., Riese, A., Xiao, B., Li, R., Sham, T.K., Liu, L.M., et al. (2016). Platinum single-atom and cluster catalysis of the hydrogen evolution reaction. Nat. Commun. *7*, 13638. https://doi.org/10.1038/ncomms13638.

275. Zhao, C., Dai, X., Yao, T., Chen, W., Wang, X., Wang, J., Yang, J., Wei, S., Wu, Y., and Li, Y. (2017). Ionic Exchange of Metal-Organic Frameworks to Access Single Nickel Sites for Efficient Electroreduction of CO2. J. Am. Chem. Soc. *139*, 8078–8081. https://doi.org/10.1021/jacs.7b02736.

276. Cao, Q., Zhang, L.L., Zhou, C., He, J.H., Marcomini, A., and Lu, J.M. (2021). Covalent organic framework-supported Zn single atom catalyst for highly efficient N-formylation of amines with CO2 under mild conditions. Appl. Catal., B *294*, 120238. https://doi.org/10.1016/j.apcatb.2021.120238.

277. Li, Y., Chen, Y., Wan, Y.L., Wang, R.S., Wang, H., and Lei, Y.Z. (2022). Single-atom Zn on bipyridine-functionalized porous organic polymers towards highly efficient N-formylation of amines with CO2under mild conditions. J. CO2 Util. *65*, 102214. https://doi.org/10.1016/j.jcou.2022.102214.

278. Subramani, V., and Gangwal, S.K. (2008). A review of recent literature to search for an efficient catalytic process for the conversion of syngas to ethanol. Energy Fuels *22*, 814–839. https://doi.org/10.1021/ef700411x.

279. Sun, Ye, and Cheng, J. (2002). Hydrolysis of lignocellulosic materials for ethanol production: a review. Bioresour. Technol. *83*, 1–11. https://doi.org/10.1016/S0960-8524(01)00212-7.

280. Wang, C., Zhang, J., Qin, G., Wang, L., Zuidema, E., Yang, Q., Dang, S., Yang, C., Xiao, J., Meng, X., et al. (2020). Direct Conversion of Syngas to Ethanol within Zeolite Crystals. Chem *6*, 646–657. https://doi.org/10.1016/j.chempr.2019.12.007.

281. Lan, E.I., and Liao, J.C. (2013). Microbial synthesis of n-butanol, isobutanol, and other higher alcohols from diverse resources. Bioresour. Technol. *135*, 339–349. https://doi.org/10.1016/j.biortech.2012.09.104.

282. Richard, A.R., and Fan, M. (2017). Low-Pressure Hydrogenation of CO2 to CH3OH Using Ni-In-Al/SiO2 Catalyst Synthesized via a Phyllosilicate Precursor. ACS Catal. *7*, 5679–5692. https://doi.org/10.1021/acscatal.7b00848.

283. Butera, V., and Detz, H. (2021). Hydrogenation of CO2to methanol by the diphosphine-ruthenium(ii) cationic complex: a DFT investigation to shed light on the decisive role of carboxylic acids as promoters. Catal. Sci. Technol. *11*, 3556–3567. https://doi.org/10.1039/d1cy00502b.

284. Hussain, I., Mustapha, U., Al-Qathmi, A.T., Malaibari, Z.O., Alotaibi, S., Ganiyu, S.A., Alhooshani, K., and Alhooshani, K. (2023). The critical role of intrinsic physicochemical properties of catalysts for CO2 hydrogenation to methanol: A state of the art review. J. Ind. Eng. Chem. *128*, 95–126. https://doi.org/10.1016/j.jiec.2023.08.012.

285. Jin, F., Gao, Y., Jin, Y., Zhang, Y., Cao, J., Wei, Z., and Smith Jr, R.L. (2011). High-yield reduction of carbon dioxide into formic acid by zero-valent metal/metal oxide redox cycles. Energy Environ. Sci. *4*, 881–884. https://doi.org/10.1039/c0ee00661k.

286. Sun, Y., Hu, H., Wang, Y., Gao, J., Tang, Y., Wan, P., Hu, Q., Lv, J., Zhang, T., and Yang, X.J. (2019). In Situ Hydrogenation of CO2 by Al/Fe and Zn/Cu Alloy Catalysts under Mild Conditions. Chem. Eng. Technol. *42*, 1223–1231. https://doi.org/10.1002/ceat.201800389.

287. Lyu, L., Zeng, X., Yun, J., Wei, F., and Jin, F. (2014). No catalyst addition and highly efficient dissociation of H2O for the reduction of CO2 to formic acid with Mn. Environ. Sci. Technol. *48*, 6003–6009. https://doi.org/10.1021/es405210d.

288. Zhong, H., Yao, G., Cui, X., Yan, P., Wang, X., and Jin, F. (2019). Selective conversion of carbon dioxide into methane with a 98% yield on an in situ formed Ni nanoparticle catalyst in water. Chem. Eng. J. *357*, 421–427. https://doi.org/10.1016/j.cej.2018.09.155.

289. Yang, Y., Zhong, H., He, R., Wang, X., Cheng, J., Yao, G., and Jin, F. (2019). Synergetic conversion of microalgae and CO2 into value-added

chemicals under hydrothermal conditions. Green Chem. *21*, 1247–1252. https://doi.org/10.1039/c8gc03645d.

290. Wang, Y., Kattel, S., Gao, W., Li, K., Liu, P., Chen, J.G., and Wang, H. (2019). Exploring the ternary interactions in Cu–ZnO–ZrO 2 catalysts for efficient CO 2 hydrogenation to methanol. Nat. Commun. *10*, 1166. https://doi.org/10.1038/s41467-019-09072-6.

291. Yan, Y., Dai, Y., He, H., Yu, Y., and Yang, Y. (2016). A novel W-doped Ni-Mg mixed oxide catalyst for CO2 methanation. Appl. Catal., B *196*, 108–116. https://doi.org/10.1016/j.apcatb.2016.05.016.

292. Kothandaraman, J., Goeppert, A., Czaun, M., Olah, G.A., and Prakash, G.K.S. (2016). Conversion of CO2 from Air into Methanol Using a Polyamine and a Homogeneous Ruthenium Catalyst. J. Am. Chem. Soc. *138*, 778–781. https://doi.org/10.1021/jacs.5b12354.

293. Jalama, K. (2017). Carbon dioxide hydrogenation over nickel-ruthenium- and copper-based catalysts: Review of kinetics and mechanism. Catal. Rev. Sci. Eng. *59*, 95–164. https://doi.org/10.1080/01614940.2017.1316172.

294. Sugiyama, H., Miyazaki, M., Sasase, M., Kitano, M., and Hosono, H. (2023). Room-Temperature CO2 Hydrogenation to Methanol over Air-Stable hcp-PdMo Intermetallic Catalyst. J. Am. Chem. Soc. *145*, 9410–9416. https://doi.org/10.1021/jacs.2c13801.

295. Kowalczyk, Z., Stołecki, K., Raróg-Pilecka, W., Miśkiewicz, E., Wilczkowska, E., and Karpiński, Z. (2008). Supported ruthenium catalysts for selective methanation of carbon oxides at very low COx/H2 ratios. Appl. Catal. Gen. *342*, 35–39. https://doi.org/10.1016/j.apcata.2007.12.040.

296. Ma, Z., Wang, B., Yang, X., Ma, C., Wang, W., Chen, C., Liang, F., Zhang, N., Zhang, H., Chu, Y., et al. (2024). P-Block Aluminum Single-Atom Catalyst for Electrocatalytic CO2 Reduction with High Intrinsic Activity. J. Am. Chem. Soc. *146*, 29140–29149. https://doi.org/10.1021/jacs.4c11326.

297. Zheng, T., Jiang, K., Ta, N., Hu, Y., Zeng, J., Liu, J., and Wang, H. (2019). Large-Scale and Highly Selective CO 2 Electrocatalytic Reduction on Nickel Single-Atom Catalyst. Joule *3*, 265–278. https://doi.org/10.1016/j.joule.2018.10.015.

298. Cao, Y., Chen, S., BO, S., Fan, W., Li, J., Jia, C., Zhou, Z., Liu, Q., Zheng, L., and Zhang, F. (2022). Singe atom Bi decorated copper alloy enables C-C coupling for electrocatalytic reduction of CO2 into C2+ products. Preprint at Angewa. Chem. 62. https://doi.org/10.21203/rs.3.rs-2298906/v1.

299. Kim, J.Y., Ahn, H.S., Kim, I., Hong, D., Lee, T., Jo, J., Kim, H., Kyung Kwak, M., Gyun Kim, H., Kang, G., et al. (2024). Selective hydrocarbon or oxygenate production in CO_2 electroreduction over metallurgical alloy catalysts. Nat. Synth. *3*, 452–465. https://doi.org/10.1038/s44160-023-00449-6.

300. Zhang, J., Wang, Y., and Li, Y. (2024). Not One, Not Two, But at Least Three: Activity Origin of Copper Single-Atom Catalysts toward CO2/CO Electroreduction to C2+ Products. J. Am. Chem. Soc. *146*, 14954–14958. https://doi.org/10.1021/jacs.4c05669.

301. Jia, C., Tan, X., Sun, Q., Liu, R., Hocking, R.K., Wang, S., Zhong, L., Shi, Z., Smith, S., and Zhao, C. (2025). Fluorine Doping-Assisted Reconstruction of Isolated Cu Sites for CO $_2$ Electroreduction Toward Multicarbon Products. Adv. Mater. *37*, e2417443. https://doi.org/10.1002/adma.202417443.

302. Sun, B., Li, Z., Xiao, D., Liu, H., Song, K., Wang, Z., Liu, Y., Zheng, Z., Wang, P., Dai, Y., et al. (2024). Unveiling pH-Dependent Adsorption Strength of *CO2− Intermediate over High-Density Sn Single Atom Catalyst for Acidic CO2-to-HCOOH Electroreduction. Angew Chem. Int. Ed. Engl. *63*, e202318874. https://doi.org/10.1002/anie.202318874.

303. Zhao, H., Yu, R., Ma, S., Xu, K., Chen, Y., Jiang, K., Fang, Y., Zhu, C., Liu, X., Tang, Y., et al. (2022). The role of Cu_1–O_3 species in single-atom Cu/ZrO_2 catalyst for CO_2 hydrogenation. Nat. Catal. *5*, 818–831. https://doi.org/10.1038/s41929-022-00840-0.

304. Zheng, K., Li, Y., Liu, B., Jiang, F., Xu, Y., and Liu, X. (2022). Ti-doped CeO2 Stabilized Single-Atom Rhodium Catalyst for Selective and Stable CO2 Hydrogenation to Ethanol. Angew Chem. Int. Ed. Engl. *61*, e202210991. https://doi.org/10.1002/anie.202210991.

305. Ye, X., Yang, C., Pan, X., Ma, J., Zhang, Y., Ren, Y., Liu, X., Li, L., and Huang, Y. (2020). Highly selective hydrogenation of CO2to ethanol via designed bifunctional Ir1-In2O3Single-atom catalyst. J. Am. Chem. Soc. *142*, 19001–19005. https://doi.org/10.1021/jacs.0c08607.

306. Li, S., Xu, Y., Wang, H., Teng, B., Liu, Q., Li, Q., Xu, L., Liu, X., and Lu, J. (2023). Tuning the CO2 Hydrogenation Selectivity of Rhodium Single-Atom Catalysts on Zirconium Dioxide with Alkali Ions. Angew Chem. Int. Ed. Engl. *62*, e202218167. https://doi.org/10.1002/anie.202218167.

307. Lee, K., Anjum, U., Araújo, T.P., Mondelli, C., He, Q., Furukawa, S., Pérez-Ramírez, J., Kozlov, S.M., and Yan, N. (2022). Atomic Pd-promoted ZnZrOx solid solution catalyst for CO2 hydrogenation to methanol. Appl. Catal., B *304*, 120994. https://doi.org/10.1016/j.apcatb.2021.120994.

308. Hwang, S.M., Han, S.J., Park, H.G., Lee, H., An, K., Jun, K.W., and Kim, S.K. (2021). Atomically alloyed Fe-Co catalyst derived from a N-coordinated Co single-atom structure for CO2hydrogenation. ACS Catal. *11*, 2267–2278. https://doi.org/10.1021/acscatal.0c04358.

309. Kim, K.Y., Lee, H., Noh, W.Y., Shin, J., Han, S.J., Kim, S.K., An, K., and Lee, J.S. (2020). Cobalt Ferrite Nanoparticles to Form a Catalytic Co-Fe Alloy Carbide Phase for Selective CO2Hydrogenation to Light Olefins. ACS Catal. *10*, 8660–8671. https://doi.org/10.1021/acscatal.0c01417.

310. Jenkins, A.H., Dunphy, E.E., Toney, M.F., Musgrave, C.B., and Medlin, J.W. (2023). Tailoring the Near-Surface Environment of Rh Single-Atom Catalysts for Selective CO2 Hydrogenation. ACS Catal. *13*, 15340–15350. https://doi.org/10.1021/acscatal.3c03768.

311. Tang, Y., Zong, X., Nguyen, L., and Tao, F. (2024). Single-Atom Catalyst Restructuring during Catalytic Reforming of CH4 by CO2. ACS Catal. *14*, 18679–18689. https://doi.org/10.1021/acscatal.4c05703.

312. Yin, Q., Shen, T., Li, J., Ning, C., Xue, Y., Chen, G., Xu, M., Wang, F., Song, Y.F., Zhao, Y., and Duan, X. (2023). Solar-driven dry reforming of methane using RuNi single-atom alloy catalyst coupled with thermal decomposition of carbonates. Chem. Eng. J. *470*, 144416. https://doi.org/10.1016/j.cej.2023.144416.

313. Song, Y., Ozdemir, E., Ramesh, S., Adishev, A., Subramanian, S., Harale, A., Albuali, M., Fadhel, B.A., Jamal, A., Moon, D., et al. (2020). Dry reforming of methane by stable Ni–Mo nanocatalysts on single-crystalline MgO. Science *367*, 777–781. https://doi.org/10.1126/science.aav2412.

314. He, C., Li, Q., Ye, Z., Wang, L., Gong, Y., Li, S., Wu, J., Lu, Z., Wu, S., and Zhang, J. (2024). Regulating Atomically-Precise Pt Sites for Boosting Light-Driven Dry Reforming of Methane. Angew Chem. Int. Ed. Engl. *63*, e202412308. https://doi.org/10.1002/anie.202412308.

315. Wang, H., Cui, G., Lu, H., Li, Z., Wang, L., Meng, H., Li, J., Yan, H., Yang, Y., and Wei, M. (2024). Facilitating the dry reforming of methane with interfacial synergistic catalysis in an Ir@CeO2−x catalyst. Nat. Commun. *15*, 3765. https://doi.org/10.1038/s41467-024-48122-6.

316. Lei, M., Cheng, B., Liao, Y., Fang, X., Xu, X., and Wang, X. (2025). Band gap effect of TiO2 on supported Ru single-atom catalysts for CO2 methanation by DFT calculations. Mol. Catal. *570*, 114665. https://doi.org/10.1016/j.mcat.2024.114665.

317. Meng, W., Sui, X., Liu, Y., He, Y., Yuan, H., Zhu, X., Zhou, Y., and Zhou, Y. (2025). Collaborative influence of Ni single atoms and oxygen defects on Bi3O4Br for boosting light-driven CO2 hydrogenation to CH4. Appl. Catal., B *366*, 125033. https://doi.org/10.1016/j.apcatb.2025.125033.

318. Li, J., Wei, M., Ji, B., Hu, S., Xue, J., Zhao, D., Wang, H., Liu, C., Ye, Y., Xu, J., et al. (2025). Copper-Catalysed Electrochemical CO2 Methanation via the Alloying of Single Cobalt Atoms. Angew Chem. Int. Ed. Engl. *64*, e202417008. https://doi.org/10.1002/anie.202417008.

319. Zhang, T., Zheng, P., Gao, J., Han, Z., Gu, F., Xu, W., Li, L., Zhu, T., Zhong, Z., Xu, G., and Su, F. (2024). Single-Atom Ru Alloyed with Ni

Nanoparticles Boosts CO2 Methanation. Small *20*, e2308193. https://doi.org/10.1002/smll.202308193.

320. Zhang, T., Zheng, P., Gu, F., Xu, W., Chen, W., Zhu, T., Han, Y.F., Xu, G., Zhong, Z., and Su, F. (2023). The dual-active-site tandem catalyst containing Ru single atoms and Ni nanoparticles boosts CO2 methanation. Appl. Catal., B *323*, 122190. https://doi.org/10.1016/j.apcatb.2022.122190.

321. Ma, Y., Chen, C., Jiang, Y., Wei, X., Liu, Y., Liao, H., Wang, H., Dai, S., An, P., and Hou, Z. (2023). Ruthenium Single-Atom Anchored in Polyoxometalate-Ionic Liquids for N-Formylation of Amines with CO2 and H2. ACS Catal. *13*, 10295–10308. https://doi.org/10.1021/acscatal.3c02336.

322. Butera, V., and Butera, V. (2024). Density Functional Theory Methods Applied to Homogeneous and Heterogeneous Catalysis: A Short Review and a Practical User Guide (Preprint at Royal Society of Chemistry). https://doi.org/10.1039/d4cp00266k.

323. Osella, S., and Goddard Iii, W.A. (2023). CO2 Reduction to Methane and Ethylene on a Single-Atom Catalyst: A Grand Canonical Quantum Mechanics Study. J. Am. Chem. Soc. *145*, 21319–21329. https://doi.org/10.1021/jacs.3c05650.

324. Detz, H., and Butera, V. (2023). Insights into the mechanistic CO2 conversion to methanol on single Ru atom anchored on MoS2 monolayer. Mol. Catal. *535*, 112878. https://doi.org/10.1016/j.mcat.2022.112878.

325. Jiao, J., Lin, R., Liu, S., Cheong, W.C., Zhang, C., Chen, Z., Pan, Y., Tang, J., Wu, K., Hung, S.F., et al. (2019). Copper atom-pair catalyst anchored on alloy nanowires for selective and efficient electrochemical reduction of CO 2. Nat. Chem. *11*, 222–228. https://doi.org/10.1038/s41557-018-0201-x.

326. Gašparič, L., Pintar, A., and Kokalj, A. (2024). A DFT study of elementary reaction steps of dry reforming of methane catalyzed by Ni: Explaining the difference between Ni particles supported on CeO2 and MnOx-doped CeO2. Appl. Surf. Sci. *648*, 159029. https://doi.org/10.1016/j.apsusc.2023.159029.

327. Wang, S.G., Cao, D.B., Li, Y.W., Wang, J., and Jiao, H. (2006). CO2 reforming of CH4 on Ni(111): A density functional theory calculation. J. Phys. Chem. B *110*, 9976–9983. https://doi.org/10.1021/jp060992g.

328. Han, Z., Yang, Z., and Han, M. (2019). Comprehensive investigation of methane conversion over Ni(111) surface under a consistent DFT framework: Implications for anti-coking of SOFC anodes. Appl. Surf. Sci. *480*, 243–255. https://doi.org/10.1016/j.apsusc.2019.02.084.

329. Wang, S.G., Cao, D.B., Li, Y.W., Wang, J., and Jiao, H. (2009). Reactivity of surface OH in CH4 reforming reactions on Ni(1 1 1): A density functional theory calculation. Surf. Sci. *603*, 2600–2606. https://doi.org/10.1016/j.susc.2009.06.009.

330. Behrens, M., Studt, F., Kasatkin, I., Kühl, S., Hävecker, M., Abild-Pedersen, F., Zander, S., Girgsdies, F., Kurr, P., Kniep, B.L., et al. (2012). The active site of methanol synthesis over Cu/ZnO/Al2O 3 industrial catalysts. Science *336*, 893–897. https://doi.org/10.1126/science.1219831.

331. Zheng, H., Narkhede, N., Han, L., Zhang, H., and Li, Z. (2020). Methanol synthesis from CO2: a DFT investigation on Zn-promoted Cu catalyst. Res. Chem. Intermed. *46*, 1749–1769. https://doi.org/10.1007/s11164-019-04061-2.

332. Liu, L., Wang, C., Xue, F., Li, J., Zhang, H., Lu, S., Su, X., Cao, B., Huo, W., and Fang, T. (2022). DFT investigation of CO2 hydrogenation to methanol over Ir-doped Cu surface. Mol. Catal. *528*, 112460. https://doi.org/10.1016/j.mcat.2022.112460.

333. Alagumalai, A., Devarajan, B., and Song, H. (2023). Unlocking the potential of catalysts in thermochemical energy conversion processes. Catal. Sci. Technol. *13*, 5632–5653. https://doi.org/10.1039/d3cy00848g.

334. Mosaad Awad, M., Kotob, E., Ahmed Taialla, O., Hussain, I., Ganiyu, S.A., and Alhooshani, K. (2024). Recent Developments and Current Trends on Catalytic Dry Reforming of Methane: Hydrogen Production, Thermodynamics Analysis, Techno Feasibility, and Machine Learning (Preprint at Elsevier Ltd). https://doi.org/10.1016/j.enconman.2024.118252.

335. Kim, A.N., and Stoltz, B.M. (2020). Recent Advances in Homogeneous Catalysts for the Asymmetric Hydrogenation of Heteroarenes. ACS Catal. *10*, 13834–13851. https://doi.org/10.1021/acscatal.0c03958.

336. Vogt, C., and Weckhuysen, B.M. (2022). The concept of active site in heterogeneous catalysis. Nat. Rev. Chem *6*, 89–111.

337. Jin, S., Hao, Z., Zhang, K., Yan, Z., and Chen, J. (2021). Advances and Challenges for the Electrochemical Reduction of CO2 to CO: From Fundamentals to Industrialization (Preprint at John Wiley and Sons Inc). https://doi.org/10.1002/anie.202101818.

338. Li, Y., Xu, L., Mei, F., and Ying, S. (2023). LaNets: Hybrid Lagrange Neural Networks for Solving Partial Differential Equations. Comput. Model. Eng. Sci. *134*, 657–672. https://doi.org/10.32604/cmes.2022.021277.

339. Cubuk, E.D., Schoenholz, S.S., Rieser, J.M., Malone, B.D., Rottler, J., Durian, D.J., Kaxiras, E., and Liu, A.J. (2015). Identifying structural flow defects in disordered solids using machine-learning methods. Phys. Rev. Lett. *114*, 108001. https://doi.org/10.1103/PhysRevLett.114.108001.

340. Aramouni, N.A.K., Touma, J.G., Tarboush, B.A., Zeaiter, J., and Ahmad, M.N. (2018). Catalyst Design for Dry Reforming of Methane: Analysis Review (Preprint at Elsevier Ltd). https://doi.org/10.1016/j.rser.2017.09.076.

341. Wu, L., Guo, T., and Li, T. (2021). Machine learning-accelerated prediction of overpotential of oxygen evolution reaction of single-atom catalysts. iScience *24*, 102398. https://doi.org/10.1016/j.isci.2021.102398.

342. Liang, H., Liu, P.F., Xu, M., Li, H., and Asselin, E. (2023). A study of two-dimensional single atom-supported MXenes as hydrogen evolution reaction catalysts using density functional theory and machine learning. Int. J. Quant. Chem. *123*, e27055. https://doi.org/10.1002/qua.27055.

343. Svetnik, V., Liaw, A., Tong, C., Culberson, J.C., Sheridan, R.P., and Feuston, B.P. (2003). Random Forest: A Classification and Regression Tool for Compound Classification and QSAR Modeling. J. Chem. Inf. Comput. Sci. *43*, 1947–1958. https://doi.org/10.1021/ci034160g.

344. Chen, A., Zhang, X., Chen, L., Yao, S., and Zhou, Z. (2020). A Machine Learning Model on Simple Features for CO2Reduction Electrocatalysts. J. Phys. Chem. C *124*, 22471–22478. https://doi.org/10.1021/acs.jpcc.0c05964.

345. Umer, M., Umer, S., Zafari, M., Ha, M., Anand, R., Hajibabaei, A., Abbas, A., Lee, G., and Kim, K.S. (2022). Machine learning assisted high-throughput screening of transition metal single atom based superb hydrogen evolution electrocatalysts. J. Mater. Chem. A Mater. *10*, 6679–6689. https://doi.org/10.1039/d1ta09878k.

346. Shu, Z., Yan, H., Chen, H., and Cai, Y. (2022). Mutual modulation via charge transfer and unpaired electrons of catalytic sites for the superior intrinsic activity of N2 reduction: From highthroughput computation assisted with a machine learning perspective. J. Mater. Chem. A Mater. *10*, 5470–5478. https://doi.org/10.1039/d1ta10688k.

347. Lu, Z., Yadav, S., and Singh, C.V. (2020). Predicting aggregation energy for single atom bimetallic catalysts on clean and O* adsorbed surfaces through machine learning models. Catal. Sci. Technol. *10*, 86–98. https://doi.org/10.1039/c9cy02070e.

348. Wu, L., and Li, T. (2023). Machine learning enabled rational design of atomic catalysts for electrochemical reactions. Mater. Chem. Front. *7*, 4445–4459. https://doi.org/10.1039/d3qm00661a.

349. Tamtaji, M., Gao, H., Hossain, M.D., Galligan, P.R., Wong, H., Liu, Z., Liu, H., Cai, Y., Goddard, W.A., and Luo, Z. (2022). Machine learning for design principles for single atom catalysts towards electrochemical reactions. J. Mater. Chem. A *10*, 15309–15331. https://doi.org/10.1039/d2ta02039d.

350. Wittich, K., Krämer, M., Bottke, N., and Schunk, S.A. (2020). Catalytic Dry Reforming of Methane: Insights from Model Systems. Preprint at Wiley Blackwell *12*, 2130–2147. https://doi.org/10.1002/cctc.201902142.

351. Guharoy, U., Reina, T.R., Liu, J., Sun, Q., Gu, S., and Cai, Q. (2021). A Theoretical Overview on the Prevention of Coking in Dry Reforming of Methane Using Non-precious Transition Metal Catalysts (Preprint at Elsevier Ltd). https://doi.org/10.1016/j.jcou.2021.101728.

352. Yentekakis, I.V., Panagiotopoulou, P., and Artemakis, G. (2021). A Review of Recent Efforts to Promote Dry Reforming of Methane (DRM) to Syngas Production via Bimetallic Catalyst Formulations (Preprint at Elsevier B.V.). https://doi.org/10.1016/j.apcatb.2021.120210.

353. Şener, A.N., Günay, M.E., Leba, A., and Yıldırım, R. (2018). Statistical review of dry reforming of methane literature using decision tree and artificial neural network analysis. Catal. Today *299*, 289–302. https://doi.org/10.1016/j.cattod.2017.05.012.

354. Ayodele, B.V., and Cheng, C.K. (2015). Modelling and optimization of syngas production from methane dry reforming over ceria-supported cobalt catalyst using artificial neural networks and Box-Behnken design. J. Ind. Eng. Chem. *32*, 246–258. https://doi.org/10.1016/j.jiec.2015.08.021.

355. Vellayappan, K., Yue, Y., Lim, K.H., Cao, K., Tan, J.Y., Cheng, S., Wang, T., Gani, T.Z.H., Karimi, I.A., and Kawi, S. (2023). Impacts of catalyst and process parameters on Ni-catalyzed methane dry reforming via interpretable machine learning. Appl. Catal., B *330*, 122593. https://doi.org/10.1016/j.apcatb.2023.122593.

356. ELMAZ, F., Yücel, Ö., and MUTLU, A.Y. (2020). Predictive Modeling of the Syngas Production from Methane Dry Reforming over Cobalt Catalyst with Statistical and Machine Learning Based Approaches. International Journal of Advances in Engineering and Pure Sciences *32*, 8–14. https://doi.org/10.7240/jeps.558373.

357. Roh, J., Park, H., Kwon, H., Joo, C., Moon, I., Cho, H., Ro, I., and Kim, J. (2024). Interpretable machine learning framework for catalyst performance prediction and validation with dry reforming of methane. Appl. Catal., B *343*, 123454. https://doi.org/10.1016/j.apcatb.2023.123454.

358. Marlin, D.S., Sarron, E., and Sigurbjörnsson, Ó. (2018). Process Advantages of Direct CO2 to Methanol Synthesis. Front. Chem. *6*, 446. https://doi.org/10.3389/fchem.2018.00446.

359. Sehested, J. (2019). Industrial and Scientific Directions of Methanol Catalyst Development (Preprint at Academic Press Inc.). https://doi.org/10.1016/j.jcat.2019.02.002.

360. Vanjari, P., Kamesh, R., and Rani, K. Y. (2023). Machine learning models representing catalytic activity for direct catalytic CO2 hydrogenation to methanol. Materials Today: Proceedings *72*, 524–532. https://doi.org/10.1016/j.matpr.2022.11.265.

361. Burkart, M.D., Hazari, N., Tway, C.L., and Zeitler, E.L. (2019). Opportunities and Challenges for Catalysis in Carbon Dioxide Utilization. ACS Catal. *9*, 7937–7956. https://doi.org/10.1021/acscatal.9b02113.

362. Galadima, A., and Muraza, O. (2019). Catalytic Thermal Conversion of CO2 into Fuels: Perspective and Challenges (Preprint at Elsevier Ltd). https://doi.org/10.1016/j.rser.2019.109333.

363. Zheng, Y., Zhang, W., Li, Y., Chen, J., Yu, B., Wang, J., Zhang, L., and Zhang, J. (2017). Energy Related CO2 Conversion and Utilization: Advanced Materials/nanomaterials, Reaction Mechanisms and Technologies (Preprint at Elsevier Ltd). https://doi.org/10.1016/j.nanoen.2017.08.049.

364. Kamkeng, A.D.N., Wang, M., Hu, J., Du, W., and Qian, F. (2021). Transformation Technologies for CO2 Utilisation: Current Status, Challenges and Future Prospects (Preprint at Elsevier B.V.). https://doi.org/10.1016/j.cej.2020.128138.

365. Grim, R.G., Huang, Z., Guarnieri, M.T., Ferrell, J.R., Tao, L., and Schaidle, J.A. (2020). Transforming the carbon economy: Challenges and opportunities in the convergence of low-cost electricity and reductive CO2 utilization. Energy Environ. Sci. *13*, 472–494. https://doi.org/10.1039/c9ee02410g.

366. Mustafa, A., Lougou, B.G., Shuai, Y., Wang, Z., and Tan, H. (2020). Current Technology Development for CO2 Utilization into Solar Fuels and Chemicals: A Review (Preprint at Elsevier B.V.). https://doi.org/10.1016/j.jechem.2020.01.023.

367. Artz, J., Müller, T.E., Thenert, K., Kleinekorte, J., Meys, R., Sternberg, A., Bardow, A., and Leitner, W. (2018). Sustainable Conversion of Carbon Dioxide: An Integrated Review of Catalysis and Life Cycle Assessment. Chem. Rev. *118*, 434–504. https://doi.org/10.1021/acs.chemrev.7b00435.

368. Zhang, J., Cai, W., Hu, F.X., Yang, H., and Liu, B. (2021). Recent advances in single atom catalysts for the electrochemical carbon dioxide reduction reaction. Chem. Sci. *12*, 6800–6819. https://doi.org/10.1039/d1sc01375k.

369. Gong, L., Zhang, D., Lin, C.Y., Zhu, Y., Shen, Y., Zhang, J., Han, X., Zhang, L., and Xia, Z. (2019). Catalytic Mechanisms and Design Principles for Single-Atom Catalysts in Highly Efficient CO2 Conversion. Adv. Energy Mater. *9*, 20191902625. https://doi.org/10.1002/aenm.201902625.

370. Song, W., Xiao, C., Ding, J., Huang, Z., Yang, X., Zhang, T., Mitlin, D., and Hu, W. (2024). Review of Carbon Support Coordination Environments for Single Metal Atom Electrocatalysts (SACS) (Preprint at John Wiley and Sons Inc). https://doi.org/10.1002/adma.202301477.

371. Zhang, L., Yang, X., Yuan, Q., Wei, Z., Ding, J., Chu, T., Rong, C., Zhang, Q., Ye, Z., Xuan, F.Z., et al. (2023). Elucidating the structure-stability relationship of Cu single-atom catalysts using operando surface-enhanced infrared absorption spectroscopy. Nat. Commun. *14*, 8311. https://doi.org/10.1038/s41467-023-44078-1.

372. Ma, Z., Zhang, T., Lin, L., Han, A., and Liu, J. (2023). Ni single-atom arrays as self-supported electrocatalysts for CO2RR. AIChE J. *69*, e18161. https://doi.org/10.1002/aic.18161.

373. Huang, Y., Rehman, F., Tamtaji, M., Li, X., Huang, Y., Zhang, T., and Luo, Z. (2021). Mechanistic understanding and design of non-noble metal-based single-atom catalysts supported on two-dimensional materials for CO2 electroreduction. J. Mater. Chem. A *10*, 5813–5834. https://doi.org/10.1039/d1ta08337f.

374. Zheng, X., Li, P., Dou, S., Sun, W., Pan, H., Wang, D., and Li, Y. (2021). Non-carbon-supported single-atom site catalysts for electrocatalysis. Energy Environ. Sci. *14*, 2809–2858. https://doi.org/10.1039/d1ee00248a.

375. Theaker, N., Strain, J.M., Kumar, B., Brian, J.P., Kumari, S., and Spurgeon, J.M. (2018). Heterogeneously catalyzed two-step cascade electrochemical reduction of CO2 to ethanol. Electrochim. Acta *274*, 1–8. https://doi.org/10.1016/j.electacta.2018.04.072.

376. Liu, J., Cai, Y., Song, R., Ding, S., Lyu, Z., Chang, Y.C., Tian, H., Zhang, X., Du, D., Zhu, W., et al. (2021). Recent Progress on Single-Atom Catalysts for CO2 Electroreduction (Preprint at Elsevier B.V.). https://doi.org/10.1016/j.mattod.2021.02.005.

377. Sun, Z., Yin, H., Liu, K., Cheng, S., Li, G.K., Kawi, S., Zhao, H., Jia, G., and Yin, Z. (2022). Machine Learning Accelerated Calculation and Design of Electrocatalysts for CO2 Reduction (Preprint at John Wiley & Sons Inc). https://doi.org/10.1002/smm2.1107.

378. Wang, Z., Sun, Z., Yin, H., Wei, H., Peng, Z., Pang, Y.X., Jia, G., Zhao, H., Pang, C.H., and Yin, Z. (2023). The role of machine learning in carbon neutrality: Catalyst property prediction, design, and synthesis for carbon dioxide reduction. eScience *3*, 100136. https://doi.org/10.1016/j.esci.2023.100136.

379. Chen, Z.W., Chen, L.X., Yang, C.C., and Jiang, Q. (2019). Atomic (single, double, and triple atoms) catalysis: Frontiers, opportunities, and challenges. J. Mater. Chem. A *7*, 3492–3515. https://doi.org/10.1039/c8ta11416a.

380. Li, Z., Zhang, X., Cheng, H., Liu, J., Shao, M., Wei, M., Evans, D.G., Zhang, H., and Duan, X. (2020). Confined Synthesis of 2D Nanostructured Materials toward Electrocatalysis (Preprint at Wiley-VCH Verlag). https://doi.org/10.1002/aenm.201900486.

381. Liu, J. (2017). Catalysis by Supported Single Metal Atoms. ACS Catal. *7*, 34–59. https://doi.org/10.1021/acscatal.6b01534.

382. Zhang, T., Walsh, A.G., Yu, J., and Zhang, P. (2021). Single-atom alloy catalysts: Structural analysis, electronic properties and catalytic activities. Chem. Soc. Rev. *50*, 569–588. https://doi.org/10.1039/d0cs00844c.

383. Zhang, W., Zhao, Y., Huang, W., Huang, T., and Wu, B. (2024). Coordination Environment Manipulation of Single Atom Catalysts: Regulation Strategies, Characterization Techniques and Applications (Preprint at Elsevier B.V.). https://doi.org/10.1016/j.ccr.2024.215952.

384. Li, S., Lu, X., Liu, S., Zhou, J., Liu, Y., Zhang, H., Shen, R., Sun, K., Jiang, J., Wang, Y., et al. (2024). Structure Design and Electrochemical Properties of Carbon-Based Single Atom Catalysts in Energy Catalysis: A Review (Preprint at Elsevier B.V.). https://doi.org/10.1016/j.jechem.2024.06.028.

385. Wang, Y., Song, E., Qiu, W., Zhao, X., Zhou, Y., Liu, J., and Zhang, W. (2019). Recent Progress in Theoretical and Computational Investigations of Structural Stability and Activity of Single-Atom Electrocatalysts (Preprint at Elsevier B.V.). https://doi.org/10.1016/j.pnsc.2019.04.004.

386. Singh, B., Sharma, V., Gaikwad, R.P., Fornasiero, P., Zbořil, R., and Gawande, M.B. (2021). Single-Atom Catalysts: A Sustainable Pathway for the Advanced Catalytic Applications (Preprint at John Wiley and Sons Inc). https://doi.org/10.1002/smll.202006473.